Edge Probability Graph Models Beyond Edge Independency: Concepts, Analyses, and Algorithms

Fanchen Bu[1], Ruochen Yang[2], Paul Bogdan[2], and Kijung Shin[1]

[1]KAIST, Republic of Korea and [2]University of Southern California, United States

[1]{boqvezen97, kijungs}@kaist.ac.kr and [2]{ruocheny, pbogdan}@usc.edu

Abstract—Desirable random graph models (RGMs) should *(i)* reproduce *common patterns* in real-world graphs (e.g., power-law degrees, small diameters, and high clustering), *(ii)* generate *variable* (i.e., not overly similar) graphs, and *(iii)* remain *tractable* to compute and control graph statistics. A common class of RGMs (e.g., Erdős-Rényi and stochastic Kronecker) outputs edge probabilities, so we need to *realize* (i.e., sample from) the output edge probabilities to generate graphs. Typically, the existence of each edge is assumed to be determined independently, for simplicity and tractability. However, with edge independency, RGMs provably cannot produce high subgraph densities and high output variability simultaneously. In this work, we explore RGMs beyond edge independence that can better reproduce common patterns while maintaining high tractability and variability. Theoretically, we propose an edge-dependent realization (i.e., sampling) framework called *binding* that provably preserves output variability, and derive *closed-form* tractability results on subgraph (e.g., triangle) densities. Practically, we propose algorithms for graph generation with binding and parameter fitting of binding. Our empirical results demonstrate that RGMs with binding exhibit high tractability and well reproduce common patterns, significantly improving upon edge-independent RGMs.

Index Terms—Random graph model, Edge dependency, Edge probability, Subgraph density

I. INTRODUCTION

Random graph models (RGMs) help us understand, analyze, and predict real-world systems [2], with various practical applications, e.g., graph algorithm testing [3], statistical testing [4], and graph anonymization [5]. Desirable RGMs should generate graphs with *common patterns* in real-world graphs, such as high clustering,[1] power-law degrees, and small diameters [8]. At the same time, the generated graphs should be *variable*, i.e., not highly-similar or even near-identical, and the RGMs should be *tractable*, i.e., we can compute and control graph statistics of the generated random graphs.

Many RGMs output individual edge probabilities and generate graphs accordingly, e.g., the Erdős-Rényi model [9], the Chung-Lu model [10], the stochastic block model [11], and the stochastic Kronecker model [12]. To generate graphs from edge probabilities, we need *realizations* (i.e., sampling), where edge independency (i.e., the existences of edges are determined independently) is widely assumed for simplicity and tractability. Although edge-independent RGMs have high tractability and may reproduce some patterns (e.g., power-law degrees and small diameters), they empirically fail to preserve some other patterns, especially high clustering [13], [14], which has also

[1]*High clustering* means high subgraph densities as in, e.g., [6] and [7].

been theoretically validated. Specifically, edge-independent RGMs provably cannot generate graphs with high triangle density and high output variability at the same time [15].

Naturally, we ask: Can we apply realization *without assuming edge independency* so that we can improve upon such RGMs to generate graphs *reproducing common patterns* and *having high variability*, while still *ensuring high tractability*? To address this question, we propose and explore the concept of *edge probability graph models* (EPGMs), i.e., RGMs that are still based on edge probabilities but do not assume edge independency, from theoretical and practical perspectives. Our key message is a positive answer to the question. Specifically, our novel contributions are fourfold:

1) **Concepts (Section IV):** We formally propose and define the *concept* of EPGMs, and theoretically show some basic *properties* of EPGMs, e.g., even with edge dependency introduced, the *output variability remains as high* as the corresponding edge-independent model.
2) **Analyses (Section V):** We propose *binding*, a *(i) pattern-reproducing*, *(ii) tractable*, and *(iii) flexible* realization scheme, to construct EPGMs with different levels of edge dependency, and derive tractability results on the *closed-form* subgraph (e.g., triangle) densities.
3) **Algorithms (Section V):** We propose practical algorithms for *(i) graph generation* with binding, and for *(ii) efficient parameter fitting* to control the graph statistics generated by EPGMs with binding.
4) **Experiments (Section VI):** Via experiments on real-world graphs, we show the power of the proposed binding and parameter-fitting algorithms to reproduce common graph patterns and their efficiency, validating the correctness of our theoretical analyses and practical algorithms.

<u>**Reproducibility.**</u> The appendix, code, and data are publicly available online in [1] (https://github.com/bokveizen/edge-probability-graph-model).

II. PRELIMINARIES

<u>**Graphs.**</u> A *graph* $G = (V, E)$ is defined by a *node set* $V = V(G)$ and an *edge set* $E = E(G) \subseteq \binom{V}{2} := \{V' \subseteq V : |V'| = 2\}$.[2] For a node $v \in V$, the set of its *neighbors* is $N(v; G) = \{u \in V : (u, v) \in E(G)\}$, and its *degree* $d(v; G) = |N(v; G)|$ is the

[2]In this work, we consider undirected unweighted graphs without self-loops following common settings for random graph models. See Appendix C-A [1] for discussions on more general graphs, e.g., directed or weighted graphs.

number of its neighbors. Given $V' \subseteq V$, the *induced subgraph* of G on V' is $G[V'] = (V', E \cap \binom{V'}{2})$.

Triangles and clustering. Given $G = (V, E)$, the number of wedges (i.e., open triangles) is $n_w(G) = \sum_{v \in V} \binom{d(v)}{2}$. The *global clustering coefficient* (GCC) of G is defined as $\text{GCC}(G) = \frac{\triangle(G)}{n_w(G)}$, where $\triangle(G)$ is the number of triangles in G. The *average local clustering coefficient* (ALCC) of G is defined as $\text{ALCC}(G) = \sum_{v:d(v) \geq 2} \frac{\triangle(v;G)}{\binom{d(v)}{2}}$, where $\triangle(v;G)$ is the number of triangles involving v in G.

Random graph models (RGMs). Fix a node set $V = [n] = \{1, 2, \ldots, n\}$ with $n \in \mathbb{N}$. Let $\mathcal{G}(V) = \{G = (V, E): E \subseteq \binom{V}{2}\}$ denote the set of all $2^{\binom{n}{2}}$ possible node-labeled (i.e., each node is assigned a distinct identifier $i \in [n]$) graphs on V. A *random graph model* (RGM) is defined as a probability distribution $f : \mathcal{G}(V) \to [0, 1]$ with $\sum_{G \in \mathcal{G}(V)} f(G) = 1$. For each graph $G \in \mathcal{G}(V)$, $f(G)$ is the probability of G being generated by the RGM f. For each node pair (u, v) with $u, v \in V$, the (marginal) *edge probability* of (u, v) under the RGM f is $\text{Pr}_f[(u, v)] := \sum_{G \in \mathcal{G}(V)} f(G)\mathbf{1}[(u, v) \in E(G)]$, where $\mathbf{1}[\cdot]$ is the indicator function.

Edge independent graph models (EIGMs). Given edge probabilities, edge independency is widely assumed in many existing RGMs, resulting in the concept of edge independent graph models (EIGMs [15]; also known as *inhomogeneous Erdős-Rényi graphs* [16]). The EIGM f_p^{EI} w.r.t. edge probabilities $p: \binom{V}{2} \to [0, 1]$ is defined by $f_p^{\text{EI}}(G) = \prod_{(u,v) \in E(G)} p(u, v) \prod_{(u',v') \notin E(G)} (1 - p(u', v')), \forall G \in \mathcal{G}(V)$.

III. RELATED WORK AND BACKGROUND

A. Limitations of EIGMs

Chanpuriya et al. [15] defined the concept of *overlap* to measure the variability of RGMs, where a high overlap value implies low variability. The overlap of an RGM f is the expected proportion of edges in two generated graphs: $\text{Ov}(f) = \frac{\mathbb{E}_f|E(G') \cap E(G'')|}{\mathbb{E}_f|E(G)|}$, where G, G', and G'' are three random graphs independently generated by f.

High variability (i.e., low overlap) is important for RGMs [17], as generating overly similar graphs undermines the effectiveness of RGMs in common applications, e.g., graph algorithm testing and graph anonymization (see Section I). Chanpuriya et al. [15] showed that EIGMs cannot generate graphs with high clustering, which is a common property in real-world graphs [8], and low overlap at the same time.

Chanpuriya et al. [18] recently extended their theoretical results to edge-dependent RGMs. However, they did not provide practical graph generation algorithms or detailed tractability results,[3] while tractability results and practical graph generation are part of our focus in this work.

Some methods shift edge probabilities from existing EIGMs by accept-reject [19] or mixing different existing EIGMs [20]. Such methods are essentially still EIGMs, and inevitably have high overlap (i.e., low variability). See Appendix D-F [1] for more discussion and evaluation on such methods.

---

[3]Their graph generation relies on time-consuming maximal clique enumeration. See Appendix C-B [1] for more discussions.

B. Edge-dependent RGMs

Edge dependency exists in various RGMs, e.g., preferential attachment models [21], small-world graphs [22], random geometric graphs [23], and exponential random graphs [24]. Recent work on exchangeable network models, which initially assume symmetry among nodes, introduce *node asymmetry* to improve expressiveness [25], [26]. In a similar spirit but from a different perspective, we introduce *edge dependence* upon EIGMs to enhance the power of RGMs.

We differ from existing edge-dependent RGMs as follows:
- We provide a novel perspective on constructing edge-dependent RGMs by decomposing RGMs into (1) the marginal edge probabilities and (2) the realization of the probabilities (see Definition IV.1).
- This new perspective allows us to improve upon existing EIGMs, inheriting their strengths (e.g., variability and tractability; see Property IV.3 and Theorem V.6) and alleviating their weaknesses (e.g., inability to generate high clustering; see Section VI-B).
- We derive *closed-form* tractability results on subgraph densities (see Theorem V.6), while only *asymptotic* results, as the number of nodes goes to infinity, are usually available for existing models [27]–[29].
- Our model empirically shows better capability in generating graphs with both high clustering and high variability than existing models (see Section VI-F).

Target. In this work, we aim to propose novel edge-dependent RGMs with the following desirable properties:
- *Reproducing common patterns* widely observed in real-world graphs, e.g., high clustering, power-law degrees, and small diameters [8].
- *Showing high output variability*, generating variable graphs with low overlap (see Section III-A).
- *Having high tractability*, with the feasibility of obtaining closed-form results of graph statistics in generated graphs.

IV. EDGE PROBABILITY GRAPH MODELS (EPGMs): CONCEPT AND BASIC PROPERTIES

In this section, we introduce the concept of edge probability graph models (EPGMs) and show some basic properties of EPGMs. EIGMs generate graphs assuming edge independency. In contrast, we explore a broader class of edge probability graph models (EPGMs) going beyond edge independency.

Definition IV.1 (EPGMs). Given edge probabilities $p: \binom{V}{2} \to [0, 1]$, the set $\mathcal{F}(p)$ of *edge probability graph models* (EPGMs) w.r.t. p consists of all the RGMs with marginal edge probabilities p, i.e., $\mathcal{F}(p) := \{f: \text{Pr}_f[(u, v)] = p(u, v), \forall u, v \in V\}$.

By EPGMs, we decompose each RGM into two factors: **(F1)** the marginal probability of each edge and **(F2)** how the edge probabilities are realized (i.e., sampled). EIGMs have overlooked (F2), simply using realization assuming edge independency. Our decomposition via EPGMs introduces a novel perspective on imposing edge dependency.

Below, we show some basic properties of EPGMs and discuss their implication and significance.

Algorithm 1: General Binding

Input : (1) edge probabilities $p: \binom{V}{2} \to [0, 1]$; (2) pair partition
$\quad\quad$ $\mathcal{P}$ s.t. $\bigcup_{P \in \mathcal{P}} P = \binom{V}{2}$ with $P \cap P' = \varnothing, \forall P \neq P' \in \mathcal{P}$

Output : generated graph G

1 $E \leftarrow \bigcup_{P \in \mathcal{P}} \texttt{binding}(p, P)$
2 **return** $G = (V, E)$
3 **Procedure** $\texttt{binding}(\hat{p}, \hat{P})$
4 $\quad$ sample a random variable $s \sim \mathcal{U}(0, 1)$
5 $\quad$ $\hat{E} \leftarrow \{(u, v) : \hat{p}(u, v) \geq s\}$ $\quad$ ▷ Decided by same s
6 $\quad$ **return** $\hat{E}$

Property IV.2 (EPGMs are general)**.** *Any RGM can be represented as an EPGM (w.r.t its marginal edge probabilities).*

Proof sketch. Any RGM is a multivariate distribution that can be represented by the marginal probabilities of each variable and the dependency among them. $\quad\square$

Note that, for all theoretical results in the paper, we provide **formal statements and/or full proofs** in Appendix A [1].
Implication. Property IV.2 shows the *generality* of EPGMs, as they encompass all possible RGMs. However, it also implies that the space of EPGMs is too vast to be fully explored, which motivates us to find *good subsets* of EPGMs.

Finally, since each individual edge probability is preserved as in p, several other quantities are consequently preserved.

Property IV.3 (EPGMs have constant expected degrees and overlap)**.** *For any $p: \binom{V}{2} \to [0, 1]$, the expected node degrees and overlap (see Section III-A) of all the EPGMs w.r.t. p are constant (i.e., depend only on p), ensuring EPGMs preserve degree distributions in expectation and have as low overlap (i.e., high output variability) as the corresponding EIGM.*

Proof sketch. It follows from the linearity of expectation. $\quad\square$

Implications. Many EIGMs can generate graphs with desirable degree distributions, and Property IV.3 ensures that EPGMs inherit such strengths (see Figure 1 for empirical evidence). Moreover, it ensures that EPGMs have as high output variability as the corresponding EIGM, which is an important and desirable property of RGMs (see Section III).

Research questions. Inspired by the basic properties of EPGMs, below, we explore EPGMs from both theoretical and practical perspectives, aiming to answer two questions:

- **(RQ1; Theory)** What good subsets of EPGMs are pattern-reproducing, flexible, and tractable?
- **(RQ2; Practice)** How to generate graphs using such EPGMs and fit the parameters of EPGMs?

V. Binding: Analyses and algorithms

The output variability of EPGMs is guaranteed by Property IV.3. Therefore, we now aim to find good subsets of EPGMs for given edge probabilities (which can be obtained by EIGMs) that *(i)* reproduce *common patterns* (especially high clustering, the bottleneck of EIGMs) and *(ii)* are *tractable* (i.e., with controllable graph statistics).

A. General binding: General mathematical framework

Desirable RGMs should generate graphs with common patterns, e.g., high clustering, power-law degrees, and small diameters. Some EIGMs (e.g., stochastic Kronecker) already do well in the latter two aspects, so we focus on the bottleneck "high clustering" and seek EPGMs that achieve it.[4] To this end, we first study and propose *binding*, a general mathematical framework that introduces positive dependency among edges to determine multiple edge existences together. Binding can be seen as a way of probability coupling [30], with given marginal distributions (i.e., edge probabilities). The process of binding is described in Algorithm 1, where edge dependence is imposed in each group of pairs, in the sense that, if a node pair is sampled as an edge, all the pairs with higher probabilities must be sampled (Line 5). Note that, Algorithm 1 describes a general framework, while our practical algorithms (Algorithms 2 and 3) do not need to choose an explicit partition $\mathcal{P}$ beforehand. See Definition A.4 in Appendix A [1] for a mathematical definition of binding.

There are two basic properties of binding: *(i)* binding is *correct*, i.e., generates EPGMs, and *(ii)* binding produces higher subgraph densities (i.e., higher clustering) than EIGMs, which aligns with our motivation to improve clustering.

Proposition V.1. *Algorithm 1 with input p (and any $\mathcal{P}$) correctly produces an EPGM w.r.t. p.*

Proof sketch. Each edge (u, v) exists when $p(u, v) \geq s$, which happens with probability $p(u, v)$ since $s \sim \mathcal{U}(0, 1)$. $\quad\square$

Proposition V.2. *Binding produces higher or equal subgraph densities, compared to the corresponding EIGMs.*

Proof sketch. When multiple edges are grouped together, the probability that all of them exist increases from the *product* of their marginal probabilities to the *minimum* of them. $\quad\square$

With binding, we can construct EPGMs with different levels of edge dependency by different ways of binding the node pairs. Let us first study two extreme cases.
Minimal binding. EIGMs are the case with minimal binding, i.e., without binding, where the partition contains only sets of a single pair, i.e., $\mathcal{P} = \{\{(u, v)\} : u, v \in V\}$.
Maximal binding. Maximal binding corresponds to the case with $\mathcal{P} = \{\binom{V}{2}\}$, i.e., all the pairs are bound together. It achieves the upper bound of subgraph densities.

Below, we explore EPGMs between the two extremes.

B. Local binding: Practical and tractable scheme

Building upon the general framework introduced in Section V-A, we propose practical binding algorithms. Intuitively, the more pairs we bind together, the higher subgraph densities we have. Between minimal binding (i.e., EIGMs) and maximal binding that achieves the upper bound of subgraph densities, we can have a *flexible* spectrum. However, the number of

---

[4]Empirically, binding maintains or even improves the generation quality w.r.t. several different graph metrics, including but not limited to degrees and diameters (see Section VI-C).

possible partitions of node pairs $\binom{V}{2}$ grows exponentially w.r.t. $|V|$. Hence, we propose to introduce edge dependency *without explicit partitions*. Specifically, we propose *local binding*, where we repeatedly sample node groups,[5] and bind pairs between each sampled node group together. Node pairs within the same node group are structurally related, and binding them together is expected to bring structurally meaningful edge dependency. **Real-world motivation.** In social networks, each group "bound together" can represent a group interaction, e.g., an offline social event (meeting, conference, party) or an online social event (group chat, Internet forum, online game). In such social events, people gather together, and the communications/relations between them likely co-occur. At the same time, not all people in such events would necessarily communicate with each other, e.g., some people are more familiar with each other. This is the point of considering binding with various edge probabilities (instead of just inserting cliques). In general, group interactions widely exist in graphs in different domains, e.g., social networks [31], biological networks [32], and web graphs [33]. See Appendix C-D [1] for more discussions.

In Algorithm 2, we repeatedly sample a subset of nodes (Line 4) and group the ungrouped pairs between the sampled nodes (Line 5). We maintain P_{rem} to ensure disjoint partitions (Line 6). For practical usage, we consider a limited number (i.e., R) of rounds for binding (Line 2) otherwise it may take a long time to exhaust all the pairs. Algorithm 2 is also a probabilistic process, and we use $f_{p;g,R}^{\text{LB}}$ to denote the corresponding RGM, i.e., $f_{p;g,R}^{\text{LB}}(G) = \Pr[\text{Algorithm 2 outputs } G \text{ with inputs } p,$ $g, \text{ and } R]$. As a special case of binding, local binding also correctly generates EPGMs.

Proposition V.3. *Algorithm 2 with input p (and any g and R) produces an EPGM w.r.t. p.*

Proof sketch. It is a direct corollary of Proposition V.1. ☐

Remark V.4. We introduce node-sampling probabilities (i.e., g) to sample node groups with better tractability, without explicit partitions. With higher node-sampling probabilities, larger node groups are bound together, and the generated graphs are expected to have higher subgraph densities. Local binding forms a spectrum between the two extreme cases (see Section V-A): $g(v) \equiv 0$ gives minimal binding and $g(v) \equiv 1$ gives maximal binding.

Theorem V.5 (Time complexity of graph generation with local binding). *Given $p: \binom{V}{2} \to [0,1]$, $g: V \to [0,1]$, and $R \in \mathbb{N}$, $f_{p;g,R}^{LB}$ generates a graph in $O\left(R\left(\sum_{v \in V} g(v)\right)^2 + |V|^2\right)$ time with high probability,[6] with the worst case $O(R|V|^2)$.*

Proof sketch. In each round, it takes $O(n^2)$, where n is the number of sampled nodes, which is $\sum_{v \in V} g(v)$ in expectation, thus $O(\sum_{v \in V} g(v))$ with high probability, and $O(|V|^2)$ at most. Dealing with the remaining pairs takes $O\left(\binom{|V|}{2}\right)$. ☐

[5] We use independent *node* sampling (yet still with *edge* dependency), which is simple, tractable, and works empirically well in our experiments. See Appendix C-C [1] for more discussions.

[6] That is, $\lim_{|V| \to \infty} \Pr[\text{it takes } O\left(R\left(\sum_{v \in V} g(v)\right)^2 + |V|^2\right)] = 1$.

Algorithm 2: Local binding

Input : (1) edge probabilities $p: \binom{V}{2} \to [0,1]$;
   (2) node-sampling probabilities $g: V \to [0,1]$;
   (3) maximum number of rounds R
Output : G: generated graph
1   $\mathcal{P} \leftarrow \varnothing; i_{round} \leftarrow 0; P_{rem} \leftarrow \binom{V}{2}$ ▷ Initialization
2   **for** $i_{round} = 1, 2, \ldots, R$ **do**
3   **if** $P_{rem} = \varnothing$ **then break**   ▷ Pairs exhausted
4   sample $V_s \subseteq V$ with $\Pr[v \in V_s] = g(v)$ independently
5    $P_s \leftarrow \binom{V_s}{2} \cap P_{rem}$ ▷ Group pairs
6    $\mathcal{P} \leftarrow \mathcal{P} \cup \{P_s\}; P_{rem} \leftarrow P_{rem} \setminus P_s$ ▷ Update
7   $\mathcal{P} \leftarrow \mathcal{P} \cup \{\{(u,v)\}: (u,v) \in P_{rem}\}$ ▷ Remaining pairs
8   **return** *the output of Algorithm 1 with inputs p and $\mathcal{P}$*

We derive tractability results of local binding on the closed-form expected number of motifs (i.e., induced subgraphs; see Section II). For this, we derive the probabilities of all the possible size-3 motifs for each node group, then we compute the expected number of each motif by taking the summation over all different node groups, which is later used for parameter fitting (see Section V-D).

Theorem V.6 (Tractable 3-motif probabilities with local binding). *For any $p: \binom{V}{2} \to [0,1]$, $g: V \to [0,1]$, $R \in \mathbb{N}$, any size-3 node group $V' = \{u, v, w\} \in \binom{V}{3}$, and any size-3 motif instance $E^* \subseteq \binom{V'}{2}$, we can compute the closed-form $\Pr_{f_{p;g,R}^{LB}}[E(G[V']) = E^*]$, as a function w.r.t. p, g, and R (the detailed formulae are in Appendix A-D [1]).*

Proof sketch. For each size-3 node group, we (1) consider all the possible cases of how the pairs among the three nodes are partitioned and grouped, (2) compute the motif probabilities conditioned on each sub-case, and (3) take the summation of motif probabilities in all the sub-cases. See Appendix A-D [1] for the full proof and detailed formulae. ☐

Closed-form motif probabilities show the tractability of EPGMs with binding, which allows us to estimate the output and fit the parameters of RGMs (see Section V-D). Regarding the parameters, higher p and g give higher clustering, while the choice of R is mainly for controlling the running time.

Remark V.7. Theorem V.6 can be extended to larger motif sizes, with practical difficulties from the increasing sub-cases as motif size increases.

Theorem V.8 (Time complexity of computing motif probabilities with local binding). *Computing $\Pr_{f_{p;g,R}^{LB}}[E(G[V']) = E^*]$ takes $O(|V|^3)$ time in total for all $E^* \subseteq \binom{V'}{2}$ and $V' \in \binom{V}{3}$.*

Proof sketch. We enumerate all $O(|V|^3)$ size-3 node groups. For each group and each motif, the calculation takes $O(1)$ with fixed arithmetic formulae. ☐

Remark V.9. The complexity can be reduced by considering node equivalence, which we will discuss in detail when discussing parameter fitting in Section V-D.

C. Parallel binding: Parallelizable icing on the cake

In local binding, the sampling order matters, i.e., later rounds are affected by earlier rounds. If one pair is already determined

in an early round, even if sampled again in later rounds, its (in)existence cannot be changed. This property hinders the parallelization and the derivation of tractability analyses, and implies that each pair can only be bound together once, entailing less flexibility in group interactions.

We thus propose *parallel binding*, a more flexible and naturally *parallelizable* binding scheme. The process is described in Algorithm 3. We let $f_{p;g,R}^{\text{PB}}$ denote the corresponding RGM defined by $f_{p;g,R}^{\text{PB}}(G) = \Pr[\text{Algorithm 3 outputs } G \text{ with inputs } p, g, \text{ and } R]$.

The high-level idea is to make each round of binding probabilistically equivalent (see Lines 4 to 6). In each round, we insert edges with some "small" probabilities r calculated from p (Line 2). Those "small" probabilities accumulate over rounds, maintaining the final edge probabilities as p (together with p_{rem}). We can straightforwardly parallelize multiple rounds of binding by, e.g., multi-threading.

Although parallel binding is algorithmically different from (local) binding (e.g., no explicit partition is used), it shares many theoretical properties with local binding. Specifically, Statements V.3 to V.8 also apply to parallel binding. This implies that we maintain (or even improve; see Remark V.10) correctness, tractability, flexibility, and efficiency when using parallel binding compared to local binding. See Appendix A-E [1] for the formal statements and proofs.

Remark V.10. We also derive tractability results of parallel binding on the expected number of (non-)isolated nodes. It is much more challenging to derive such results for local binding where later rounds are affected by earlier rounds. Since our main focus is on subgraph densities, see Appendix B [1] for all the analysis regarding (non-)isolated nodes.

D. Efficient parameter fitting with node equivalence

With tractability results, we can fit parameters (p, g, and R) of binding (Algorithms 2 and 3) to the graph statistics of a given graph G, to generate random graphs that are similar to G, which is useful for the typical applications of RGMs, e.g., graph algorithm testing [34], statistical testing [35], and graph anonymization [36].

By default, we consider the cases where the number R of rounds is fixed, edge probabilities p are obtained by applying an EIGM to the given graph G, and we aim to fit the node-sampling probabilities g. It is also possible to jointly optimize both p and g (see Section VI-E), or generate graphs "from scratch" with different levels of clustering by directly setting the parameters (see Appendix D-G [1]).

Since our closed-form tractability results are functions involving only arithmetic operations on the parameters, differentiable optimization techniques (e.g., Newton-Raphson and gradient descent) are possible for parameter fitting. The fitting objective can be any function of 3-motif probabilities. For example, one can fit the (expected) number of triangles ($\mathbb{E}_{f_{p;g,R}^{\text{X}}}[\triangle(G)]$) to the ground-truth number in an input graph ($\triangle(G_{input})$) by minimizing the "difference" between them, e.g., $(1 - \frac{\mathbb{E}_{f_{p;g,R}^{\text{X}}}[\triangle(G)]}{\triangle(G_{input})})^2$, where $\mathbb{E}_{f_{p;g,R}^{\text{X}}}[\triangle(G)] = \sum_{V' \in \binom{V}{3}} \Pr_{f_{p;g,R}^{\text{X}}}[E(G[V']) = \binom{V'}{2}]$ are

---

Algorithm 3: Parallel binding

Input : (1) edge probabilities $p\colon \binom{V}{2} \to [0,1]$
(2) node-sampling probabilities $g : V \to [0,1]$
(3) the number of rounds R

Output : G: generated graph

1   $E \leftarrow \varnothing$ ▷ Initialization
2   $r(u,v) \leftarrow \min(\frac{1-(1-p(u,v))^{1/R}}{g(u)g(v)}, 1), \forall u,v \in V$
3   $p_{rem}(u,v) \leftarrow \max(1 - \frac{1-p(u,v)}{(1-g(u)g(v))^R}, 0), \forall u,v \in V$
4   **for** $i_{round} = 1, 2, \ldots, R$ **do**
5   sample $V_s \subseteq V$ with $\Pr[v \in V_s] = g(v)$ independently
6      $E \leftarrow E \cup \texttt{binding}(r, \binom{V_s}{2})$ ▷ See Alg. 1
7   sample a random variable $s \sim \mathcal{U}(0,1)$
8   $E \leftarrow E \cup \{(u,v) : p_{rem}(u,v) \geq s\}$
9   **return** $G = (V, E)$

---

obtainable by the tractability results (see Theorem V.6) with $X \in \{\text{LB}, \text{PB}\}$ indicating the binding scheme (LB represents local binding and PB represents parallel binding).

Efficient evaluation of the fitting objective is important. A key challenge is that the naive computation takes $O(|V|^3)$ time in total by considering all $O(|V|^3)$ different possible node groups V' (see Theorem V.6). We aim to improve the speed of computing the tractability results by considering *node equivalence* and thus reducing the total number of distinct node groups we need to consider.

Erdős-Rényi (ER) model. The ER model [9] outputs edge probabilities with two parameters: n_0 and p_0, and the output is p_{n_0,p_0}^{ER} with $p_{n_0,p_0}^{ER}(u,v) = p_0, \forall u,v \in \binom{V}{2}$ with $V = [n_0]$. Given a graph $G = (V = [n], E)$, ER outputs $n_0 = n$ and $p_0 = \frac{2|E|}{n(n-1)}$. ER outputs uniform edge probabilities, and all nodes are equivalent. We use uniform node-sampling probabilities, i.e., $g(v) = g_0, \forall v \in V$ for a single parameter $g_0 \in [0,1]$.

Lemma V.11. *For ER, the time of computing 3-motif probabilities can be reduced from $O(|V|^3)$ to $O(1)$.*

Chung-Lu (CL) model. The CL model [10] outputs edge probabilities with a sequence of expected degrees $D = (d_1, d_2, \ldots, d_n)$, and the output is p_D^{CL} with $p_D^{CL}(u,v) = \min(\frac{d_u d_v}{\sum_{i=1}^n d_i}, 1), \forall u,v \in \binom{V}{2}$ with $V = [n]$. Given a graph $G = (V = [n], E)$, CL outputs $d_i = d(i; G)$ for each node $i \in V$. CL outputs edge probabilities to match node degrees $D = (d_1, d_2, \ldots, d_n)$, and nodes with the same degree are equivalent. We set node-sampling probabilities as a function of degree (i.e., nodes with the same degree share the same node-sampling probability) with k_{deg} parameters, where $k_{deg} \coloneqq |\{d_1, d_2, \ldots, d_n\}|$ is the number of distinct degrees.

Lemma V.12. *For CL, the time of computing 3-motif probabilities can be reduced from $O(|V|^3)$ to $O(k_{deg}^3)$.*

Stochastic block (SB) model. Given a graph $G = (V = [n], E)$ and a node partition $f_B\colon [n] \to [c]$ with $c \in \mathbb{N}$, let $V_i = \{v \in V : f_B(v) = i\}$ denote the set of nodes partitioned in the i-th group for $i \in [c]$. The fitting of the edge probabilities in the SB [11] model gives $p_B\colon [c] \times [c] \to [0,1]$ with

$p_B(i,i) = \frac{|E(G[V_i])|}{\binom{|V_i|}{2}}$ and $p_B(i,j) = \frac{|E \cap \{(v,v'):v \in V_i, v' \in V_j\}|}{|V_i||V_j|}$, for $i \neq j \in [c]$. SB outputs edge probabilities with nodes assigned to different "blocks", and nodes partitioned in the same block are equivalent. We set the node-sampling probabilities as a function of the block index, i.e., nodes in the same block share the same node-sampling probabilities, with the number of parameters equal to the total number c of blocks.

Lemma V.13. *For SB, the time of computing 3-motif probabilities can be reduced from $O(|V|^3)$ to $O(c^3)$.*

Stochastic Kronecker (KR) model. With a seed matrix $\theta \in [0,1]^{2 \times 2}$ and $k_{KR} \in \mathbb{N}$, the KR model [12] outputs edge probabilities as the k_{KR}-th Kronecker power of θ (see Appendix A-F4 [1] for a formal definition). In practice, the fitting of KR typically uses `KronFit` [12], as proposed by the original authors of KR. In KR, each node $i \in [2^{k_{KR}}]$ is associated with a binary vector of length k_{KR}, and nodes with the same number of ones in their vectors are equivalent. We set node-sampling probabilities as a function of the number of ones in the binary vectors, with $k_{KR} + 1$ parameters, where $k_{KR} = O(\log|V|)$.

Lemma V.14. *For KR, the time of computing 3-motif probabilities can be reduced from $O(|V|^3)$ to $O(k_{KR}^7)$.*

Remark V.15. The equivalence in KR is weaker than that in the other three models. This is why the reduced time complexity in Lemma V.14 is $O(k_{KR}^7)$ instead of $O(k_{KR}^3)$. See Appendix A-F4 [1] for more details.

Note. See Appendix A-F [1] for more details, e.g., formal definitions of the models and more details of node equivalence.

VI. Experiments

In this section, we empirically evaluate EPGMs with our binding schemes and show the superiority of realization schemes beyond edge independency. Specifically, we show the following two points:

- **(P1)** When we use our tractability results to fit the parameters of EPGMs, we improve upon EIGMs and reproduce high triangle densities (high clustering), which is a common pattern in real-world graphs; this also validates the correctness of our tractability results and algorithms.
- **(P2)** We can reproduce other common patterns, e.g., power-law degrees and small diameters, especially when the corresponding EIGMs can do so; this shows that improving EIGMs w.r.t. clustering by binding does not harm the generation quality w.r.t. other common patterns.

A. Experimental settings

Datasets. We use six real-world datasets: (1) social networks *hamsterster (Hams)* and *facebook (Fcbk)*, (2) web graphs *polblogs (Polb)* and *spam (Spam)*, and (3) biological graphs *CE-PG (Cepg)* and *SC-HT (Scht)*. See Table I for the basic statistics of the datasets. We also upscale *Hams* by duplicating the original graph for scalability analysis (see Section VI-D).
Models. We consider the four edge-probability models analyzed in Section V-D: the Erdős-Rényi (ER) model, the Chung-Lu

TABLE I: The basic statistics of the datasets, where $\triangle$ represents the number of triangles, GCC represents global clustering coefficient, and ALCC represents average local clustering coefficient (see Section II). The upscaled versions of *Hams* are obtained by duplicating the original graph, which are used for scalability analysis (see Section VI-D).

dataset	$|V|$	$|E|$	$\triangle$	GCC	ALCC
Hams	2,000	16,097	157,953	0.229	0.540
Fcbk	4,039	88,234	4,836,030	0.519	0.606
Polb	1,222	16,717	303,129	0.226	0.320
Spam	4,767	37,375	387,051	0.145	0.286
Cepg	1,692	47,309	2,353,812	0.321	0.447
Scht	2,077	63,023	4,192,980	0.377	0.350
(Upscaled versions of Hams used for scalability analysis)					
Synthetic	4,000 - 64,000,000	32,194 - 515,104,000	315,906 - 5,054,496,000	0.229	0.540

(CL) model, the stochastic block (SB) model, and the stochastic Kronecker (KR) model. Given an input graph, we fit each model to the graph and obtain the output edge probabilities (see Section V-D and Appendix A-F [1] for more details).
Realization methods. We compare edge-probability graph models with three different realization methods: EIGMs (EdgeInd) assuming edge dependency, and EPGMs with the two proposed binding schemes: local binding (LoclBdg) and parallel binding (ParaBdg).
Fitting. As in Section V-D, by default, we use the edge probabilities p provided by the models, and we only fit the node-sampling probabilities g. Since our main focus is to improve clustering (see our motivation for binding at the start of Section V), in our main experiments, we use the number of triangles, an important indicator of clustering [37], [38], as the objective of the fitting algorithms. We use gradient descent to optimize parameters. In the main experiments, the edge probabilities are fixed as those output by the edge-probability models, while we also consider joint optimization of edge probabilities and node-sampling probabilities (see Section VI-E). Instead of fitting specific graphs, it is also possible to use EPGMs with binding to generate graphs "from scratch" with different levels of clustering by directly setting the parameters (see Appendix D-G [1]).
Hardware and software. All the experiments of fitting are run on a machine with two Intel Xeon® Silver 4210R (10 cores, 20 threads) processors, a 512GB RAM, and RTX A6000 (48GB) GPUs. A single GPU is used for each fitting process. The code for fitting is written in Python, using Pytorch [39]. All the experiments of graph generation are run on a machine with one Intel i9-10900K (10 cores, 20 threads) processor, a 64GB RAM. The code for generation is written in C++, compiled with G++ with O2 optimization and OpenMP [40] parallelization. See Appendix D-A [1] for the detailed experimental settings.

B. P1: EPGMs reproduce high clustering (Table II)

EPGMs with binding reproduce high clustering in real-world graphs. In Table II, for each dataset and each model, we compare three clustering-related metrics, the number of triangles ($\triangle$), the global clustering coefficient (GCC), and the average local clustering coefficient (ALCC), in the ground-truth (GroundT) graph and the graphs generated with each realization method. For each dataset and each model, we

TABLE II: The clustering metrics of generated graphs. The number of triangles (△) is normalized. For each dataset and each model, the best result is in bold and the second best is underlined. AR represents average ranking. The statistics are averaged over 100 random trials. See Table VIII in Appendix D-B [1] for the full results with standard deviations. **Our binding schemes (LoclBdg and ParaBdg) are consistently and clearly beneficial for improving clustering, and generating graphs with close-to-ground-truth clustering metrics.**

| dataset		*Hams*			*Fcbk*			*Polb*			*Spam*			*Cepg*			*Scht*			AR over dataset		
metric		△	GCC	ALCC	△	GCC	ALCC	△	GCC	ALCC	△	GCC	ALCC	△	GCC	ALCC	△	GCC	ALCC	△	GCC	ALCC
model	GroundT	1.00	0.23	0.54	1.00	0.52	0.61	1.00	0.23	0.32	1.00	0.14	0.29	1.00	0.32	0.45	1.00	0.38	0.35	N/A	N/A	N/A
ER	EdgeInd	0.01	0.01	0.01	0.01	0.01	0.01	0.03	0.02	0.02	0.01	**0.00**	0.00	0.04	0.03	0.03	0.03	0.03	0.03	3.0	2.7	2.5
	LoclBdg	**1.00**	**0.32**	0.24	1.01	0.45	0.22	0.95	**0.34**	**0.25**	0.99	0.34	**0.23**	**1.02**	**0.40**	**0.26**	1.01	**0.42**	0.25	1.7	1.3	1.3
	ParaBdg	0.99	0.39	**0.64**	**1.00**	**0.57**	**0.81**	**1.02**	0.41	0.66	**0.99**	0.40	0.66	0.97	0.51	0.75	**0.99**	0.56	0.79	1.3	2.0	2.2
CL	EdgeInd	0.30	0.07	0.06	0.12	0.06	0.06	0.79	0.18	0.17	0.50	0.07	0.06	0.68	0.23	0.22	0.64	0.24	**0.23**	3.0	3.0	2.5
	LoclBdg	0.99	0.17	0.26	**1.03**	0.26	0.30	**1.00**	0.21	**0.34**	1.03	0.12	0.26	**1.00**	0.29	0.43	1.04	**0.32**	0.47	1.7	1.8	1.5
	ParaBdg	**1.00**	**0.18**	**0.47**	1.01	**0.34**	**0.63**	1.01	**0.22**	0.47	**1.01**	**0.13**	0.44	**1.00**	**0.31**	0.58	**1.14**	0.29	0.61	1.3	1.2	2.0
SB	EdgeInd	0.26	0.08	0.04	0.15	0.14	0.08	0.48	0.14	0.16	0.53	0.09	0.04	0.66	0.26	0.20	0.64	0.27	0.13	3.0	3.0	3.0
	LoclBdg	1.04	**0.22**	0.24	0.93	0.43	0.33	**0.99**	**0.24**	**0.35**	0.98	**0.15**	0.22	0.99	**0.32**	**0.41**	1.03	**0.35**	**0.39**	1.7	1.2	1.3
	ParaBdg	**0.99**	0.24	**0.52**	**1.03**	**0.53**	**0.56**	1.01	0.18	0.25	**0.99**	0.16	**0.36**	1.05	0.33	0.36	**0.97**	0.34	0.44	1.3	1.8	1.7
KR	EdgeInd	0.18	0.04	0.06	0.05	0.04	0.04	0.10	0.04	0.07	0.06	0.01	0.03	0.13	0.07	0.12	0.03	0.03	0.05	3.0	3.0	3.0
	LoclBdg	1.09	0.15	0.23	0.93	0.24	0.27	**1.06**	0.14	**0.23**	0.94	0.12	0.19	0.99	0.17	0.31	**1.44**	0.18	**0.28**	2.0	2.0	1.7
	ParaBdg	**1.00**	**0.17**	**0.39**	**0.97**	**0.35**	**0.60**	0.94	**0.22**	0.42	**1.05**	**0.16**	**0.38**	**1.00**	**0.28**	**0.46**	1.07	**0.35**	0.58	1.0	1.0	1.3
AR over models	EdgeInd	3.0	3.0	3.0	3.0	3.0	3.0	3.0	3.0	2.5	3.0	2.5	2.8	3.0	3.0	3.0	3.0	3.0	2.3	3.0	2.9	2.8
	LoclBdg	1.8	**1.5**	2.0	2.0	2.0	2.0	1.5	1.5	**1.0**	2.0	**1.8**	1.3	1.5	**1.5**	1.3	1.8	**1.3**	1.3	1.8	1.6	1.5
	ParaBdg	**1.3**	**1.5**	**1.0**	**1.0**	**1.0**	**1.0**	**1.5**	**1.5**	2.5	**1.0**	**1.8**	2.0	**1.5**	**1.5**	**1.8**	**1.3**	1.8	2.5	**1.3**	1.5	1.8
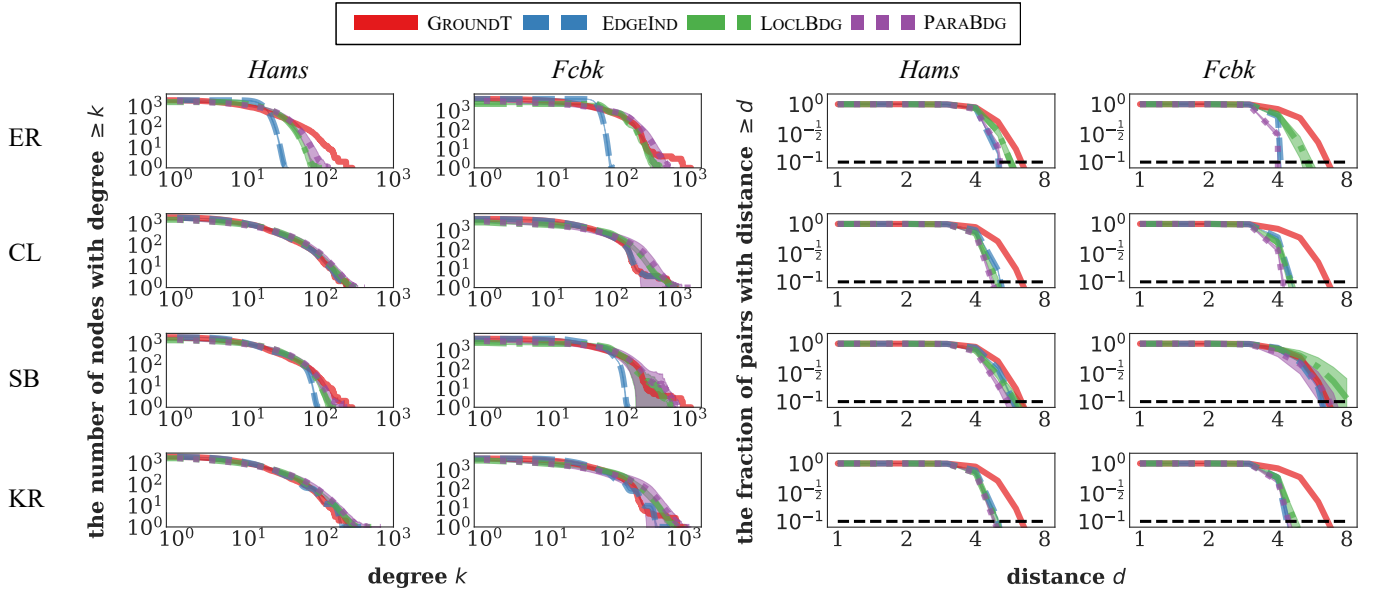
Fig. 1: The degree (left) and distance (right) distributions of generated graphs. Each shaded area represents one standard deviation. The plots are on a log-log scale. **Our binding schemes (LoclBdg and ParaBdg) do not negatively affect degree or distance distributions, and provide improvements sometimes (e.g., for the ER model).**

compute the ranking of each method according to the absolute error w.r.t. each metric. We also show the average rankings (ARs) over datasets and models. The statistics are averaged over 100 generated graphs. See Appendix D-B [1] for the full results with standard deviations.

EPGMs with both LoclBdg and ParaBdg almost perfectly reproduce the number of triangles in real-world graphs, while EIGMs (i.e., EdgeInd in Table II) often fail to generate graphs with enough triangles. GCC and ALCC are also significantly improved (upon EIGMs) in most cases, while ParaBdg has noticeably higher ALCC than LoclBdg. In some rare cases, ParaBdg generates graphs with exceedingly high GCC and/or ALCC and haves higher absolute errors compared to EIGMs.

C. P2: EPGMs reproduce other patterns (Figures 1 and 2)

EPGMs with binding (LoclBdg and ParaBdg) also reproduce other common patterns in real-world graphs. In Figure 1, for each dataset (each column) and each model (each row), we compare the degree distributions and distance distributions in the ground-truth graph and the graphs generated with each realization method. Specifically, for each realization method, we count the number of nodes with degree at least k for each $k \in \mathbb{N}$ and count the number of pairs in the largest connected component with distance at least d for each $d \in \mathbb{N}$ in each generated graph, and take the average number over 100 generated graphs. See Appendix D-C [1] for the full results.

EPGMs with binding generate graphs with common patterns: power-law degrees and small diameters (i.e., small distances).
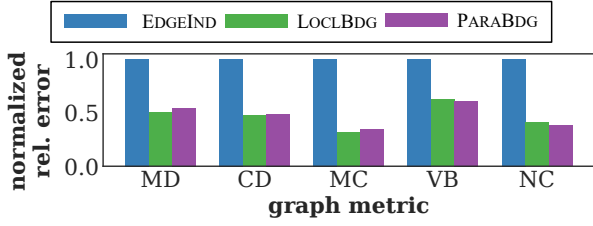
Fig. 2: The normalized relative error w.r.t. different graph metrics of generated graphs. For each graph metric: modularity (MD), conductance (CD), max core numbers (MC), vertex betweenness (VB), and natural connectivity (NC), the relative errors are computed and averaged over all datasets and all models, and normalized so that the relative error of EDGEIND is 1. See Appendix D-C [1] for the detailed results. **Our binding schemes (LOCLBDG and PARABDG) generate graphs that are closer to the ground truth w.r.t. various graph metrics, consistently improving upon EDGEIND.**

Both schemes (LOCLBDG and PARABDG) perform comparably well while LOCLBDG performs noticeably better with ER and PARABDG performs noticeably better with KR. Importantly, when the edge probabilities output power-law expected degrees (e.g., CL and KR), the degree distributions are well preserved with binding. Edge-independent ER cannot generate power-law degrees [41], and binding alleviates this problem. Also, it is known that oscillations exist in the degree distributions of graphs generated by edge-independent KR [14], [42], which is also alleviated by binding.

Other graph metrics. With binding, the generated graphs are also closer to the ground truth w.r.t. some other graph metrics: modularity, core numbers, conductance, vertex betweenness, and natural connectivity. See Figure 2 for a summary of the results, and see Appendix D-C [1] for the detailed results.

D. Graph generation speed and scalability (Tables III and IV)

In Table III, we compare the running time of graph generation (averaged over 100 random trials) using EDGEIND, LOCLBDG, PARABDG, and serialized PARABDG without parallelization (PARABDG-s) with the stochastic Kronecker (KR) model. For EDGEIND, we use `krongen` [43], which is an algorithm parallelized and optimized for KR.

TABLE III: The time (in seconds) for graph generation with different realization methods.

	Hams	*Fcbk*
EDGEIND	0.1	0.1
LOCLBDG	4.7	49.0
PARABDG	0.3	1.7
PARABDG-S	3.2	12.6

Among the competitors, EDGEIND is the fastest with the simplest algorithmic nature. Between the two binding schemes, PARABDG is noticeably faster than LOCLBDG, and is even faster with parallelization. Fitting the same number of triangles, PARABDG usually requires lower node-sampling probabilities and thus deals with fewer pairs in each round, and is thus faster even when serialized.

We also conduct scalability experiments by upscaling the *Hams* dataset (see Table I). As shown in Table IV, with 32GB RAM, all the proposed algorithms can run with 128,000 nodes. Notably, for PARABDG, an optimized implementation scales to up to 64 million nodes (over 512 million edges), by storing compact summaries (e.g., cliques and bi-cliques) instead of individual edges. See Appendix D-D [1] for more details.

TABLE IV: The time (in seconds) for graph generation when upscaling the *Hams* dataset by duplicating the graph. **With 32GB RAM, all the proposed algorithms can run with 128,000 nodes, and the scalable implementation of PARABDG can run with 64 million nodes (over 512 million edges).**

model	$|V|$	2k	4k	8k	16k	32k	64k	128k
ER	LOCLBDG	3.2	6.5	16.4	45.6	143.4	494.5	1859.2
	PARABDG	0.0	0.1	0.1	0.2	0.6	1.7	5.4
CL	LOCLBDG	4.0	9.6	35.4	123.9	472.3	2162.3	8402.2
	PARABDG	0.3	0.5	1.0	2.1	4.4	11.2	31.1
SB	LOCLBDG	4.0	9.5	29.6	99.2	362.9	1648.4	8398.1
	PARABDG	0.3	0.5	1.0	2.1	5.3	14.9	46.0
KR	LOCLBDG	8.6	31.2	124.5	506.9	2097.2	8681.0	33918.4
	PARABDG	0.4	1.2	4.3	20.3	113.5	705.6	4351.6

model	$|V|$	1m	2m	4m	8m	16m	32m	64m
ER		5.9	12.4	28.2	61.0	121.9	262.7	491.0
CL	PARABDG (scalable version)	102.2	220.2	423.8	815.9	1685.6	3135.2	6179.3
SB		106.0	213.7	429.0	869.0	1798.3	3829.6	8639.0
KR		105.1	219.4	439.1	875.4	1751.3	3504.7	7014.9

TABLE V: The clustering metrics of the graphs generated by three variants of parallel binding. The number of triangles ($\triangle$) is normalized. For each dataset and each model, the best result is in bold, and the second best is underlined. **Using joint optimization further enhances the power of our binding scheme PARABDG to fit graph statistics and reproduce graph patterns.**

dataset		*Hams*			*Fcbk*	
metric	$\triangle$	GCC	ALCC	$\triangle$	GCC	ALCC
GROUNDT	1.000	0.229	0.540	1.000	0.519	0.606
PARABDG	0.997	0.165	0.394	0.971	0.347	**0.605**
PARABDG-W	0.964	0.176	0.260	1.021	0.408	0.458
PARABDG-JW	**0.999**	**0.230**	**0.448**	1.018	0.521	0.644

E. Joint optimization (Table V)

In addition to optimizing node-sampling probabilities for given edge probabilities, we can also jointly optimize both kinds of probabilities. In Table V, we compare the ground-truth clustering and that generated by EPGMs using three variants of parallel binding: (1) PARABDG with the number of triangles as the objective (the one used in Table II), (2) PARABDG-W with the numbers of triangles and wedges as the objective (given edge probabilities), (3) PARABDG-JW jointly optimizing both kinds of probabilities, with the numbers of triangles and wedges as the objective.

On both *Hams* and *Fcbk*, PARABDG and PARABDG-W can well fit the number of triangles but have noticeable errors w.r.t. the number of wedges (and thus GCC), while PARABDG-JW with joint optimization accurately fits both triangles and wedges. On the other datasets, the three variants perform similarly well because PARABDG already preserves both triangles and wedges well, and there is not much room for improvement. Notably, with joint optimization, the degree and distance distributions are still well preserved (see Appendix D-E [1]).

F. Comparison with advanced RGMs (Table VI)

We test other edge-dependent RGMs: preferential attachment (PA) model [21]) and random geometric graphs (RGG) model [23]), and advanced EIGMs: block two-level Erdős-Rényi (BTER) model [20] and Lancichinetti-Fortunato-
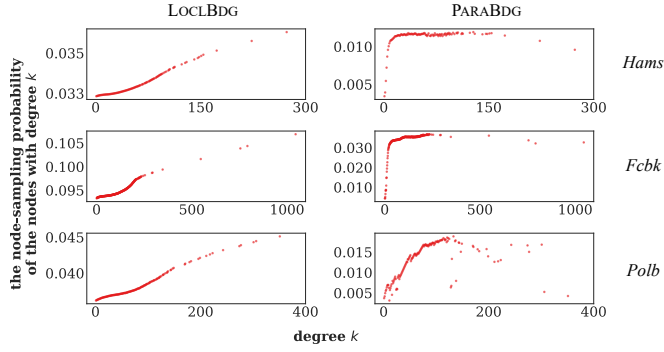
Fig. 3: The relations between node degrees and node-sampling probabilities. See Appendix D-A [1] for the full results.

Radicchi (LFR) model [44]. In Table VI, we report clustering-related metrics and overlap (low overlap indicates high output variability; see Section III-A) of the graphs generated by each model for *Hams* and *Fcbk* datasets. See Appendix D-F [1] for full results on other datasets.

We fit PA and RGG to the numbers of nodes and edges of each input graph. As discussed in Section III-B, closed-form tractability results on subgraph densities are not unavailable for PA and RGG. PA fails to generate graphs with high clustering. For RGG, sometimes enough triangles are generated with small d values, but the GCC and ALCC are too high in such cases. We also tried exchangeable network models and exponential random graphs, which failed to generate comparable results. See Appendix D-B [1] for more details.

BTER essentially uses a mixture of multiple Chung-Lu models to generate high clustering, and LFR imposes community structures on top of Chung-Lu. We empirically validate that, compared to EIGMs, EPGMs with binding (we report the results based on Chung-Lu; one may achieve even better performance with binding based on other edge-probability models, as shown in Table II) achieve comparable or better performance in generating high-clustering graphs, with much higher output variability (i.e., low overlap), which is important and desirable for RGMs (see Section III).

In Appendix D-F [1], we also evaluate three deep graph generative models: CELL [45], GraphVAE [46], and GraphRNN [47]. All of them failed to generate comparable results: CELL and GraphVAE produce highly overlapping graphs (i.e., low output variability), while GraphRNN generates graphs with many more edges but much lower clustering than the ground truth.

G. Extra experimental results

See Figure 3 for analyses on node-sampling probabilities assigned by our fitting algorithms. We observe that our fitting algorithms assign different node-sampling probabilities to different nodes, implying that different nodes have different levels of importance in binding. Full results are in Appendix D [1]. See Appendix B [1] for the theoretical analyses and experimental results on fitting the number of (non-)isolated nodes, which further shows the tractability of our binding schemes.

TABLE VI: The clustering metrics and overlap (lower the better) of the graphs generated by binding and other models. For each dataset and each model, the best result is in bold, and the second best is underlined. **Overall, binding achieves promising performance in generating high-clustering graphs, with high variability.**

dataset	*Hams*				*Fcbk*			
metric	$\triangle$	GCC	ALCC	overlap	$\triangle$	GCC	ALCC	overlap
GROUNDT	1.000	0.229	0.540	N/A	1.000	0.519	0.606	N/A
LOCLBDG-CL	<u>0.992</u>	0.165	0.255	5.8%	<u>1.026</u>	0.255	0.305	6.3%
PARABDG-CL	**1.000**	**0.185**	0.471	5.9%	**1.006**	0.336	0.626	6.2%
PA	0.198	0.049	0.049	4.7%	0.120	0.061	0.061	6.2%
RGG ($d = 1$)	1.252	0.751	0.751	**0.8%**	0.607	0.751	0.752	**1.1%**
RGG ($d = 2$)	1.011	0.595	0.604	0.8%	0.492	0.596	<u>0.607</u>	1.1%
RGG ($d = 3$)	0.856	0.491	<u>0.513</u>	0.8%	0.421	<u>0.494</u>	0.518	1.1%
BTER	0.991	<u>0.290</u>	**0.558**	53.8%	0.880	**0.525**	**0.605**	68.0%
LFR ($\mu = 0.0$)	1.140	0.262	0.546	43.5%	N/A	N/A	N/A	N/A
LFR ($\mu = 0.5$)	0.296	0.068	0.081	13.4%	0.161	0.084	0.120	17.0%
LFR ($\mu = 1.0$)	0.197	0.045	0.047	7.0%	0.105	0.055	0.059	6.7%

VII. CONCLUSION AND DISCUSSIONS

We show that realization beyond edge independence can better reproduce common patterns while ensuring high tractability and variability. We formally define EPGMs and show their basic properties (Section IV). We propose a pattern-reproducing, tractable, and flexible realization framework called *binding* (Algorithm 1) with two practical variants: local binding (Algorithm 2) and parallel binding (Algorithm 3). We derive tractability results (Theorem V.6) on the closed-form subgraph densities, and propose efficient parameter fitting (Section V-D; Lemmas V.11-V.14). We conduct extensive experiments to show the empirical power of EPGMs with binding (Section VI).

Limitations and future directions. EPGMs with binding generate more isolated nodes than EIGMs due to higher variance. Fortunately, we can address the limitation by fitting and controlling the number of isolated nodes with the tractability results, as mentioned in Remark V.10.

The performance of EPGMs depends on both the underlying edge probabilities and the way to realize (i.e., sample from) them. In this work, we focus on the latter, while finding valuable edge probabilities is an independent problem. Notably, as shown in Section VI-E, it is possible to jointly optimize both edge probabilities and their realization.

Binding only covers a subset of EPGMs, and we will explore the other types of EPGMs (e.g., EPGMs with lower subgraph densities). Combining binding with other mechanisms in existing edge-dependent RGMs to create even stronger RGMs, and developing practical algorithms for higher-order motifs, are some interesting future directions.

REFERENCES

[1] F. Bu, R. Yang, P. Bogdan, and K. Shin, "Edge probability graph models beyond edge independency: Appendix, code, and datasets," https://github.com/bokveizen/edge-probability-graph-model, 2025.

[2] M. Drobyshevskiy and D. Turdakov, "Random graph modeling: A survey of the concepts," *ACM Computing Surveys*, vol. 52, no. 6, pp. 1–36, 2019.

[3] R. C. Murphy, K. B. Wheeler, B. W. Barrett, and J. A. Ang, "Introducing the graph 500," *Cray Users Group*, vol. 19, pp. 45–74, 2010.

[4] D. Ghoshdastidar, M. Gutzeit, A. Carpentier, and U. von Luxburg, "Two-sample tests for large random graphs using network statistics," in *COLT*, 2017.

[5] L. Backstrom, C. Dwork, and J. Kleinberg, "Wherefore art thou r3579x? anonymized social networks, hidden patterns, and structural steganography," in *TheWebConf (WWW)*, 2007.

[6] M. E. Newman, "Properties of highly clustered networks," *Physical Review E*, vol. 68, no. 2, p. 026121, 2003.

[7] J. J. Pfeiffer, T. La Fond, S. Moreno, and J. Neville, "Fast generation of large scale social networks while incorporating transitive closures," in *PASSAT-SocialCom*, 2012.

[8] D. Chakrabarti and C. Faloutsos, "Graph mining: Laws, generators, and algorithms," *ACM Computing Surveys*, vol. 38, no. 1, pp. 2–es, 2006.

[9] P. Erdős and A. Rényi, "On random graphs i," *Publicationes Mathematicae Debrecen*, vol. 6, pp. 290–297, 1959.

[10] F. Chung and L. Lu, "Connected components in random graphs with given expected degree sequences," *Annals of Combinatorics*, vol. 6, no. 2, pp. 125–145, 2002.

[11] P. W. Holland, K. B. Laskey, and S. Leinhardt, "Stochastic blockmodels: First steps," *Social Networks*, vol. 5, no. 2, pp. 109–137, 1983.

[12] J. Leskovec, D. Chakrabarti, J. Kleinberg, C. Faloutsos, and Z. Ghahramani, "Kronecker graphs: An approach to modeling networks," *Journal of Machine Learning Research*, vol. 11, no. 2, 2010.

[13] S. Moreno, J. Neville, and S. Kirshner, "Tied kronecker product graph models to capture variance in network populations," *ACM Transactions on Knowledge Discovery from Data*, vol. 12, no. 3, pp. 1–40, 2018.

[14] C. Seshadri, A. Pinar, and T. G. Kolda, "An in-depth analysis of stochastic kronecker graphs," *Journal of the ACM*, vol. 60, no. 2, pp. 1–32, 2013.

[15] S. Chanpuriya, C. Musco, K. Sotiropoulos, and C. Tsourakakis, "On the power of edge independent graph models," in *NeurIPS*, 2021.

[16] O. Klopp, A. B. Tsybakov, and N. Verzelen, "Oracle inequalities for network models and sparse graphon estimation," *Annals of Statistics*, vol. 45, no. 1, pp. 316–354, 2017.

[17] N. De Cao and T. Kipf, "MolGAN: An implicit generative model for small molecular graphs," *arXiv:1805.11973*, 2018.

[18] S. Chanpuriya, C. Musco, K. Sotiropoulos, and C. Tsourakakis, "On the role of edge dependency in graph generative models," in *ICML*, 2024.

[19] S. Mussmann, J. Moore, J. Pfeiffer, and J. Neville, "Incorporating assortativity and degree dependence into scalable network models," in *AAAI*, 2015.

[20] T. G. Kolda, A. Pinar, T. Plantenga, and C. Seshadri, "A scalable generative graph model with community structure," *SIAM Journal on Scientific Computing*, vol. 36, no. 5, pp. C424–C452, 2014.

[21] A.-L. Barabási and R. Albert, "Emergence of scaling in random networks," *Science*, vol. 286, no. 5439, pp. 509–512, 1999.

[22] D. J. Watts and S. H. Strogatz, "Collective dynamics of small-world networks," *Nature*, vol. 393, no. 6684, pp. 440–442, 1998.

[23] M. Penrose, *Random geometric graphs*. OUP Oxford, 2003, vol. 5.

[24] D. Lusher, J. Koskinen, and G. Robins, *Exponential random graph models for social networks: Theory, methods, and applications*. Cambridge University Press, 2013.

[25] H. Crane and W. Dempsey, "Edge exchangeable models for interaction networks," *Journal of the American Statistical Association*, vol. 113, no. 523, pp. 1311–1326, 2018.

[26] W. Wu, S. Olhede, and P. Wolfe, "Tractably modelling dependence in networks beyond exchangeability," *Bernoulli*, vol. 31, no. 1, pp. 584–608, 2025.

[27] L. Ostroumova Prokhorenkova, "General results on preferential attachment and clustering coefficient," *Optimization Letters*, vol. 11, pp. 279–298, 2017.

[28] L. Gu, H. L. Huang, and X. D. Zhang, "The clustering coefficient and the diameter of small-world networks," *Acta Mathematica Sinica, English Series*, vol. 29, no. 1, pp. 199–208, 2013.

[29] U. Bhat, P. Krapivsky, R. Lambiotte, and S. Redner, "Densification and structural transitions in networks that grow by node copying," *Physical Review E*, vol. 94, no. 6, p. 062302, 2016.

[30] H. Thorisson, "Coupling methods in probability theory," *Scandinavian Journal of Statistics*, pp. 159–182, 1995.

[31] D. Felmlee and R. Faris, "Interaction in social networks," in *Handbook of social psychology*. Springer, 2013, pp. 439–464.

[32] M. A. Naoumkina, L. V. Modolo, D. V. Huhman, E. Urbanczyk-Wochniak, Y. Tang, L. W. Sumner, and R. A. Dixon, "Genomic and coexpression analyses predict multiple genes involved in triterpene saponin biosynthesis in medicago truncatula," *The Plant Cell*, vol. 22, no. 3, pp. 850–866, 2010.

[33] Y. Dourisboure, F. Geraci, and M. Pellegrini, "Extraction and classification of dense implicit communities in the web graph," *ACM Transactions on the Web*, vol. 3, no. 2, pp. 1–36, 2009.

[34] R. Mishra, S. Shukla, D. Arora, and M. Kumar, "An effective comparison of graph clustering algorithms via random graphs," *International Journal of Computer Applications*, vol. 22, no. 1, pp. 22–27, 2011.

[35] S. Wandelt, X. Sun, E. Menasalvas, A. Rodríguez-González, and M. Zanin, "On the use of random graphs as null model of large connected networks," *Chaos, Solitons & Fractals*, vol. 119, pp. 318–325, 2019.

[36] J. Casas-Roma, J. Herrera-Joancomartí, and V. Torra, "A survey of graph-modification techniques for privacy-preserving on networks," *Artificial Intelligence Review*, vol. 47, pp. 341–366, 2017.

[37] C. E. Tsourakakis, U. Kang, G. L. Miller, and C. Faloutsos, "Doulion: counting triangles in massive graphs with a coin," in *KDD*, 2009.

[38] T. G. Kolda, A. Pinar, T. Plantenga, C. Seshadri, and C. Task, "Counting triangles in massive graphs with mapreduce," *SIAM Journal on Scientific Computing*, vol. 36, no. 5, pp. S48–S77, 2014.

[39] A. Paszke, S. Gross, F. Massa, A. Lerer, J. Bradbury, G. Chanan, T. Killeen, Z. Lin, N. Gimelshein, L. Antiga *et al.*, "PyTorch: An imperative style, high-performance deep learning library," in *NeurIPS*, 2019.

[40] L. Dagum and R. Menon, "OpenMP: An industry standard api for shared-memory programming," *IEEE Computational Science and Engineering*, vol. 5, no. 1, pp. 46–55, 1998.

[41] B. Bollobás and O. M. Riordan, "Mathematical results on scale-free random graphs," *Handbook of Graphs and Networks: From the Genome to the Internet*, pp. 1–34, 2003.

[42] A. Pinar, C. Seshadri, and T. G. Kolda, "The similarity between stochastic kronecker and chung-lu graph models," in *SCM*, 2012.

[43] J. Leskovec and R. Sosič, "SNAP: A general-purpose network analysis and graph-mining library," *ACM Transactions on Intelligent Systems and Technology*, vol. 8, no. 1, pp. 1–20, 2016.

[44] A. Lancichinetti, S. Fortunato, and F. Radicchi, "Benchmark graphs for testing community detection algorithms," *Physical Review E*, vol. 78, no. 4, p. 046110, 2008.

[45] L. Rendsburg, H. Heidrich, and U. Von Luxburg, "NetGAN without GAN: From random walks to low-rank approximations," in *ICML*, 2020.

[46] M. Simonovsky and N. Komodakis, "GraphVAE: Towards generation of small graphs using variational autoencoders," in *ICANN*, 2018.

[47] J. You, R. Ying, X. Ren, W. Hamilton, and J. Leskovec, "GraphRNN: Generating realistic graphs with deep auto-regressive models," in *ICML*, 2018.

[48] G. Seroussi and F. Ma, "On the arithmetic complexity of matrix Kronecker powers," *Information Processing Letters*, vol. 17, no. 3, pp. 145–148, 1983.

[49] C. Brissette and G. M. Slota, "Limitations of Chung Lu random graph generation," in *International Workshop on Complex Networks and Their Applications*, 2021.

[50] C. Brissette, D. Liu, and G. M. Slota, "Correcting output degree sequences in Chung-Lu random graph generation," in *COMPLEX NETWORKS*, 2022.

[51] M. Mahdian and Y. Xu, "Stochastic kronecker graphs," in *WAW*, 2007.

[52] R. Milo, S. Shen-Orr, S. Itzkovitz, N. Kashtan, D. Chklovskii, and U. Alon, "Network motifs: Simple building blocks of complex networks," *Science*, vol. 298, no. 5594, pp. 824–827, 2002.

[53] F. Bu, S. Kang, and K. Shin, "Interplay between topology and edge weights in real-world graphs: Concepts, patterns, and an algorithm," *Data Mining and Knowledge Discovery*, vol. 37, pp. 2139 – 2191, 2023.

[54] J. D. Eblen, C. A. Phillips, G. L. Rogers, and M. A. Langston, "The maximum clique enumeration problem: Algorithms, applications, and implementations," in *BMC bioinformatics*, vol. 13, 2012, pp. 1–11.

[55] S. M. Xie and S. Ermon, "Reparameterizable subset sampling via continuous relaxations," in *IJCAI*, 2019.

[56] A. Pervez, P. Lippe, and E. Gavves, "Scalable subset sampling with neural conditional poisson networks," in *ICLR*, 2023.

[57] K. Ahmed, Z. Zeng, M. Niepert, and G. V. d. Broeck, "SIMPLE: A gradient estimator for k-subset sampling," in *ICLR*, 2023.

[58] T. M. Sutter, A. Ryser, J. Liebeskind, and J. E. Vogt, "Differentiable random partition models," *arXiv 2305.16841*, 2023.

[59] V. Levorato, "Group measures and modeling for social networks," *Journal of Complex Systems*, vol. 2014, 2014.

[60] S. Purushotham and C. C. Jay Kuo, "Modeling group dynamics for personalized group-event recommendation," in *SBP*, 2015.

[61] H. Jang, S. P. Choe, S. N. Gunkel, S. Kang, and J. Song, "A system to analyze group socializing behaviors in social parties," *IEEE Transactions on Human-Machine Systems*, vol. 47, no. 6, pp. 801–813, 2016.

[62] A. Li, L. Zhou, Q. Su, S. P. Cornelius, Y.-Y. Liu, L. Wang, and S. A. Levin, "Evolution of cooperation on temporal networks," *Nature Communications*, vol. 11, no. 1, p. 2259, 2020.

[63] I. Iacopini, G. Petri, A. Baronchelli, and A. Barrat, "Group interactions modulate critical mass dynamics in social convention," *Communications Physics*, vol. 5, no. 1, p. 64, 2022.

[64] R. Plomin, "The role of inheritance in behavior," *Science*, vol. 248, no. 4952, pp. 183–188, 1990.

[65] D. Anastassiou, "Computational analysis of the synergy among multiple interacting genes," *Molecular Systems Biology*, vol. 3, no. 1, p. 83, 2007.

[66] I. I. Gottesman and D. R. Hanson, "Human development: Biological and genetic processes," *Annual Review of Psychology*, vol. 56, pp. 263–286, 2005.

[67] Y. Pritykin, D. Ghersi, and M. Singh, "Genome-wide detection and analysis of multifunctional genes," *PLoS Computational Biology*, vol. 11, no. 10, p. e1004467, 2015.

[68] J. D. Storey, J. Madeoy, J. L. Strout, M. Wurfel, J. Ronald, and J. M. Akey, "Gene-expression variation within and among human populations," *The American Journal of Human Genetics*, vol. 80, no. 3, pp. 502–509, 2007.

[69] G. Lee, M. Choe, and K. Shin, "How do hyperedges overlap in real-world hypergraphs? patterns, measures, and generators," in *TheWebConf (WWW)*, 2021.

[70] T. LaRock and R. Lambiotte, "Encapsulation structure and dynamics in hypergraphs," *Journal of Physics: Complexity*, vol. 4, no. 4, p. 045007, 2023.

[71] R. A. Rossi and N. K. Ahmed, "The network data repository with interactive graph analytics and visualization," in *AAAI*, 2015.

[72] J. Leskovec and A. Krevl, "SNAP Datasets: Stanford large network dataset collection," http://snap.stanford.edu/data, Jun. 2014.

[73] Hamsterster, "Hamsterster social network," http://www.hamsterster.com.

[74] J. Leskovec and J. Mcauley, "Learning to discover social circles in ego networks," in *NeurIPS*, 2012.

[75] L. A. Adamic and N. Glance, "The political blogosphere and the 2004 US election: Divided they blog," in *LinkKDD workshop*, 2005.

[76] C. Castillo, K. Chellapilla, and L. Denoyer, "Web spam challenge 2008," in *AIRWeb workshop*, 2008.

[77] A. Cho, J. Shin, S. Hwang, C. Kim, H. Shim, H. Kim, H. Kim, and I. Lee, "WormNet v3: A network-assisted hypothesis-generating server for caenorhabditis elegans," *Nucleic Acids Research*, vol. 42, no. W1, pp. W76–W82, 2014.

[78] J. Chung, B. D. Pedigo, E. W. Bridgeford, B. K. Varjavand, H. S. Helm, and J. T. Vogelstein, "GraSPy: Graph statistics in Python," *Journal of Machine Learning Research*, vol. 20, pp. 1–7, 2019.

[79] U. Von Luxburg, "A tutorial on spectral clustering," *Statistics and Computing*, vol. 17, pp. 395–416, 2007.

[80] D. L. Sussman, M. Tang, D. E. Fishkind, and C. E. Priebe, "A consistent adjacency spectral embedding for stochastic blockmodel graphs," *Journal of the American Statistical Association*, vol. 107, no. 499, pp. 1119–1128, 2012.

[81] K. Rohe, S. Chatterjee, and B. Yu, "Spectral clustering and the high-dimensional stochastic blockmodel," *The Annals of Statistics*, pp. 1878–1915, 2011.

[82] D. A. Reynolds *et al.*, "Gaussian mixture models," *Encyclopedia of Biometrics*, vol. 741, no. 659-663, 2009.

[83] D. P. Kingma and J. Ba, "Adam: A method for stochastic optimization," in *ICLR*, 2015.

[84] F. I. Stamm, M. Scholkemper, M. Strohmaier, and M. T. Schaub, "Neighborhood structure configuration models," in *WWW*, 2023.

[85] S. Chan and E. Airoldi, "A consistent histogram estimator for exchange-able graph models," in *ICML*, 2014.

[86] T. A. Snijders, P. E. Pattison, G. L. Robins, and M. S. Handcock, "New specifications for exponential random graph models," *Sociological Methodology*, vol. 36, no. 1, pp. 99–153, 2006.

[87] G. Robins, "Exponential random graph models for social networks," *The Sage Handbook of Social Network Analysis*, pp. 484–500, 2011.

[88] G. G. V. Yon, A. Slaughter, and K. de la Haye, "Exponential random graph models for little networks," *Social Networks*, vol. 64, pp. 225–238, 2021.

[89] W. An, "Fitting ERGMs on big networks," *Social Science Research*, vol. 59, pp. 107–119, 2016.

[90] M. E. Newman, "Modularity and community structure in networks," *Proceedings of the National Academy of Sciences*, vol. 103, no. 23, pp. 8577–8582, 2006.

[91] D. Gleich, "Hierarchical directed spectral graph partitioning," *Information Networks*, vol. 443, 2006.

[92] S. B. Seidman, "Network structure and minimum degree," *Social Networks*, vol. 5, no. 3, pp. 269–287, 1983.

[93] L. Freeman, "A set of measures of centrality based on betweenness," *Sociometry*, vol. 40, no. 1, pp. 35–41, 1977.

[94] U. Brandes, "On variants of shortest-path betweenness centrality and their generic computation," *Social Networks*, vol. 30, no. 2, pp. 136–145, 2008.

[95] H. Chan, L. Akoglu, and H. Tong, "Make it or break it: Manipulating robustness in large networks," in *SDM*, 2014.

[96] V. D. Blondel, J.-L. Guillaume, R. Lambiotte, and E. Lefebvre, "Fast unfolding of communities in large networks," *Journal of Statistical Mechanics: Theory and Experiment*, vol. 2008, no. 10, p. P10008, 2008.

[97] B. W. Kernighan and S. Lin, "An efficient heuristic procedure for partitioning graphs," *The Bell System Technical Journal*, vol. 49, no. 2, pp. 291–307, 1970.

[98] J. G. Siek, L.-Q. Lee, and A. Lumsdaine, *The Boost Graph Library: User guide and reference manual*. Pearson Education, 2001.

[99] C. L. Staudt, A. Sazonovs, and H. Meyerhenke, "NetworKit: A tool suite for large-scale complex network analysis," *Network Science*, vol. 4, no. 4, pp. 508–530, 2016.

[100] G. Melancon, "Just how dense are dense graphs in the real world? a methodological note," in *BELIV*, 2006.

[101] S. Fortunato, "Community detection in graphs," *Physics Reports*, vol. 486, no. 3-5, pp. 75–174, 2010.

Edge Probability Graph Models Beyond Edge Independency: Appendix

CONTENTS

APPENDIX A
PROOFS

In this section, we show the proofs of our theoretical results.

A. EPGMs

Proposition A.1 (EIGMs are special EPGMs). *For any p, the EIGM w.r.t. p is an EPGM w.r.t. p, i.e., $f_p^{EI} \in \mathcal{F}(p)$.*

Proof. By the definition of EIGMs,

$$
\begin{aligned}
&\Pr\nolimits_{f_p^{EI}}[(u,v)] \\
&= \sum_{G \in \mathcal{G}(V)} f_p^{EI}(G)\mathbf{1}[(u,v) \in G] \\
&= \sum_{(u,v) \in G \in \mathcal{G}(V)} f_p^{EI}(G) \\
&= \sum_{(u,v) \in G \in \mathcal{G}(V)} p(u,v) \prod_{(u,v) \neq (u^+,v^+) \in G} p(u^+, v^+) \prod_{(u^-,v^-) \notin G} (1 - p(u^-, v^-)) \\
&= p(u,v), \forall u,v,
\end{aligned}
$$

completing the proof. $\qquad\square$

Proposition IV.2 (EPGMs are general). *For any $f: \mathcal{G}(V) \to [0,1]$, there exists $p: \binom{V}{2} \to [0,1]$ such that $f \in \mathcal{F}(p)$.*

Proof. Let $p: \binom{V}{2} \to [0,1]$ be that $p(u,v) = \Pr_f[(u,v)], \forall u, v \in V$, then by Definition IV.1, $f \in \mathcal{F}(p)$. $\qquad\square$

Proposition A.2 (Upper bound of edge-group probabilities). *For any $p: \binom{V}{2} \to [0,1]$ and any edge group $P \subseteq \binom{V}{2}$, $\Pr_f[P \subseteq E(G)] \leq \min_{(u,v) \in P} p(u,v), \forall f \in \mathcal{F}(p)$.*

Proof. By definition, $\Pr_f[(u,v)] = p(u,v), \forall (u,v)$. Hence,

$$
\begin{aligned}
\Pr\nolimits_f[P \subseteq E(G)] &= \Pr\nolimits_f[\bigwedge_{(u,v) \in P} (u,v) \in G] \\
&\leq \min_{(u,v) \in P} \Pr\nolimits_f[(u,v)] \\
&= \min_{(u,v) \in P} p(u,v),
\end{aligned}
$$

where we have used the fact that $\bigwedge_{(u,v) \in P}(u,v) \in G$ is a subevent of $(u,v) \in G$ for any $(u,v) \in P$. $\qquad\square$

Proposition IV.3 (EPGMs have constant expected degrees and overlap). *For any $p: \binom{V}{2} \to [0,1]$, the expected degree of each node and the overlap of all the EPGMs w.r.t. p are constant. Specifically, $\mathbb{E}_f[d(v;G)] = \sum_{u \in V} p(u,v)$ and $\mathrm{Ov}(f) = \frac{\sum_{u,v \in V} p^2(u,v)}{\sum_{u,v \in V} p(u,v)}, \forall f \in \mathcal{F}(p)$.*

Proof. By linearity of expectation,

$$
\mathbb{E}_f[d(v;G)] = \sum_{u \in V} \Pr[u \in N(v)] = \sum_{u \in V} \Pr[(u,v) \in G] = \sum_{u \in V} p(u,v),
$$

which does not depend on anything else but p.

By the definition of overlap,

$$
\begin{aligned}
&\mathrm{Ov}(f) \\
&= \frac{\mathbb{E}_{G',G''\sim f}\,|E(G')\cap E(G'')|}{\mathbb{E}_f\,|E(G)|} \\
&= \frac{\sum_{u,v}\Pr[(u,v)\in G' \wedge (u,v)\in G'']}{\sum_{u,v}\Pr[(u,v)\in G]} \\
&= \frac{\sum_{u,v}\Pr[(u,v)\in G']\Pr[(u,v)\in G'']}{\sum_{u,v}\Pr[(u,v)\in G]} \\
&= \frac{\sum_{u,v\in V}p^2(u,v)}{\sum_{u,v\in V}p(u,v)},\ \forall f\in\mathcal{F}(p),
\end{aligned}
$$

where we have used linearity of expectation and the independence between G' and G'', completing the proof. $\qquad\square$

Corollary A.3. *For any $p\colon \binom{V}{2}\to[0,1]$, $\mathbb{E}_f[\triangle(G)]\le\sum_{\{u,v,w\}\in\binom{V}{3}}\min(p(u,v),p(u,w),p(v,w)),\ \forall f\in\mathcal{F}(p)$, where $\triangle(G)$ is the number of triangles in G.*

Proof. By linearity of expectation and Proposition A.2,

$$
\begin{aligned}
\mathbb{E}_f[\triangle(G)] &= \sum_{\{u,v,w\}\in\binom{V}{3}}\Pr_f[\{(u,v),(u,w),(v,w)\in E(G)\}] \\
&\le \sum_{\{u,v,w\}\in\binom{V}{3}}\min(p(u,v),p(u,w),p(v,w)).
\end{aligned}
$$

$\qquad\square$

B. General binding

Definition A.4 (Formal definition of binding). Given edge probabilities $p\colon\binom{V}{2}\to[0,1]$ and a partition $\mathcal{P}$ of node pairs, binding results the RGM $f_{p;\mathcal{P}}^{\mathrm{BD}}$ defined as follows:

- For each $P_i\in\mathcal{P}$, write $P_i=\{(u_{i1},v_{i1}),\ldots,(u_{i|P_i|},v_{i|P_i|})\}$ in the descending order w.r.t. edge probabilities, i.e., $p(u_{i1},v_{i1})\ge\cdots\ge p(u_{i|P_i|},v_{i|P_i|})$.
- Let $P_{i;k}\coloneqq\{(u_{i1},v_{i1}),\ldots,(u_{ik},v_{ik})\}$.
- For G with edges $\bigcup_i P_{i;k_i}$ for some k_i's, $f_{p;\mathcal{P}}^{\mathrm{BD}}(G)=\prod_i(p(u_{ik_i},v_{ik_i})-p(u_{i,k_i+1},v_{i,k_i+1}))$, where we take $p(u_{i,|P_i|+1},v_{i,|P_i|+1})=0$.
- For any other G, $f_{p;\mathcal{P}}^{\mathrm{BD}}(G)=0$.

Proposition V.1 (Binding produces EPGMs). *For any $p\colon\binom{V}{2}\to[0,1]$ and any pair partition $\mathcal{P}$, $f_{p;\mathcal{P}}^{BD}\in\mathcal{F}(p)$.*

Proof. For each pair (u,v), the existence of the corresponding edge is determined in the "binding" procedure on the group P such that $(u,v)\in P$, where (u,v) is added into $\hat{E}$ and thus E if and only if $s\le\hat{p}(u,v)=p(u,v)$, which happens with probability $p(u,v)$ since $s\sim\mathcal{U}(0,1)$. $\qquad\square$

Proposition V.2 (Binding produces higher edge-group probabilities). *For any $p\colon\binom{V}{2}\to[0,1]$, any pair partition $\mathcal{P}$, and any $P\subseteq\binom{V}{2}$, $\Pr_{f_{p;\mathcal{P}}^{BD}}[P\subseteq E(G)]\ge\Pr_{f_p^{EI}}[P\subseteq E(G)]$.*

Proof. Let $\mathcal{P}'$ be a partition of P such that $\mathcal{P}'\coloneqq\{P_0\cap P\colon P_0\in\mathcal{P},P_0\cap P\ne\varnothing\}$. Then

$$
\begin{aligned}
\Pr_{f_{p;\mathcal{P}}^{\mathrm{BD}}}[P\subseteq E(G)] &= \prod_{P'\in\mathcal{P}'}\min_{(u,v)\in P'}p(u,v) \\
&= \prod_{(u,v)\in P\colon\exists P'\in\mathcal{P}',(u,v)=\arg\min_{(u',v')\in P'}p(u,v)}p(u,v) \\
&\ge \prod_{(u,v)\in P}p(u,v),
\end{aligned}
$$

since each $p(u,v)\le 1$. $\qquad\square$

C. Maximal binding

The upper bound in Proposition A.2 is tight, i.e., we can find EPGMs achieving the upper bound.

Indeed, we shall show below in Lemma A.6 that, as mentioned in Section V-A, *maximal binding* (i.e., binding with all the pairs bound together $\mathcal{P} = \{\binom{V}{2}\}$) achieves the upper bound.

In order to prove Lemma A.6, let us prove the following lemma first.

Lemma A.5 (The graph distribution with maximal binding). *For any $p: \binom{V}{2} \to [0,1]$, we first index the pairs (i.e., assign each pair a number) in $\binom{V}{2}$ in the descending order w.r.t. probabilities, i.e.,*

$$\binom{V}{2} = \{(u_1, v_1), (u_2, v_2), \ldots, (u_M, v_M)\}$$

with $M = \binom{|V|}{2}$ such that

$$p(u_1, v_1) \geq p(u_2, v_2) \geq \cdots \geq p(u_M, V_M),$$

then the graph distribution with maximal binding is

$$f^{BD}_{p;\{\binom{V}{2}\}}(G) = \begin{cases} 1 - p(u_1, v_1), & \text{if } G = (V, \varnothing), \\ p(u_M, v_M), & \text{if } G = (V, \binom{V}{2}), \\ p(u_i, v_i) - p(u_{i+1}, v_{i+1}), & \text{if } G = (V, \{(u_j, v_j) : 1 \leq j \leq i\}), \forall i \in [M-1], \\ 0, & \text{otherwise.} \end{cases}$$

Proof. With $\mathcal{P} = \{\binom{V}{2}\}$, all the edge existences are determined by the same random variable s. Hence, if a pair (u, v) exists, then all the pairs (u', v') with $p(u', v') \geq p(u, v)$ must exist. The possible outputs are either $G = (V, \varnothing)$ or $G = (V, \{(u_j, v_j) : 1 \leq j \leq i\})$ for some $i \in [M]$. The case $G = (V, \varnothing)$ happens when $s > \max_{u,v \in V} p(u, v) = p(u_1, v_1)$ with probability $1 - p(u_1, v_1)$. The case $G = (V, \binom{V}{2})$ happens when $s \leq \min_{u,v \in V} p(u, v) = p(u_M, v_M)$ with probability $p(P_{\binom{|V|}{2}})$. For each remaining case $G = (V, \{(u_j, v_j) : 1 \leq j \leq i\}$ with $i \in [M-1]$, it happens when $p(u_{i+1}, v_{i+1}) < s \leq p(u_i, v_i)$ with probability $p(u_i, v_i) - p(u_{i+1}, v_{i+1})$. $\square$

Lemma A.6 (Maximal binding achieves maximum edge-group probabilities). *For any $p: \binom{V}{2} \to [0,1]$ and any edge-group $P \subseteq \binom{V}{2}$, we have*

$$\Pr_{f^{BD}_{p;\{\binom{V}{2}\}}} [P \subseteq E(G)] = \min_{(u,v) \in P} p(u, v), \forall f \in \mathcal{F}(p),$$

where $f^{BD}_{p;\mathcal{P}}$ denotes the RGM defined by $f^{BD}_{p;\mathcal{P}}(G) = \Pr[Algorithm\ 1\ outputs\ G\ with\ inputs\ p\ and\ \mathcal{P}]$.

Proof. By Lemma A.5, in a graph G generated by $f^{BD}_{p;\binom{V}{2}}$, $P \subseteq E(G)$ if and only if $\arg\min_{(u,v) \in P} p(u, v) \in G$., which happens with probability $\min_{(u,v) \in P} p(u, v)$. $\square$

D. Local binding

Proposition V.3 (Local binding produces EPGMs). *For any $p: \binom{V}{2} \to [0,1]$, $g: V \to [0,1]$ and $R \in \mathbb{N}$, $f^{LB}_{p;g,R} \in \mathcal{F}(p)$.*

Proof. For each pair (u, v), $\Pr_{f^{LB}_{p;g,R}}[(u, v)] = \sum_{\mathcal{P}} \Pr_{\mathcal{P} \sim g}[\mathcal{P}] \Pr_{f^{BD}_{p;\mathcal{P}}}[(u, v)]$. By Proposition V.1, $\Pr_{f^{BD}_{p;\mathcal{P}}}[(u, v)] = p(u, v), \forall \mathcal{P}$. Hence, $\Pr_{f^{LB}_{p;g,R}}[(u, v)] = \sum_{\mathcal{P}} \Pr_{\mathcal{P} \sim g}[\mathcal{P}] p(u, v) = p(u, v)$. $\square$

Theorem V.5 (Time complexities of graph generation with local binding). *Given $p: \binom{V}{2} \to [0,1]$, $g: V \to [0,1]$, and $R \in \mathbb{N}$, $f^{LB}_{p;g,R}$ generates a graph in $O(R(\sum_{v \in V} g(v))^2 + |V|^2)$ time with high probability, with the worst case $O(R|V|^2)$.*

Proof. We have at most R rounds of sampling and binding, where each round samples at most $|V|$ nodes and thus at most $\binom{|V|}{2}$ pairs. More specifically, the number of nodes sampled in each round is $\sum_{v \in V} g(v)$ in expectation, and thus $O(\sum_{v \in V} g(v))$ with high probability (e.g., you can use a Chernoff bound). Hence, it takes $O(R \sum_{v \in V} g(v))$ time with high probability, and at most $O(\binom{|V|}{2} R)$ time for the R rounds. The number of remaining pairs is at most $\binom{|V|}{2}$ so dealing with them takes $O(\binom{|V|}{2})$ time. For the generation, we need to enumerate all the node groups and each pair in each group. Since the partition is disjoint, i.e., each pair is in exactly one group, each pair is visited exactly once, which takes $O(\binom{|V|}{2})$ time. In conclusion, generating a graph takes $O(R \sum_{v \in V} g(v) + |V|^2)$ with high probability, and $O(\binom{|V|}{2} R)$ time in the worst case. $\square$

Theorem V.6 (Tractable motif probabilities with local binding). *For any $p: \binom{V}{2} \to [0,1]$, $g: V \to [0,1]$, $R \in \mathbb{N}$, and $V' = \{u, v, w\} \in \binom{V}{3}$, we can compute the closed-form $\Pr_{f^{LB}_{p;g,R}}[E(G[V']) = E^*], \forall E^* \subseteq \binom{V'}{2}$ as a function w.r.t. p, g, and R.*

Proof. The overall idea is that we (1) consider all the sub-cases of how all the pairs $\binom{V'}{2}$ are partitioned and grouped during the whole process, (2) compute the motif probabilities conditioned on each sub-case, and (3) finally take the summation of the motif probabilities in all the sub-cases.

We first consider all the cases of how all the pairs are sampled and grouped until $\binom{V'}{2}$ are fully determined. We divided the cases w.r.t. how the pairs in $\binom{V'}{2}$ are eventually grouped by the sampled node sets. First let us define some "short-cut" variables:

- the probability that among V', exactly V^* is sampled together in a round

$$p_g(V^*) \coloneqq \mathrm{Pr}_g[\{u,v,w\} \cap V_s = V^*] = \prod_{v \in V^*} g(v) \prod_{v' \notin V^*} (1 - g(v)), \forall V^* \subseteq V'$$

- the probability that among V', at least two nodes (and thus at least one pair) are sampled together in a round

$$
\begin{aligned}
p_g(\mathcal{V}_{\geq 2}) &\coloneqq \sum_{V^*:|V^*|\geq 2} p_g(V^*) = p_g(\{u,v\}) + p_g(\{u,w\}) + p_g(\{v,w\}) + p_g(\{u,v,w\}) \\
&= g(u)g(v)(1 - g(w)) + g(u)g(w)(1 - g(v)) \\
&\quad + g(v)g(w)(1 - g(u)) + g(u)g(v)g(w)
\end{aligned}
$$

- the probability that among V', at most one node (and thus no pair) is sampled together in a round

$$p_g(\mathcal{V}_{<2}) \coloneqq 1 - p_g(\mathcal{V}_{\geq 2})$$

WLOG, we assume that $p(u,v) \geq p(u,w) \geq p(v,w)$.

$\{u,v,w\}$. The first time any pair in $\binom{V'}{2}$ is sampled in the R rounds is when u, v, and w are sampled by g together, which happens with probability

$$
\begin{aligned}
q(\{u,v,w\}) &= p_g(V') + p_g(\mathcal{V}_{<2})p_g(V') + p_g^2(\mathcal{V}_{<2})p_g(V') + \cdots + p_g^{R-1}(\mathcal{V}_{<2})p_g(V') \\
&= \prod_{i=0}^{R-1} p_g^i(\mathcal{V}_{<2})p_g(V') = \frac{1 - p_g^R(\mathcal{V}_{<2})}{1 - p_g(\mathcal{V}_{<2})} p_g(V'),
\end{aligned}
$$

where each term $p_g^i(\mathcal{V}_{<2})p_g(V')$ is the probability that in the first i rounds at most one node among V' is sampled and V' is sampled altogether in the $(i+1)$-th round. Conditioned on that, it generates

- $\{(u,v),(u,w),(v,w)\}$ with probability $p(v,w)$; when the random variable s in binding satisfies $s \leq p(v,w)$,
- $\{(u,v),(u,w)\}$ with probability $p(u,w) - p(v,w)$; when $p(v,w) < s \leq p(u,w)$,
- $\{(u,v)\}$ with probability $p(u,v) - p(u,w)$; when $p(u,w) < s \leq p(u,v)$, and
- $\varnothing$ with probability $1 - p(u,v)$; when $s > p(u,v)$.

$\{u,v\} \to \{u,v,w\}$. All the pairs in $\binom{V'}{2}$ are covered in twice in the R rounds. At the first time, u and v are sampled together by g but not w. At the second time, u, v, and w are sampled together by g. This happens with probability

$$
\begin{aligned}
q(\{u,v\} \to \{u,v,w\}) &= p_g(V') + (p_g(\mathcal{V}_{<2}) + p_g(\{u,v\}))\,p_g(V') + \cdots \\
&\quad + (p_g(\mathcal{V}_{<2}) + p_g(\{u,v\}))^{R-1} p_g(V') - q(\{u,v,w\}) \\
&= \sum_{i=0}^{R-1} (p_g(\mathcal{V}_{<2}) + p_g(\{u,v\}))^i p_g(V') - q(\{u,v,w\}) \\
&= \left(\frac{1 - (p_g(\mathcal{V}_{<2}) + p_g(\{u,v\}))^R}{1 - (p_g(\mathcal{V}_{<2}) + p_g(\{u,v\}))} - \frac{1 - p_g^R(\mathcal{V}_{<2})}{1 - p_g(\mathcal{V}_{<2})} \right) p_g(V'),
\end{aligned}
$$

where $(p_g(\mathcal{V}_{<2}) + p_g(\{u,v\}))^i p_g(V')$ is the probability that in the first i rounds we either sample no pair between V' or just (u,v), and we sample V' altogether in the $(i+1)$-th round, and $q(\{u,v,w\})$ is subtracted to exclude the cases where (u,v) is not sampled in the first i rounds. In such cases, when (u,v) is sampled for the first time, we decide the existence of (u,v), and then after that, when V' is sampled altogether for the first time, we decide the existences of the remaining two pair (u,w) and (v,w). Hence, conditioned on that, it generates

- $\{(u,v),(u,w),(v,w)\}$ with probability $p(u,v)p(v,w)$; when $s_1 \leq p(u,v)$ in the round (u,v) is sampled for the first time and $s_2 \leq p(v,w)$ in the round V' is sampled altogether for the first time,
- $\{(u,v),(u,w)\}$ with probability $p(u,v)\,(p(u,w) - p(v,w))$; when $s_1 \leq p(u,v)$ and $p(v,w) < s_2 \leq p(u,w)$,
- $\{(u,v)\}$ with probability $p(u,v)\,(1 - p(u,w))$; when $s_1 \leq p(u,v)$ and $s_2 > p(u,w)$,
- $\{(u,w),(v,w)\}$ with probability $(1 - p(u,v))\,p(v,w)$; when $s_1 > p(u,v)$ and $s_2 \leq p(v,w)$,
- $\{(u,w)\}$ with probability $(1 - p(u,v))\,(p(u,w) - (v,w))$; when $s_1 > p(u,v)$ and $p(v,w) < s_2 \leq p(u,w)$, and
- $\varnothing$ with probability $(1 - p(u,v))\,(1 - p(u,w))$; when $s_1 > p(u,v)$ and $s_2 > p(u,w)$.

$\underline{\{u,w\} \to \{u,v,w\}}$. Similarly, this happens with probability

$$q(\{u,w\} \to \{u,v,w\}) = \left(\frac{1 - (p_g(\mathcal{V}_{<2}) + p_g(\{u,w\}))^R}{1 - (p_g(\mathcal{V}_{<2}) + p_g(\{u,w\}))} - \frac{1 - p_g^R(\mathcal{V}_{<2})}{1 - p_g(\mathcal{V}_{<2})} \right) p_g(V')$$

Conditioned on that, it generates

- $\{(u,v),(u,w),(v,w)\}$ with probability $p(u,w)p(v,w)$; when $s_1 \le p(u,w)$ and $s_2 \le p(v,w)$,
- $\{(u,v),(u,w)\}$ with probability $p(u,w)(p(u,v) - p(v,w))$; when $s_1 \le p(u,w)$ and $p(v,w) < s_2 \le p(u,v)$,
- $\{(u,w)\}$ with probability $p(u,w)(1 - p(u,v))$; when $s_1 \le p(u,w)$ and $s_2 > p(u,v)$,
- $\{(u,v),(v,w)\}$ with probability $(1 - p(u,w))p(v,w)$; when $s_1 > p(u,w)$ and $s_2 \le p(v,w)$,
- $\{(u,v)\}$ with probability $(1 - p(u,w))(p(u,v) - (v,w))$; when $s_1 > p(u,w)$ and $p(v,w) < s_2 \le p(u,v)$, and
- $\varnothing$ with probability $(1 - p(u,w))(1 - p(u,v))$; when $s_1 > p(u,w)$ and $s_2 > p(u,v)$.

$\underline{\{v,w\} \to \{u,v,w\}}$. Similarly, this happens with probability

$$q(\{v,w\} \to \{u,v,w\}) = \left(\frac{1 - (p_g(\mathcal{V}_{<2}) + p_g(\{v,w\}))^R}{1 - (p_g(\mathcal{V}_{<2}) + p_g(\{v,w\}))} - \frac{1 - p_g^R(\mathcal{V}_{<2})}{1 - p_g(\mathcal{V}_{<2})} \right) p_g(V')$$

Conditioned on that, it generates

- $\{(u,v),(u,w),(v,w)\}$ with probability $p(v,w)p(u,w)$; when $s_1 \le p(v,w)$ and $s_2 \le p(u,w)$,
- $\{(u,v),(v,w)\}$ with probability $p(v,w)(p(u,v) - p(u,w))$; when $s_1 \le p(v,w)$ and $p(u,w) < s_2 \le p(u,v)$,
- $\{(v,w)\}$ with probability $p(v,w)(1 - p(u,v))$; when $s_1 \le p(v,w)$ and $s_2 > p(u,v)$,
- $\{(u,v),(u,w)\}$ with probability $(1 - p(v,w))p(u,w)$; when $s_1 > p(v,w)$ and $s_2 \le p(u,w)$,
- $\{(u,v)\}$ with probability $(1 - p(v,w))(p(u,v) - (u,w))$; when $s_1 > p(v,w)$ and $p(u,w) < s_2 \le p(u,v)$, and
- $\varnothing$ with probability $(1 - p(v,w))(1 - p(u,v))$; when $s_1 > p(v,w)$ and $s_2 > p(u,v)$.

The remaining cases. Three edges are determined independently. This happens with the remaining probability

$$q_{indep} = 1 - q(\{u,v,w\}) - q(\{u,v\} \to \{u,v,w\}) - q(\{u,w\} \to \{u,v,w\}) - q(\{v,w\} \to \{u,v,w\})$$

Conditioned on that, it generates each $E^* \subseteq \binom{V'}{2}$ with probability

$$\prod_{(x,y) \in E^*} p(x,y) \prod_{(x',y') \in \binom{V'}{2} \setminus E^*} (1 - p(x',y')).$$

Taking the summation of all the sub-cases gives the results as follows.

$\underline{E^* = \{(u,v),(u,w),(v,w)\}}$

$$\begin{aligned}
\Pr_{f_{p;g,R}^{LB}}[E(G[V']) = \{(u,v),(u,w),(v,w)\}] = \; & q(\{u,v,w\})p(v,w) + \\
& q(\{u,v\} \to \{u,v,w\})p(u,v)p(v,w) + \\
& q(\{u,w\} \to \{u,v,w\})p(u,w)p(v,w) + \\
& q(\{v,w\} \to \{u,v,w\})p(v,w)p(u,w) + \\
& q_{indep}p(u,v)p(u,w)p(v,w)
\end{aligned}$$

$\underline{E^* = \{(u,v),(u,w)\}}$

$$\begin{aligned}
\Pr_{f_{p;g,R}^{LB}}[E(G[V']) = \{(u,v),(u,w)\}] = \; & q(\{u,v,w\})(p(u,w) - p(v,w)) + \\
& q(\{u,v\} \to \{u,v,w\})p(u,v)(p(u,w) - p(v,w)) + \\
& q(\{u,w\} \to \{u,v,w\})p(u,w)(p(u,v) - p(v,w)) + \\
& q(\{v,w\} \to \{u,v,w\})(1 - p(v,w))p(u,w) + \\
& q_{indep}p(u,v)p(u,w)(1 - p(v,w))
\end{aligned}$$

$\underline{E^* = \{(u,v),(v,w)\}}$

$$\begin{aligned}
\Pr_{f_{p;g,R}^{LB}}[E(G[V']) = \{(u,v),(v,w)\}] = \; & q(\{u,w\} \to \{u,v,w\})(1 - p(u,w))p(v,w) + \\
& q(\{v,w\} \to \{u,v,w\})p(v,w)(p(u,v) - p(u,w)) + \\
& q_{indep}p(u,v)p(v,w)(1 - p(u,w))
\end{aligned}$$

$\underline{E^* = \{(u,w),(v,w)\}}$

$$\begin{aligned}
\Pr_{f_{p;g,R}^{LB}}[E(G[V']) = \{(u,w),(v,w)\}] = \; & q(\{u,v\} \to \{u,v,w\})(1 - p(u,v))p(v,w) + \\
& q_{indep}p(u,w)p(v,w)(1 - p(u,v))
\end{aligned}$$

$E^* = \{(u,v)\}$

$$\Pr\nolimits_{f^{\text{LB}}_{p;g,R}}[E(G[V']) = \{(u,v)\}] = q(\{u,v,w\})\,(p(u,v) - p(u,w)) +$$
$$q(\{u,v\} \to \{u,v,w\})p(u,v)\,(1 - p(u,w)) +$$
$$q(\{u,w\} \to \{u,v,w\})\,(1 - p(u,w))\,(p(u,v) - p(v,w)) +$$
$$q(\{v,w\} \to \{u,v,w\})\,(1 - p(v,w))\,(p(u,v) - p(u,w)) +$$
$$q_{indep}p(u,v)\,(1 - p(u,w))\,(1 - p(v,w))$$

$E^* = \{(u,w)\}$

$$\Pr\nolimits_{f^{\text{LB}}_{p;g,R}}[E(G[V']) = \{(u,w)\}] = q(\{u,v\} \to \{u,v,w\})\,(1 - p(u,v))\,(p(u,w) - p(v,w)) +$$
$$q(\{u,w\} \to \{u,v,w\})p(u,w)\,(1 - p(u,v)) +$$
$$q_{indep}p(u,w)\,(1 - p(u,v))\,(1 - p(v,w))$$

$E^* = \{(v,w)\}$

$$\Pr\nolimits_{f^{\text{LB}}_{p;g,R}}[E(G[V']) = \{(u,w)\}] = q(\{v,w\} \to \{u,v,w\})p(v,w)\,(1 - p(u,v)) +$$
$$q_{indep}p(v,w)\,(1 - p(u,v))\,(1 - p(u,w))$$

$E^* = \varnothing$

$$\Pr\nolimits_{f^{\text{LB}}_{p;g,R}}[E(G[V']) = \{(u,w)\}] = q(\{u,v,w\})\,(1 - p(u,v)) +$$
$$q(\{u,v\} \to \{u,v,w\})\,(1 - p(u,v))\,(1 - p(u,w)) +$$
$$q(\{u,w\} \to \{u,v,w\})\,(1 - p(u,w))\,(1 - p(u,v)) +$$
$$q(\{v,w\} \to \{u,v,w\})\,(1 - p(v,w))\,(1 - p(u,v)) +$$
$$q_{indep}\,(1 - p(u,v))\,(1 - p(u,w))\,(1 - p(v,w))$$

$\square$

Discussion on higher orders. As mentioned in Remark V.7, the reasoning in the proof above can be extended to higher orders. When the order of motifs increases, enumerating the cases of how all the pairs are sampled and grouped becomes more and more challenging. When considering 3-motifs, we are essentially considering the possible sequences of subsets up to order 3, where (1) each sequence should cover all the node pairs, and (2) each subset in the sequence should cover at least one pair that has not been covered by the subsets before it. The high-level idea would be similar, but the number increases exponentially:

- for 3-motifs, we need to consider 16 cases, 4 of which involve edge dependency, as shown above;
- for 4-motifs, we need to consider 16205 cases, 5261 of which involve edge dependency.

The above numbers are obtained using a recursive search. In principle, we can also derive the variance of the number of 3-motifs by considering the probabilities of 6-motifs, since the co-existence of two 3-motifs involves motifs up to order 6. We leave the efficient computation for higher-order motifs as a future direction.

Theorem V.8 (Time complexity of computing motif probabilities with local binding). *Given $p\colon \binom{V}{2} \to [0,1]$, $g\colon V \to [0,1]$, and $R \in \mathbb{N}$, computing $\Pr_{f^{\text{LB}}_{p;g,R}}[E(G[V']) = E^*]$ takes $O(|V|^3)$ time in total for all $E^* \subseteq \binom{V'}{2}$ and $V' \in \binom{V}{3}$.*

Proof. For computing motif probabilities, we need to enumerate all triplets $V' = \{u,v,w\} \in \binom{V}{3}$ and compute the motif probability for each 3-motif. For each motif, the calculation only involves arithmetic operations, which takes $O(1)$ time since the formulae are fixed. In conclusion, computing 3-motif probabilities takes $O(\binom{|V|}{3})$ time. $\square$

E. Parallel binding

Proposition A.7 (Parallel binding produces EPGMs). *For any $p\colon \binom{V}{2} \to [0,1]$, $g\colon V \to [0,1]$, and $R \in \mathbb{N}$, $f^{PB}_{p;g,R} \in \mathcal{F}(p)$.*

Proof. For each pair (u,v), if $\frac{1-(1-p(u,v))^{1/R}}{g(u)g(v)} \le 1$, i.e., $p(u,v) \le 1 - (1 - g(u)g(v))^R$, then $p_{rem}(u,v) = 0$ and

$$\Pr\nolimits_{f^{PB}_{p;g,R}}[(u,v)] = 1 - \Pr[(u,v) \text{ not inserted in the } R \text{ rounds}]\Pr[(u,v) \text{ not inserted when dealing with } p_{rem}]$$
$$= 1 - (1 - g(u)g(v)r(u,v))^R(1 - p_{rem})$$
$$= 1 - (1 - p(u,v))$$
$$= p(u,v).$$

Otherwise, if $p(u,v) > 1 - (1 - g(u)g(v))^R$, then $r(u,v) = 1$ and

$$\Pr_{f_{p;g,R}^{\text{PB}}}[(u,v)] = 1 - \Pr[(u,v) \text{ not inserted in the } R \text{ rounds}]\Pr[(u,v) \text{ not inserted when dealing with } p_{rem}]$$
$$= 1 - (1 - g(u)g(v)r(u,v))^R(1 - p_{rem})$$
$$= 1 - (1 - g(u)g(v))^R \frac{1 - p(u,v)}{(1 - g(u)g(v))^R}$$
$$= 1 - (1 - p(u,v))$$
$$= p(u,v).$$

$\square$

Theorem A.8 (Time complexities of graph generation with parallel binding). *Given* $p: \binom{V}{2} \to [0,1]$, $g: V \to [0,1]$, *and* $R \in \mathbb{N}$, $f_{p;g,R}^{PB}$ *generates a graph in* $O(R(\sum_{v \in V} g(v))^2 + |V|^2)$ *time with high probability, with the worst case* $O(R|V|^2)$.

Proof. We have at most R rounds of sampling and binding, where each round samples at most $|V|$ nodes and thus at most $\binom{|V|}{2}$ pairs. More specifically, the number of nodes sampled in each round is $\sum_{v \in V} g(v)$ in expectation, and thus $O(\sum_{v \in V} g(v))$ with high probability (e.g., one can use a Chernoff bound). Hence, it takes $O(R \sum_{v \in V} g(v))$ time with high probability, and at most $O(\binom{|V|}{2}R)$ time for the R rounds. The number of pairs with $p_{rem} > 0$ is at most $\binom{|V|}{2}$ so dealing with them takes $O(\binom{|V|}{2})$ time. In conclusion, generating a graph takes $O(R \sum_{v \in V} g(v) + |V|^2)$ with high probability, and $O(\binom{|V|}{2}R)$ time in the worst case. $\square$

Theorem A.9 (Tractable motif probabilities with parallel binding). *For any* $p: \binom{V}{2} \to [0,1]$, $g: V \to [0,1]$, $R \in \mathbb{N}$, *and* $V' = \{u,v,w\} \in \binom{V}{3}$, *we can compute the closed-form* $\Pr_{f_{p;g,R}^{\text{PB}}}[E(G[V']) = E^*], \forall E^* \subseteq \binom{V'}{2}$ *as a function w.r.t.* p, g, *and* R.

Proof. The overall idea is that we (1) compute the probabilities of each subset of $\binom{V'}{2}$ being inserted in each round and (2) accumulate the probabilities in R rounds to obtain the final motif probabilities.

We first compute the probability of each subset of $\binom{V'}{2}$ being inserted in each round. We divide the cases w.r.t. different sets of sampled nodes $V_s \cap V'$. First, let us define some "short-cut" variables:

- the probability that among V', exactly V^* is sampled together in a round

$$p_g(V^*) := \Pr_g[\{u,v,w\} \cap V_s = V^*] = \prod_{v \in V^*} g(v) \prod_{v' \notin V^*} (1 - g(v)), \forall V^* \subseteq V'$$

- the probability that among V', at least two nodes (and thus at least one pair) are sampled together in a round

$$p_g(\mathcal{V}_{\geq 2}) := \sum_{V^*:|V^*|\geq 2} p_g(V^*) = p_g(\{u,v\}) + p_g(\{u,w\}) + p_g(\{v,w\}) + p_g(\{u,v,w\})$$
$$= g(u)g(v)(1 - g(w)) + g(u)g(w)(1 - g(v)) + g(v)g(w)(1 - g(u))$$

- the probability that among V', at most one node (and thus no pair) is sampled together in a round

$$p_g(\mathcal{V}_{<2}) := 1 - p_g(\mathcal{V}_{\geq 2})$$

- the variables r and p_{rem} are defined as in Algorithm 3.

WLGO, we assume that $p(u,v) \geq p(u,w) \geq p(v,w)$.

$\underline{V_s = \{u,v,w\}}$. This happens with probability $p_g(V')$. Conditioned on that, it generates
- $\{(u,v),(u,w),(v,w)\}$ with probability $r(v,w)$; when $s \leq r(v,w)$,
- $\{(u,v),(u,w)\}$ with probability $r(u,w) - r(v,w)$; when $r(v,w) < s \leq r(u,w)$,
- $\{(u,v)\}$ with probability $r(u,v) - r(u,w)$; when $r(u,w) < s \leq r(u,v)$, and
- $\varnothing$ with probability $1 - r(u,v)$; when $s > r(u,v)$.

$\underline{V_s = \{u,v\}}$. This happens with probability $p_g(\{u,v\})$. Conditioned on that, it generates
- $\{(u,v)\}$ with probability $r(u,v)$; when $s \leq r(u,v)$, and
- $\varnothing$ with probability $1 - r(u,v)$l when $s > r(u,v)$.

$\underline{V_s = \{u,w\}}$. This happens with probability $p_g(\{u,w\})$. Conditioned on that, it generates
- $\{(u,w)\}$ with probability $r(u,w)$; when $s \leq r(u,w)$,
- $\varnothing$ with probability $1 - r(u,w)$; when $s > r(u,w)$.

$\underline{V_s\{v,w\}}$. This happens with probability $p_g(\{v,w\})$. Conditioned on that, it generates
- $\{(v,w)\}$ with probability $r(v,w)$; when $s \leq r(v,w)$,
- $\varnothing$ with probability $1 - r(v,w)$; when $s > r(v,w)$.

The remaining cases (i.e., $|V_s \cap V'| \leq 1$). This happens with probability $p_g(\mathcal{V}_{<2})$. Conditioned on that, it generates

- $\varnothing$ with probability 1.

Summary for each round. Let $p_{round}(E^*)$ denote the probability of E^* being generated in each round, for each $E^* \subseteq \binom{V'}{2}$. We have

- $p_{round}(\{(u,v),(u,w),(v,w)\}) = p_g(V')r(v,w)$,
- $p_{round}(\{(u,v),(u,w)\}) = p_g(V')(r(u,w) - r(v,w))$,
- $p_{round}(\{(u,v)\}) = p_g(V')(r(u,v) - r(u,w)) + p_g(\{u,v\})r(u,v)$,
- $p_{round}(\{(u,w)\}) = p_g(\{u,w\})r(u,w)$,
- $p_{round}(\{(v,w)\}) = p_g(\{v,w\})r(v,w)$, and
- $p_{round}(\varnothing) = 1 - p_g(V')r(u,v) - p_g(\{u,v\})r(u,v) - p_g(\{u,w\})r(u,w) - p_g(\{v,w\})r(v,w)$.

We are now ready to compute the motif probabilities.

$E^* = \varnothing$. This happens when $\varnothing$ is generated in all R rounds and for the remaining probabilities p_{rem}, with probability

$$\Pr_{f^{\text{PB}}_{p;g,R}}[E(G[V']) = \varnothing] = (p_{round}(\varnothing))^R(1 - p_{rem}(u,v))(1 - p_{rem}(u,w))(1 - p_{rem}(v,w)).$$

$E^* = \{(u,v)\}$. This happens when either $\varnothing$ or $\{(u,v)\}$ is generated in all R rounds and for p_{rem}, and (u,v) is generated in at least one round, which has probability

$$\Pr_{f^{\text{PB}}_{p;g,R}}[E(G[V']) = \{(u,v)\}]$$
$$= (p_{round}(\varnothing))^R p_{rem}(u,v)(1 - p_{rem}(u,w))(1 - p_{rem}(v,w))+$$
$$((p_{round}(\varnothing) + p_{round}(\{(u,v)\}))^R - (p_{round}(\varnothing))^R)(1 - p_{rem}(u,w))(1 - p_{rem}(v,w)),$$

where $((p_{round}(\varnothing) + p_{round}(\{(u,v)\}))^R - (p_{round}(\varnothing))^R)$ is the probability that in the R rounds, only (u,v) is inserted.

$E^* = \{(u,w)\}$. Similarly, this happens with probability

$$\Pr_{f^{\text{PB}}_{p;g,R}}[E(G[V']) = \{(u,w)\}]$$
$$= (p_{round}(\varnothing))^R p_{rem}(u,w)(1 - p_{rem}(u,v))(1 - p_{rem}(v,w))+$$
$$((p_{round}(\varnothing) + p_{round}(\{(u,w)\}))^R - (p_{round}(\varnothing))^R)(1 - p_{rem}(u,v))(1 - p_{rem}(v,w)).$$

$E^* = \{(v,w)\}$. Similarly, this happens with probability

$$\Pr_{f^{\text{PB}}_{p;g,R}}[E(G[v']) = \{(u,w)\}]$$
$$= (p_{round}(\varnothing))^R p_{rem}(v,w)(1 - p_{rem}(u,v))(1 - p_{rem}(u,w))+$$
$$((p_{round}(\varnothing) + p_{round}(\{(v,w)\}))^R - (p_{round}(\varnothing))^R)(1 - p_{rem}(u,v))(1 - p_{rem}(u,w)).$$

$E^* = \{(u,v),(u,w)\}$. This happens when one among $\varnothing$, $\{(u,v)\}$, $\{(u,w)\}$, and $\{(u,v),(u,w)\}$ is generated in all R rounds and for R_{rem}, while excluding the cases ending up with $\varnothing$, $\{(u,v)\}$, or $\{(u,w)\}$. This happens with probability

$$\Pr_{f^{\text{PB}}_{p;g,R}}[E(G[V']) = \{(u,v),(u,w)\}]$$
$$= (p_{round}(\varnothing))^R p_{rem}(u,v)p_{rem}(u,w)(1 - p_{rem}(v,w))+$$
$$((p_{round}(\varnothing) + p_{round}(\{(u,v)\}))^R - (p_{round}(\varnothing))^R)p_{rem}(u,w)(1 - p_{rem}(v,w))+$$
$$((p_{round}(\varnothing) + p_{round}(\{(u,w)\}))^R - (p_{round}(\varnothing))^R)p_{rem}(u,v)(1 - p_{rem}(v,w))+$$
$$\tilde{p}(\{(u,v),(u,w)\}; R)(1 - p_{rem}(v,w)),$$

where

$$\tilde{p}(\{(u,v),(u,w)\}; R)$$
$$= (p_{round}(\varnothing) + p_{round}(\{(u,v)\}) + p_{round}(\{(u,w)\}) + p_{round}(\{(u,v),(u,w)\}))^R -$$
$$(p_{round}(\varnothing) + p_{round}(\{(u,v)\}))^R -$$
$$(p_{round}(\varnothing) + p_{round}(\{(u,w)\}))^R +$$
$$(p_{round}(\varnothing))^R$$

is the probability that exactly (u,v) and (u,w) are inserted in the R rounds, using the inclusion-exclusion principle.

$E^* = \{(u,v),(v,w)\}$. Similarly, this happens with probability

$$
\begin{aligned}
&\mathrm{Pr}_{f^{\mathrm{PB}}_{p;g,R}}[E(G[V']) = \{(u,v),(v,w)\}]\\
&= (p_{round}(\varnothing))^R p_{rem}(u,v) p_{rem}(v,w)(1 - p_{rem}(u,w)) +\\
&\quad ((p_{round}(\varnothing) + p_{round}(\{(u,v)\}))^R - (p_{round}(\varnothing))^R) p_{rem}(v,w)(1 - p_{rem}(u,w)) +\\
&\quad ((p_{round}(\varnothing) + p_{round}(\{(v,w)\}))^R - (p_{round}(\varnothing))^R) p_{rem}(u,v)(1 - p_{rem}(u,w)) +\\
&\quad \tilde{p}(\{(u,v),(v,w)\};R)(1 - p_{rem}(u,w)),
\end{aligned}
$$

where

$$
\begin{aligned}
\tilde{p}(\{(u,v),(v,w)\};R) = {}&(p_{round}(\varnothing) + p_{round}(\{(u,v)\}) + p_{round}(\{(v,w)\}))^R -\\
&(p_{round}(\varnothing) + p_{round}(\{(u,v)\}))^R -\\
&(p_{round}(\varnothing) + p_{round}(\{(v,w)\}))^R +\\
&(p_{round}(\varnothing))^R.
\end{aligned}
$$

Note that $p_{round}(\{(u,v),(v,w)\}) = 0$.

$E^* = \{(u,w),(v,w)\}$. Similarly, this happens with probability

$$
\begin{aligned}
&\mathrm{Pr}_{f^{\mathrm{PB}}_{p;g,R}}[E(G[V']) = \{(u,w),(v,w)\}]\\
&= (p_{round}(\varnothing))^R p_{rem}(u,w) p_{rem}(v,w)(1 - p_{rem}(u,v)) +\\
&\quad ((p_{round}(\varnothing) + p_{round}(\{(u,w)\}))^R - (p_{round}(\varnothing))^R) p_{rem}(v,w)(1 - p_{rem}(u,v)) +\\
&\quad ((p_{round}(\varnothing) + p_{round}(\{(v,w)\}))^R - (p_{round}(\varnothing))^R) p_{rem}(u,w)(1 - p_{rem}(u,v)) +\\
&\quad \tilde{p}(\{(u,w),(v,w)\};R)(1 - p_{rem}(u,v)),
\end{aligned}
$$

where

$$
\begin{aligned}
\tilde{p}(\{(u,w),(v,w)\};R) = {}&((p_{round}(\varnothing) + p_{round}(\{(u,w)\}) + p_{round}(\{(v,w)\}))^R -\\
&(p_{round}(\varnothing) + p_{round}(\{(u,w)\}))^R -\\
&(p_{round}(\varnothing) + p_{round}(\{(v,w)\}))^R +\\
&(p_{round}(\varnothing))^R)
\end{aligned}
$$

Note that $p_{round}(\{(u,w),(v,w)\}) = 0$.

$E^* = \{(u,v),(u,w),(v,w)\}$. This happens with the remaining probability, i.e.,

$$
\mathrm{Pr}_{f^{\mathrm{PB}}_{p;g,R}}[E(G[V']) = \{(u,v),(u,w),(v,w)\}] = 1 - \sum_{E' \subsetneq \binom{V'}{2}} \mathrm{Pr}_{f^{\mathrm{PB}}_{p;g,R}}[E(G[V']) = E'].
$$

$\square$

Discussion on higher orders. Similar to the counterpart for local binding, the reasoning in the proof above can be extended to higher orders. When the order of motifs increases, both considering the cases in each round and accumulating them in multiple rounds become increasingly challenging. For the cases in each round, we first need to consider more cases of V_s, i.e., all the subsets of V'. For accumulating the probabilities, for each E^*, we first need to consider all the cases (i.e., all the subsets of E^*) in each round that can accumulate to $E*$, and we need to use the inclusion-exclusion principle to avoid counting some sub-motifs multiple times, where again all the subsets of E^* need to be considered. Hence, for motifs of order k, the number of cases is at least $O(2^{\binom{k}{2}})$.

Theorem A.10 (Time complexity of computing motif probabilities with parallel binding). *Given $p: \binom{V}{2} \to [0,1]$, $g: V \to [0,1]$, and $R \in \mathbb{N}$, computing $\mathrm{Pr}_{f^{\mathrm{PB}}_{p;g,R}}[E(G[V']) = E^*]$ takes $O(|V|^3)$ time in total for all $E^* \subseteq \binom{V'}{2}$ and $V' \in \binom{V}{3}$.*

Proof. For computing motif probabilities, we need to enumerate all triplets $V' = \{u,v,w\} \in \binom{V}{3}$ and compute the motif probability for each 3-motif. For each motif, the calculation only involves arithmetic operations, which takes $O(1)$ time since the formulae are fixed. In conclusion, computing 3-motif probabilities takes $O(\binom{|V|}{3})$ time. $\square$

F. Fitting

1) The Erdős-Rényi (ER) model:

Definition. The Erdős-Rényi (ER) model [9] outputs edge probabilities with two parameters: n_0 and p_0, and the output is p_{n_0,p_0}^{ER} with $p_{n_0,p_0}^{ER}(u,v) = p_0, \forall u,v \in \binom{V}{2}$ with $V = [n_0]$. Given a graph $G = (V = [n], E)$, ER outputs $n_0 = n$ and $p_0 = \frac{2|E|}{n(n-1)}$.

Lemma V.11 (Reduced time complexity with ER). *Given $n_0 \in \mathbb{N}$, $p_0 \in [0,1]$, $g_0 \in [0,1]$, and $R \in \mathbb{N}$, computing both* $\Pr_{f_{p;g,R}^{LB}}[E(G[V']) = E^*]$ *and* $\Pr_{f_{p;g,R}^{PB}}[E(G[V']) = E^*]$ *takes $O(1)$ times in total for all $E^* \subseteq \binom{V'}{2}$ and $V' \in \binom{V}{3}$ with $p = p_{n_0,p_0}^{ER}$ and $g(v) = g_0, \forall v \in V = [n_0]$.*

Proof. When $p(u,v) \equiv v_0$ and $g(v) \equiv g_0$, both $\Pr_{f_{p;g,R}^{LB}}[E(G[V']) = E^*]$ and $\Pr_{f_{p;g,R}^{PB}}[E(G[V']) = E^*]$ become the same functions for all $V' \in \binom{V}{3}$, which only involve arithmetic operations on p_0 and g_0 and thus take $O(1)$ time for computation. Since the functions are the same for all $V' \in \binom{V}{3}$, we only need to calculate for a single V'. Hence, the total time complexity is still $O(1)$. The detailed formulae are as follows.

Local binding. Fix any $V' \in \binom{V}{3}$, we have

$$p_g(V^*) = g_0^{|V^*|}(1 - g_0)^{3-|V^*|}, \forall V^* \subseteq V',$$

$$p_g(\mathcal{V}_{\geq 2}) = 3g_0^2(1 - g_0) + g_0^3,$$

and

$$p_g(\mathcal{V}_{<2}) = 3g_0(1 - g_0)^2 + (1 - g_0)^3.$$

Hence

$$q(\{u,v,w\}) = \frac{1 - (3g_0(1 - g_0)^2 + (1 - g_0)^3)^R}{3g_0^2(1 - g_0) + g_0^3} g_0^3,$$

$$q_2 := q(\{u,v\} \to \{u,v,w\}) = q(\{u,w\} \to \{u,v,w\}) = q(\{v,w\} \to \{u,v,w\})$$
$$= \left(\frac{1 - (3g_0(1 - g_0)^2 + (1 - g_0)^3 + g_0^2(1 - g_0))^R}{2g_0^2(1 - g_0) + g_0^3} - \frac{1 - (3g_0(1 - g_0)^2 + (1 - g_0)^3)^R}{3g_0^2(1 - g_0) + g_0^3} \right),$$

and

$$q_{indep} = 1 - q(\{u,v,w\}) - 3q_2.$$

$\underline{E^* = \{(u,v),(u,w),(v,w)\}}$

$$\Pr_{f_{p;g,R}^{LB}}[E(G[V']) = \{(u,v),(u,w),(v,w)\}] = q(\{u,v,w\})p_0 + 3q_2p_0^2 + q_{indep}p_0^3$$

$\underline{|E^*| = 2}$

For each E^* with $|E^*| = 2$, i.e., $E^* = \{(u,v),(u,w)\}$ or $\{(u,v),(v,w)\}$ or $(u,w),(v,w)$, we have

$$\Pr_{f_{p;g,R}^{LB}}[E(G[V']) = E^*] = q_2p_0(1 - p_0) + q_{indep}p_0^2(1 - p_0)$$

$\underline{|E^*| = 1}$

For each E^* with $|E^*| = 1$, i.e., $E^* = \{(u,v)\}$ or $\{(u,w)\}$ or (v,w), we have

$$\Pr_{f_{p;g,R}^{LB}}[E(G[V']) = E^*] = q_2p_0(1 - p_0) + q_{indep}p_0(1 - p_0)^2$$

$\underline{E^* = \varnothing}$

$$\Pr_{f_{p;g,R}^{LB}}[E(G[V']) = \{(u,w)\}] = q(\{u,v,w\})(1 - p_0) + 3q_2(1 - p_0)^2 + q_{indep}(1 - p_0)^3$$

$\square$

2) The Chung-Lu (CL) model:

Definition. The Chung-Lu (CL) model [10] outputs edge probabilities with a sequence of expected degrees $D = (d_1, d_2, \ldots, d_n)$, and the output is p_D^{CL} with $p_D^{CL}(u, v) = \min\left(\frac{d_u d_v}{\sum_{i=1}^n d_i}, 1\right)$, $\forall u, v \in \binom{V}{2}$ with $V = [n]$. Given a graph $G = (V = [n], E)$, CL outputs $d_i = d(i; G)$ for each node $i \in V$.

Lemma V.12 (Reduced time complexity with CL). *Given $D = (d_1, d_2, \ldots, d_n)$, g_d for $d \in \{d_1, d_2, \ldots, d_n\}$, and $R \in \mathbb{N}$, computing both $\Pr_{f_{p;g,R}^{LB}}[E(G[V']) = E^*]$ and $\Pr_{f_{p;g,R}^{PB}}[E(G[V']) = E^*]$ for all $E^* \subseteq \binom{V'}{2}$ and $V' \in \binom{[n]}{3}$ takes $O(k_{deg}^3)$ times with $p = p_D^{CL}$ and $g(i) = g_{d_i}, \forall i \in [n]$.*

Proof. The key idea is that given $V' = \{i, j, k\} \in \binom{V}{3}$, both the three edge probabilities (i.e., $p(i, j)$, $p(i, k)$, and $p(j, k)$) and the three node-sampling probabilities (i.e., $g(i)$, $g(j)$, and $g(k)$) are fully determined by the degrees of the three nodes.

Hence, we only need to calculate motif probabilities for each degree combination instead of each node combination. Since we have k_{deg} different degrees, the total number of degree combinations of size 3 is $O(k_{deg}^3)$, and the calculation for each combination takes $O(1)$ time on arithmetic operations with fixed formulae. In conclusion, the total time complexity is $O(k_{deg}^3)$.

Some details are as follows. Let $k_{deg} = \{d_1, d_2, \ldots, d_n\} = \{\tilde{d}_1, \tilde{d}_2, \ldots, \tilde{d}_{k_{deg}}\}$, and let n_i denote the number of nodes with degree $\tilde{d}_i$, for $i \in [k_{deg}]$. Given three degrees $\tilde{d}_i$, $\tilde{d}_j$, and $\tilde{d}_k$, we have

- $n_i n_j n_k$ such combinations, when $i \neq j$, $i \neq k$, and $j \neq k$
- $\binom{n_i}{2} n_k$ such combinations, when $i = j$ and $i \neq k$; similarly for $i = k$ and $i \neq j$ or $j = k$ and $i \neq j$
- $\binom{n_i}{3}$ such combinations, when $i = j = k$.

□

3) The stochastic block (SB) model:

Definition. Given a graph $G = (V = [n], E)$ and a node partition $f_B: [n] \to [c]$ with $c \in \mathbb{N}$, let $V_i = \{v \in V: f_B(v) = i\}$ denote the set of nodes partitioned in the i-th group for $i \in [c]$. The fitting of the edge probabilities in the stochastic block (SB) model gives $p_B: [c] \times [c] \to [0, 1]$ with $p_B(i, i) = \frac{|E(G[V_i])|}{\binom{|V_i|}{2}}$ and $p_B(i, j) = \frac{|E \cap \{(v, v'): v \in V_i, v' \in V_j\}|}{|V_i||V_j|}$, for $i \neq j \in [c]$.

Lemma V.13 (Reduced time complexity with SB). *Given $f_B: [n_0] \to [c]$, $f_B: [n_0] \to [c]$, g_i for $i \in [c]$, and $R \in \mathbb{N}$, computing both $\Pr_{f_{p;g,R}^{LB}}[E(G[V']) = E^*]$ and $\Pr_{f_{p;g,R}^{PB}}[E(G[V']) = E^*]$ takes $O(c^3)$ times in total for all $E^* \subseteq \binom{V'}{2}$ and $V' \in \binom{[n]}{3}$ with $p = p_{f_B, p_B}^{SB}$ and $g(v) = g_{f_B(v)}$ for each $v \in V = [n]$.*

Proof. The key idea is that given $V' = \{i, j, k\} \in \binom{V}{3}$, both the three edge probabilities (i.e., $p(i, j)$, $p(i, k)$, and $p(j, k)$) and the three node-sampling probabilities (i.e., $g(i)$, $g(j)$, and $g(k)$) are fully determined by the membership the three nodes, i.e., $f_B(i)$, $f_B(j)$, and $f_B(k)$.

Hence, we only need to calculate motif probabilities for each membership combination instead of each node combination. Since we have c different groups, the total number of degree combinations of size 3 is $O(c^3)$, and the calculation for each combination takes $O(1)$ time on arithmetic operations with fixed formulae. In conclusion, the total time complexity is $O(c^3)$.

Some details are as follows. Let $n_i = |V_i|$ denote the number of nodes in the i-th group. Given three group membership indicators i, j, and k, we have

- $n_i n_j n_k$ such combinations, when $i \neq j$, $i \neq k$, and $j \neq k$
- $\binom{n_i}{2} n_k$ such combinations, when $i = j$ and $i \neq k$; similarly for $i = k$ and $i \neq j$ or $j = k$ and $i \neq j$
- $\binom{n_i}{3}$ such combinations, when $i = j = k$.

□

4) The stochastic Kronecker (KR) model:

Definition A.11 (Kronecker product and Kronecker power). Given two matrices $A \in \mathbb{R}^{m \times n}$ and $B \in \mathbb{R}^{p \times q}$, the Kronecker product between A and B is

$$\mathbf{A} \otimes \mathbf{B} = \begin{bmatrix} a_{11}b_{11} & a_{11}b_{12} & \cdots & a_{11}b_{1q} & \cdots & \cdots & a_{1n}b_{11} & a_{1n}b_{12} & \cdots & a_{1n}b_{1q} \\ a_{11}b_{21} & a_{11}b_{22} & \cdots & a_{11}b_{2q} & \cdots & \cdots & a_{1n}b_{21} & a_{1n}b_{22} & \cdots & a_{1n}b_{2q} \\ \vdots & \vdots & \ddots & \vdots & & & \vdots & \vdots & \ddots & \vdots \\ a_{11}b_{p1} & a_{11}b_{p2} & \cdots & a_{11}b_{pq} & \cdots & \cdots & a_{1n}b_{p1} & a_{1n}b_{p2} & \cdots & a_{1n}b_{pq} \\ \vdots & \vdots & & \vdots & \ddots & & \vdots & \vdots & & \vdots \\ \vdots & \vdots & & \vdots & & \ddots & \vdots & \vdots & & \vdots \\ a_{m1}b_{11} & a_{m1}b_{12} & \cdots & a_{m1}b_{1q} & \cdots & \cdots & a_{mn}b_{11} & a_{mn}b_{12} & \cdots & a_{mn}b_{1q} \\ a_{m1}b_{21} & a_{m1}b_{22} & \cdots & a_{m1}b_{2q} & \cdots & \cdots & a_{mn}b_{21} & a_{mn}b_{22} & \cdots & a_{mn}b_{2q} \\ \vdots & \vdots & \ddots & \vdots & & & \vdots & \vdots & \ddots & \vdots \\ a_{m1}b_{p1} & a_{m1}b_{p2} & \cdots & a_{m1}b_{pq} & \cdots & \cdots & a_{mn}b_{p1} & a_{mn}b_{p2} & \cdots & a_{mn}b_{pq} \end{bmatrix}.$$
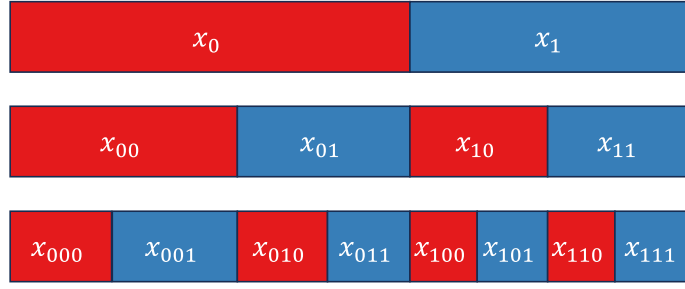
Fig. 4: The node combinations in KR.

Given $k \in \mathbb{N}$, the k Kronecker power of A is

$$\underbrace{A \otimes (A \cdots (A \otimes (A \otimes A)))}_{k-1 \text{ times of Kronecker products}}.$$

Definition. The stochastic Kronecker (KR) model [12] outputs edge probabilities with a seed matrix $\theta \in [0,1]^{2 \times 2}$ and $k_{KR} \in \mathbb{N}$,[7], and the output $p_{\theta,k_{KR}}^{KR}$ is the k_{KR}-th Kronecker power of θ.

Lemma A.12 (Node equivalence in KR). *Given $\theta \in [0,1]^{2 \times 2}$, $k_{KR} \in \mathbb{N}$, g_i for $0 \le i \le k_{KR}$, and $R \in \mathbb{N}$, computing both $\Pr_{f_{p;g,R}^{LB}}[E(G[V']) = E^*]$ and $\Pr_{f_{p;g,R}^{PB}}[E(G[V']) = E^*]$ takes $O(k_{KR}^7)$ times in total for all $E^* \subseteq \binom{V'}{2}$ and $V' \in \binom{[n]}{3}$ with $p = p_{\theta,k_{KR}}^{KR}$ and $g(v) = g_i$ with i being the number of ones in the binary representation of $v - 1$, for each $v \in [2^{k_{KR}}]$.*

Proof. A square binary matrix $P \in \{0,1\}^{n \times n}$ for some $n \in \mathbb{N}$ is a permutation matrix if exactly one entry in each row or column of P is 1, i.e., $\sum_k P_{ik} = \sum_k P_{kj} = 1, \forall i, j \in [n]$.

With binary node labels, given two nodes

$$u = (u_1 u_2 \cdots u_{k_{KR}})_2$$

and

$$v = (v_1 v_2 \cdots v_{k_{KR}})_2,$$

we have

$$\theta_{uv}^{(k_{KR})} = \prod_{i=1}^{k_{KR}} \theta_{u_i v_i},$$

which implies that for any permutation $\pi \in S_{k_{KR}}$,

$$\theta_{uv}^{(k_{KR})} = \theta_{\pi(u)\pi(v)}^{(k_{KR})}, \forall u, v,$$

where with a slight abuse of notation,

$$\pi(u) = (u_{\pi(1)} u_{\pi(2)} \cdots u_{\pi(k_{KR})})_2$$

and

$$\pi(v) = (v_{\pi(1)} v_{\pi(2)} \cdots v_{\pi(k_{KR})})_2.$$

On the other hand, for any two nodes with the same number of ones in the binary representations, we can find a permutation π between the two binary representations by seeing them as sequences. Let $P = P_\pi \in \{0,1\}^{2^{k_{KR}} \times 2^{k_{KR}}}$ with $P_{ij} = 1$ if and only if π converts the binary presentation of $i - 1$ to that of $j - 1$, and we have $P^\top \theta_{uv}^{(k_{KR})} P = \theta_{uv}^{(k_{KR})}$. $\qquad \square$

Remark A.13. The equivalence in KR is slightly weaker than that in the other three models (ER, CL, and SB). Specifically, in the other three models, "two nodes i and j are equivalent" means that, when you swap i and j while keeping the other nodes unchanged, the RGM is kept unchanged. For KR, the equivalence is weaker in that you have to swap i and j together with all the other nodes w.r.t. a permutation. This is also why the reduced time complexity is $O(k_{KR}^7)$ instead of $O(k_{KR}^3)$ in Lemma V.14.

Lemma V.14 (Reduced time complexity with KR). *Given $\theta \in [0,1]^{2 \times 2}$, $k_{KR} \in \mathbb{N}$, g_i for $0 \le i \le k_{KR}$, and $R \in \mathbb{N}$, computing both $\Pr_{f_{p;g,R}^{LB}}[E(G[V']) = E^*]$ and $\Pr_{f_{p;g,R}^{PB}}[E(G[V']) = E^*]$ for all $E^* \subseteq \binom{V'}{2}$ and $V' \in \binom{[n]}{3}$ takes $O(k_{KR}^7)$ times with $p = p_{\theta,k_{KR}}^{KR}$ and $g(v) = g_i$ with i being the number of ones in the binary representation of $v - 1$, for each $v \in [2^{k_{KR}}]$.*

Proof. We divide node combinations w.r.t the binary node labels. As shown in the proof of Lemma A.12, node combinations are equivalent with permutations on the binary node labels. Hence, in each equivalent class of node combinations, we can

---

[7]We consider the commonly used 2-by-2 seed matrices.

consider only the one with the form as shown in Figure 4, where each number (x_0, x_1, x_{00}, etc.) represents the number of zeros and ones. Here,

- the first node v_1 (more precisely, its binary node representation) has x_0 zeros first and then x_1 ones,
- the second node v_2 has x_{00} zeros, then x_{01} ones, then x_{10} zeros, and finally x_{11} ones, and
- the third node v_3 has x_{000} zeros, then x_{001} ones, then x_{010} zeros, then x_{011} ones, then x_{100} zeros, then x_{101} ones, then x_{110} zeros, and finally x_{111} ones.

As indicated in the figure, we have

- $x_0 + x_1 = k_{KR}$
- $x_{00} + x_{01} = x_0$, $x_{10} + x_{11} = x_1$
- $x_{000} + x_{001} = x_{00}$, $x_{010} + x_{011} = x_{01}$, $x_{100} + x_{101} = x_{10}$, and $x_{110} + x_{111} = x_{11}$.

The number of different equivalent classes is upper-bounded by

$$\sum_{x_0=0}^{k_{KR}} \sum_{x_{00}=0}^{x_0} \sum_{x_{10}=0}^{k_{KR}-x_0} \sum_{x_{000}=0}^{x_00} \sum_{x_{010}=0}^{x_0-x_00} \sum_{x_{100}=0}^{x_{10}} \sum_{x_{110}=0}^{k_{KR}-x_0-x_{10}} 1$$

$$= \frac{(k_{KR}+1)(k_{KR}+2)(k_{KR}+3)(k_{KR}+4)(k_{KR}+5)(k_{KR}+6)(k_{KR}+7)}{5040} = O(k_{KR}^7).$$

For each equivalent class, the calculation only involves arithmetic with a fixed formula and thus takes $O(1)$ time. Note that the Kronecker power can be computed beforehand with much lower time complexity, i.e., $o(k_{KR}^7)$ [48]. In conclusion, the total time complexity is $O(k_{KR}^7)$. $\qquad \square$

APPENDIX B
ON (NON-)ISOLATED NODES

A. Tractable number of (non-)isolated nodes with parallel binding

Theorem B.1 (Tractable number of (non-)isolated nodes with parallel binding). *For any $p \colon \binom{V}{2} \to [0,1]$, $g \colon V \to [0,1]$, $R \in \mathbb{N}$, we can compute the closed-form (w.r.t. p, g, and R) $\mathbb{E}_{f_{p;g,R}^{PB}}[|\{v \in G \colon d(v;G) \geq 1\}|]$.*

Proof. By the linearity of expectation,

$$\mathbb{E}_{f_{p;g,R}^{PB}}[|\{v \in G \colon d(v;G) \geq 1\}|] = \sum_{v \in V} \Pr_{f_{p;g,R}^{PB}}[d(v;G) \geq 1].$$

Hence, we only need to compute the probability of each node v being (non-)isolated. A node v is isolated if and only if no edge incident to v is inserted in each round. In each round, when v is sampled, i.e., $v \in V_s$, the probability that no edge incident to v is inserted is $1 - \max_{u \in V_s} p(u,v)$. Let $p_{iso}(v)$ denote the aforementioned probability and sort $V \smallsetminus \{v\} = \{u_1, u_2, \ldots, u_{n-1}\}$ with $n = |V|$ and $p(u_1,v) \geq p(u_2,v) \geq \cdots \geq p(u_{n-1},v)$. We have

$$p_{iso}(v) = (1 - \Pr[v \in V_s]) + \Pr[v \in V_s]\left(1 - \mathbb{E}_{f_{p;g,R}^{PB}}\left[\max_{u \in V_s} p(u,v)\right]\right) = 1 - g(v)\mathbb{E}_{f_{p;g,R}^{PB}}\left[\max_{u \in V_s} p(u,v)\right],$$

where

$$\mathbb{E}_{f_{p;g,R}^{PB}}\left[\max_{u \in V_s} p(u,v)\right]$$

$$= \Pr[u_1 \in V_s]p(u_1,v) + \Pr[u_1 \notin V_s \wedge u_2 \in V_s]p(u_2,v) + \cdots + \Pr\left[\left(\bigwedge_{i=1}^{n-2} u_i \notin V_s\right) \wedge u_{n-1} \in V_s\right]p(u_{n-1},v)$$

$$= g(u_1)p(u_1,v) + (1 - g(u_1))g(u_2)p(u_2,v) + \cdots + \prod_{i=1}^{n-2}(1 - g(u_i))g(u_{n-1})p(u_{n-1},v).$$

Finally, the probability that v is isolated after R rounds and dealing with p_{rem} is

$$\tilde{p}_{iso}(v) = (p_{iso}(v))^R(1 - p_{rem}(v)),$$

and thus the expected number of non-isolated nodes is

$$\mathbb{E}_{f_{p;g,R}^{PB}}[|\{v \in G \colon d(v;G) \geq 1\}|] = \sum_{v \in V}(1 - \tilde{p}_{iso}(v)).$$

$\qquad \square$

The expected number of degree-1 nodes We can extend the reasoning above to compute the expected number of degree-1 nodes. Fix a node v, for each node u_k, we shall compute the probability that no other $(u_{k'},v)$ with $k' \neq k$ is inserted, denoted

by $p_s(v; u_k)$, which is the probability of v being isolated plus the probability of v being only adjacent to u_k. In other words, we compute the probability of v being isolated while ignoring u_k. We have

$$p_s(v; u_k) = (1 - g(v)) + g(v)\tilde{p}_s(v; u_k),$$

where

$$\tilde{p}_s(v; u_k) = g(u_1)(1 - p(u_1, v)) +$$
$$(1 - g(u_1))g(u_2)(1 - p(u_2, v)) + \cdots +$$
$$\prod_{i=1}^{k-2}(1 - g(u_i))g(u_{k-1})(1 - p(u_{k-1}, v)) +$$
$$\prod_{i=1}^{k-1}(1 - g(u_i))g(u_k)\hat{p}_s(v; u_k) +$$
$$\prod_{i=1}^{k+1}(1 - g(u_i))g(u_{k+1})(1 - p(u_{k+1}, v)) + \cdots +$$
$$\prod_{i=1}^{n-2}(1 - g(u_i))g(u_{n-1})p(u_{n-1}, v) +$$
$$\prod_{i=1}^{n-1}(1 - g(u_i))$$

with

$$\hat{p}_s(v; u_k) = g(u_{k+1})(1 - p(u_{k+1}, v)) +$$
$$(1 - g(u_{k+1}))g(u_{k+2})(1 - p(u_{k+2}, v)) + \cdots +$$
$$\prod_{i=k+1}^{n-2}(1 - g(u_i))g(u_{n-1})(1 - p(u_{n-1}, v)) +$$
$$\prod_{i=k+1}^{n-1}(1 - g(u_i)).$$

Finally, the probability of v being degree-1 is

$$\sum_{i=1}^{n-1}(p_s(v; u_i) - p_{iso}(v)).$$

Theorem B.2 (Time complexity of computing the expected number of (non-)isolated nodes with parallel binding). *Given* $p \colon \binom{V}{2} \to [0, 1]$, $g \colon V \to [0, 1]$, *and* $R \in \mathbb{N}$, *computing* $\mathbb{E}_{f_{p;g,R}^{PB}}[|\{v \in G \colon d(v; G) \geq 1\}|]$ *takes* $O(|V|^2 \log |V|)$ *time.*

Proof. For computing the expected number of non-isolated nodes, for each node v, we need to first sort the other nodes $u \in V \setminus \{v\}$ w.r.t. $p(u, v)$, which takes $O(|V| \log |V|)$ times. After that, the calculation only arithmetic operations, which takes $O(1)$ time since the formulae are fixed. Hence, for each node v it takes $O(\log |V|)$ times. In conclusion, for all the nodes in V, it takes $O(|V| \log |V|)$ time in total. $\square$

Remark B.3. Considering node equivalence (see Section V-D) can also be used to reduce the time complexity of computing the number of (non-)isolated nodes.

B. Experimental results

Since we have the tractability results on the number of (non-)isolated nodes, we can also fit and control the number of (non-)isolated nodes with our binding schemes. Specifically, in our main experiments, the objective of fitting is merely the number of triangles. Here, we further consider variants with the fitting objective including both the number of triangles and the number of (non-)isolated nodes, trying to preserve both numbers as the ground truth.

In Table VII, for each dataset and each model, we compare the ground-truth graph, the corresponding EIGM, and the following two variants of EPGMs:
1) PARABDG: parallel binding with the number of triangles as the objective
2) PARABDG-N: parallel binding with both the number of triangles and the number of (non-)isolated nodes[8]
and report the following statistics of the generated graphs:
1) n_{ni}: the number of non-isolated nodes

[8]We only have tractability results with parallel binding.

TABLE VII: The number of non-isolated nodes and clustering metrics of graphs generated by different realization methods. The number of non-isoalted nodes n_{ni} and the number of triangles ($\triangle$) are normalized. For each dataset and each model, the best result is in bold and the second best is underlined.

dataset		*Hams*				*Fcbk*				*Polb*			
metric		n_{ni}	$\triangle$	GCC	ALCC	n_{ni}	$\triangle$	GCC	ALCC	n_{ni}	$\triangle$	GCC	ALCC
model	GROUNDT	1.000	1.000	0.229	0.540	1.000	1.000	0.519	0.606	1.000	1.000	0.226	0.320
ER	EDGEIND	**1.000**	0.013	_0.008_	0.008	**1.000**	0.009	0.011	0.011	**1.000**	0.034	_0.022_	**0.022**
	PARABDG	0.812	_0.988_	**0.385**	**0.640**	0.555	**1.002**	**0.574**	**0.815**	0.801	_1.025_	**0.412**	_0.659_
	PARABDG-N	_0.996_	**0.990**	0.481	0.748	_1.007_	_0.584_	_0.594_	_0.835_	_1.007_	**1.012**	0.532	0.787
CL	EDGEIND	**0.964**	_0.299_	_0.067_	0.058	**0.988**	0.124	0.064	0.063	**0.944**	0.792	_0.183_	_0.173_
	PARABDG	0.771	**1.000**	**0.185**	**0.471**	0.656	**1.006**	**0.336**	**0.626**	0.789	**1.010**	**0.221**	0.468
	PARABDG-N	_0.959_	0.257	0.027	0.069	_0.969_	1.098	0.125	0.151	_0.935_	0.794	0.135	**0.219**
SB	EDGEIND	**0.996**	0.263	0.080	0.038	**1.000**	0.153	0.145	0.080	**0.975**	_0.478_	_0.145_	0.164
	PARABDG	0.719	**0.993**	**0.241**	**0.521**	0.608	**1.035**	**0.529**	**0.557**	0.899	**1.010**	**0.183**	**0.251**
	PARABDG-N	_0.991_	1.168	_0.154_	_0.092_	_1.000_	_1.036_	_0.423_	_0.204_	_0.953_	0.475	0.094	_0.217_
KR	EDGEIND	**0.996**	0.185	_0.039_	0.060	_1.014_	0.052	0.035	0.042	1.598	0.101	0.040	0.075
	PARABDG	0.856	**0.997**	**0.165**	**0.394**	0.781	**0.971**	**0.347**	**0.605**	_1.194_	_0.942_	**0.219**	_0.420_
	PARABDG-N	_0.996_	_0.301_	0.028	_0.099_	**1.000**	_0.953_	_0.254_	_0.262_	**0.987**	**0.976**	_0.268_	**0.368**

dataset		*Spam*				*Cepg*				*Scht*			
metric		n_{ni}	$\triangle$	GCC	ALCC	n_{ni}	$\triangle$	GCC	ALCC	n_{ni}	$\triangle$	GCC	ALCC
model	GROUNDT	1.000	1.000	0.145	0.286	1.000	1.000	0.321	0.447	1.000	1.000	0.377	0.350
ER	EDGEIND	**1.000**	0.005	**0.003**	**0.003**	**1.000**	0.037	0.033	0.033	**1.000**	0.027	0.029	**0.029**
	PARABDG	0.783	**0.993**	_0.401_	_0.663_	0.688	**0.968**	**0.508**	**0.750**	0.617	**0.991**	0.559	_0.794_
	PARABDG-N	_1.006_	_1.009_	0.526	0.787	_1.008_	_0.832_	_0.606_	_0.839_	_1.002_	0.669	_0.604_	0.839
CL	EDGEIND	_0.906_	_0.496_	_0.072_	0.060	**0.953**	0.683	_0.230_	0.223	**0.964**	_0.644_	_0.245_	_0.234_
	PARABDG	0.700	**1.007**	**0.131**	**0.436**	0.698	**0.999**	**0.310**	_0.578_	0.866	**1.135**	**0.294**	0.610
	PARABDG-N	**0.908**	0.445	0.033	_0.071_	_0.927_	_0.725_	0.198	**0.334**	_0.932_	0.639	0.200	**0.347**
SB	EDGEIND	**0.982**	0.528	_0.094_	0.036	**0.994**	0.662	0.258	0.200	**0.992**	0.644	0.272	0.128
	PARABDG	0.685	**0.994**	**0.158**	**0.356**	0.911	**1.047**	_0.333_	**0.363**	0.792	**0.975**	**0.340**	**0.437**
	PARABDG-N	_0.957_	_0.537_	0.070	_0.109_	_0.990_	_1.056_	**0.329**	_0.202_	_0.972_	_0.956_	_0.292_	_0.205_
KR	EDGEIND	1.438	0.061	0.014	0.025	1.210	0.132	0.069	0.120	1.953	0.032	0.033	0.052
	PARABDG	_1.024_	_1.049_	_0.161_	**0.378**	_1.043_	**1.001**	_0.279_	**0.461**	_1.211_	_1.069_	0.346	**0.581**
	PARABDG-N	**0.995**	**0.981**	**0.161**	_0.385_	**0.996**	_1.118_	**0.296**	_0.478_	**0.997**	**1.030**	**0.370**	_0.640_

2) $\triangle$: the number of triangles
3) GCC: the global clustering coefficient
4) ALCC: the average clustering coefficient

As in the main text, the statistics are averaged on 100 random trials, i.e., 100 generated graphs.

For ER, we relax both the number of total nodes and the uniform edge probability, i.e., n_0 and p_0, for fitting. For the other three models (CL, SB, and KR), we still use the edge probabilities obtained from the original model and only add an additional term to the objective.

As shown in the results, in most cases, PARABDG generates graphs with fewer non-isolated nodes compared to the ground truth, and PARABDG-n well fits the number of non-isolated nodes while still improving clustering compared to EIGMs. Notably, since the total number of nodes for KR can only be a power of the seed-matrix size (i.e., a power of 2 in our experiments), the corresponding EIGM generates graphs with too many non-isolated nodes in many cases, while PARABDG-n generates graphs with a more similar number of non-isolated nodes (i.e., closer to the ground truth). Moreover, it is also known that even without binding, some models may suffer from the problem of isolated nodes, e.g., CL [49], [50] and KR [14], [51].

Overall, the results validate that, our tractability results allow practitioners to fit the number of non-isolated nodes (if that is one of their main concerns) while improving other aspects, e.g., clustering.

APPENDIX C
ADDITIONAL DISCUSSIONS

A. General graphs

As mentioned in Section II, we focus on undirected unweighted graphs without self-loops following common settings for random graph models in the main text. Below, we shall discuss different more general cases.

Directed edges and self-loops. In our binding schemes (Algorithms 1 to 3), if we consider directed edges and/or self-loops, we can further consider them after sampling a group of nodes. Regarding theoretical analysis, we can further consider subgraphs (motifs) with directed edges and self-loops [52] and the high-level ideas still apply.

Weighted edges. Our graph generation algorithms only determine the (in)existence of edges and we may need additional schemes to generate edge weights. For example, we can use algorithms that generate proper edge weights when given graph topology [53]. Since in our graph generation algorithms, nodes (and thus edges) can be sampled multiple times, an alternative way to have edge weights is to allow each edge to be inserted multiple times and use the times of repetition as edge weights.

B. Overlap-related triangle-density results

As mentioned in Section III-A, Chanpuriya et al. [18] have recently extended their theoretical analysis to other categories of RGMs. In addition to EIGMs, they further considered two other categories: node independent graph models (NIGMs) and fully dependent graph models (FDGMs). Between the two, FDGMs means any distribution of graphs, i.e., any RGM, is allowed.

They only discussed general overlap-related triangle-density upper bounds in those categories of RGMs, without detailed tractability results for practical graph generations. Specifically, their graph generation algorithm is based on maximal clique enumeration (MCE). However, given a graph, MCE itself can take exponential time [54].

Also, what we focus on in this work, i.e., the category of binding-based EPGMs, is a subset of EPGMs and are not "fully general" as FDGMs. On the other hand, NIGMs are associated with node embeddings, where we have a node embedding space (i.e., a distribution) $\mathcal{E}$ and a symmetric function $e: \mathcal{E} \times \mathcal{E} \to [0, 1]$, and each node i has a node embedding $\boldsymbol{x}_i$ sampled from $\mathcal{E}$ i.i.d., and each edge (i, j) exists with probability $e(\boldsymbol{x}_i, \boldsymbol{x}_j)$ independently. Our binding-based EPGMs do not fall in this category either.

C. Subset sampling

As mentioned in Footnote 5 in Section V-B, we use independent *node* sampling (yet still with *edge* dependency) which is simple, tractable, and works well. Specifically, independent node sampling allows us to easily compute the marginal probability of each node binding sampled in each round, which is involved in the derivation of our tractability results. Also, as shown in our experiments, with binding schemes using independent node sampling, we still achieve significant empirical improvement over EIGMs. In the most general case, considering the sampling probabilities of all $2^{|V|}$ subsets would be intractable. Recently, a line of works has been proposed for tractable and differentiable subset sampling [55]–[58], and exploring more flexible node sampling schemes is an interesting future direction to be explored.

D. Practical meaning of binding

As we mentioned in Section V-B, local binding (and parallel binding as a parallel version) binds node pairs *locally among a group of nodes* (instead of some irrelevant node pairs). Such node pairs are structurally related, and are expected to be meaningfully related in the corresponding real-world systems. We shall discuss two specific real-world scenarios below.

Group interactions in social networks. In typical social networks, nodes represent people, and edges represent social communications/relations between people. Each group "bound together" by our binding algorithms can represent a group interaction, e.g., an offline social event (meeting, conference, party) or an online social event (group chat, Internet forum, online game). In such social events, people gather together and the communications/relations between them likely co-occur. Certainly, not necessarily all people in such events would communicate with each other, e.g., some people are more familiar with each other. This is exactly the point of considering binding with various edge probabilities (instead of just inserting cliques).

Specifically, the random variable s represents the overall "social power" of an event, while individual edge probabilities $p(u, v)$'s represent some local factors (e.g., their personal relationship) between each pair of people. A line of research studies group interactions in social networks [31], [59]–[63].

Gene functional associations in gene networks. In typical gene networks, nodes represent genes, and edges represent gene functional associations, i.e., connections between genes that contribute jointly to a biological function. Each group "bound together" by our binding algorithms can represent a biological function, since typically (1) a single biological function involves multiple genes [32], [64], [65] (represented by a group of nodes bound together), and (2) the same biological function may involve different genes in different cases [66]–[68] (represented by the probabilistic nature of binding).

On parallel binding. Specifically, as mentioned in Section V-C, compared to local binding where each pair can only participate in a single group, parallel binding allows each pair to participate in multiple groups (in different rounds). This is also true for real-world group interactions, where different groups overlap and intersect with each other [69], [70].

APPENDIX D
ADDITIONAL DETAILS OF THE EXPERIMENTS

A. Experimental settings

Datasets. We use six real-world datasets from three different domains: (1) social networks *hamsterster (Hams)* and *facebook (Fcbk)*, (2) web graphs *polblogs (Polb)* and *spam (Spam)*, and (3) biological graphs *CE-PG (Cepg)* and *SC-HT (Scht)*.

The datasets are available online [71], [72]:

- *hamsterster (Hams)* [73] is available at https://networkrepository.com/soc-hamsterster.php
- *facebook (Fcbk)* [74] is available at https://snap.stanford.edu/data/ego-Facebook.html
- *polblogs (Polb)* [75] is available at https://networks.skewed.de/net/polblogs
- *spam (Spam)* [76] is available at https://networkrepository.com/web-spam.php
- *CE-PG (Cepg)* [77] is available at https://networkrepository.com/bio-CE-PG.php
- *SC-HT (Scht)* [77] is available at https://networkrepository.com/bio-SC-HT.php

In Table I, we show the basic statistics (e.g., the numbers of nodes and edges) of the datasets.

We provide the formal definitions of some basic statistics below.

Definition D.1 (Clustering coefficients). Given $G = (V, E)$, the number of wedges (i.e., open triangles) is $n_w(G) = \sum_{v \in V} \binom{d(v)}{2}$. The *global clustering coefficient* (GCC) of G is defined as

$$\mathrm{GCC}(G) = \frac{3 \triangle (G)}{n_w(G)},$$

where $\triangle(G)$ is the number of triangles in G and it is multiplied by 3 because each triangle corresponds to three wedges (consider three different nodes as the center of the wedge). The *average local clustering coefficient* (ALCC) of G is defined as

$$\mathrm{ALCC}(G) = \sum_{v:d(v) \geq 2} \frac{\triangle(v; G)}{\binom{d(v)}{2}},$$

where $\triangle(v; G)$ is the number of triangles involving v in G.

Models. The Erdős-Rényi (ER) model outputs edge probabilities with two parameters: n_0 and p_0, and the output is p_{n_0,p_0}^{ER} with $p_{n_0,p_0}^{ER}(u, v) = p_0, \forall u, v \in \binom{V}{2}$ with $V = [n_0]$. Given a graph $G = (V = [n], E)$, the standard fitting of ER gives $n_0 = n$ and $p_0 = \frac{|E|}{\binom{|V|}{2}}$.

The Chung-Lu (CL) model outputs edge probabilities with a sequence of expected degrees $D = (d_1, d_2, \ldots, d_n)$, and the output is p_D^{CL} with $p_D^{CL}(u, v) = \min(\frac{d_u d_v}{\sum_{i=1}^n d_i}, 1), \forall u, v \in \binom{V}{2}$ with $V = [n]$. Given a graph $G = (V = [n], E)$, the standard fitting of CL gives $d_i = d(i; G)$ for each node $i \in V$.

The stochastic block (SB) model outputs edge probabilities with (1) a partition of nodes which can be represented by an assignment function $f_B: [n_0] \to [c]$ with n_0 nodes and c blocks and (2) the edge probability between each pair of blocks (including between two identical blocks), which can be represented by $p_B: [c] \times [c] \to [0, 1]$, and the output is p_{f_B,p_B}^{SB} with $p_{f_B,p_B}^{SB}(u, v) = p_B(f_B(u), f_B(v)), \forall u, v \in [n_0]$. In our experiments, we use the Python library Graspologic [78] which contains a fitting algorithm for SB. Specifically, it uses spectral embedding [79]–[81] and a Gaussian mixture model [82] to obtain node partitions.

The stochastic Kronecker (KR) model outputs edge probabilities with a seed matrix $\theta \in [0, 1]^{2 \times 2}$ and a Kronecker power $k_{KR} \in \mathbb{N}$, and the output is $p_{\theta,k_{KR}}^{KR}$ with $p_{\theta,k_{KR}}^{KR}(u, v) = \theta_{uv}^{(k_{KR})}, \forall u, v \in \binom{V}{2}$ with $V = [2^{k_{KR}}]$, where $\theta^{(k_{KR})} \in [0, 1]^{2^{k_{KR}} \times 2^{k_{KR}}}$ is the k_{KR}-th Kronecker power of θ. In our experiments, we use `kronfit` [12] proposed by the original authors of KR.

Fitting. For fitting the parameters for our binding schemes, we use the Adam optimizer [83] with learning rate $\eta = 0.001$ and $n_{ep} = 10,000$ epochs for training. In our experiments, we consistently use $R = 100,000$ rounds for both of our binding schemes. By default, the input edge probabilities p are provided and fixed as described above. By default, the objective is the expected number of triangles. More specifically, it is

$$(1 - \frac{\mathbb{E}_{f_{p;g,R}^{\mathrm{x}}}[\triangle(G)]}{\triangle(G_{input})})^2$$

where

$$\mathbb{E}_{f_{p;g,R}^{\mathrm{x}}}[\triangle(G)] = \sum_{V' \in \binom{V}{3}} \Pr_{f_{p;g,R}^{\mathrm{x}}} \left[E(G[V']) = \binom{V'}{2} \right]$$

is the expected number of triangles in a generated graph with $X \in \{\textsc{LoclBdg}, \textsc{ParaBdg}\}$ indicating the binding scheme, and $\triangle(G_{input})$ is the ground-truth number of triangles in the input graph.

We observe that our fitting algorithms assign different node-sampling probabilities to different nodes, which implies that different nodes have different levels of importance in binding. In Figure 5, for the CL model and for each dataset, we show the relations between nodes' degrees and their node-sampling probabilities in $\textsc{LoclBdg}$ and $\textsc{ParaBdg}$. For $\textsc{LoclBdg}$, we observe strong positive correlations between node degrees and node-sampling probabilities. For $\textsc{ParaBdg}$, similar trends are observed, but the patterns are quite different. Also, we can observe that the node-sampling probabilities for $\textsc{ParaBdg}$ are overall lower than those for $\textsc{LoclBdg}$, as mentioned in Section VI-D.

TABLE VIII: The clustering metrics of graphs generated by different realization methods, with the standard deviations. The number of triangles ($\triangle$) is normalized.

dataset		*Hams*			*Fcbk*			*Polb*		
metric		$\triangle$	GCC	ALCC	$\triangle$	GCC	ALCC	$\triangle$	GCC	ALCC
model	GROUNDT	1.000	0.229	0.540	1.000	0.519	0.606	1.000	0.226	0.320
ER	EDGEIND	0.013	0.008	0.008	0.009	0.011	0.011	0.034	0.022	0.022
	(std)	0.001	0.000	0.000	0.000	0.000	0.000	0.001	0.000	0.000
	LOCLBDG	0.997	0.321	0.236	1.010	0.448	0.223	0.955	0.336	0.247
	(std)	0.279	0.028	0.022	0.445	0.077	0.042	0.320	0.038	0.032
	PARABDG	0.988	0.385	0.640	1.002	0.574	0.815	1.025	0.412	0.659
	(std)	0.081	0.014	0.018	0.155	0.036	0.026	0.135	0.022	0.028
CL	EDGEIND	0.299	0.067	0.058	0.124	0.064	0.063	0.792	0.183	0.173
	(std)	0.010	0.002	0.002	0.002	0.001	0.001	0.017	0.002	0.005
	LOCLBDG	0.992	0.165	0.255	1.026	0.255	0.305	1.002	0.214	0.341
	(std)	0.353	0.030	0.026	1.033	0.095	0.050	0.132	0.008	0.021
	PARABDG	1.000	0.185	0.471	1.006	0.336	0.626	1.010	0.221	0.468
	(std)	0.144	0.013	0.013	0.261	0.035	0.018	0.068	0.003	0.009
SB	EDGEIND	0.263	0.080	0.038	0.153	0.145	0.080	0.478	0.145	0.164
	(std)	0.007	0.001	0.001	0.002	0.001	0.000	0.012	0.002	0.004
	LOCLBDG	1.039	0.219	0.240	0.934	0.429	0.331	0.994	0.237	0.355
	(std)	0.419	0.042	0.026	0.732	0.086	0.074	0.386	0.025	0.037
	PARABDG	0.993	0.241	0.521	1.035	0.529	0.557	1.010	0.183	0.251
	(std)	0.118	0.013	0.012	0.504	0.064	0.042	1.819	0.076	0.054
KR	EDGEIND	0.185	0.039	0.060	0.052	0.035	0.042	0.101	0.040	0.075
	(std)	0.006	0.001	0.002	0.001	0.000	0.001	0.003	0.001	0.003
	LOCLBDG	1.095	0.152	0.230	0.927	0.239	0.270	1.061	0.141	0.234
	(std)	0.580	0.047	0.028	1.090	0.117	0.048	2.234	0.106	0.054
	PARABDG	0.997	0.165	0.394	0.971	0.347	0.605	0.942	0.219	0.420
	(std)	0.210	0.021	0.016	0.395	0.055	0.017	0.601	0.075	0.035

dataset		*Spam*			*Cepg*			*Scht*		
metric		$\triangle$	GCC	ALCC	$\triangle$	GCC	ALCC	$\triangle$	GCC	ALCC
model	GROUNDT	1.000	0.145	0.286	1.000	0.321	0.447	1.000	0.377	0.350
ER	EDGEIND	0.005	0.003	0.003	0.037	0.033	0.033	0.027	0.029	0.029
	(std)	0.000	0.000	0.000	0.001	0.000	0.000	0.000	0.000	0.000
	LOCLBDG	0.993	0.336	0.234	1.016	0.397	0.258	1.012	0.420	0.251
	(std)	0.158	0.022	0.013	0.557	0.083	0.057	0.687	0.094	0.063
	PARABDG	0.993	0.401	0.663	0.968	0.508	0.750	0.991	0.559	0.794
	(std)	0.047	0.010	0.011	0.183	0.039	0.038	0.198	0.043	0.035
CL	EDGEIND	0.496	0.072	0.060	0.683	0.230	0.223	0.644	0.245	0.234
	(std)	0.010	0.001	0.002	0.008	0.001	0.004	0.006	0.001	0.003
	LOCLBDG	1.028	0.124	0.260	0.996	0.293	0.430	1.036	0.318	0.469
	(std)	0.214	0.016	0.019	0.241	0.018	0.033	0.367	0.028	0.042
	PARABDG	1.007	0.131	0.436	0.999	0.310	0.578	1.135	0.294	0.610
	(std)	0.074	0.006	0.011	0.107	0.004	0.010	1.290	0.079	0.033
SB	EDGEIND	0.528	0.094	0.036	0.662	0.258	0.200	0.644	0.272	0.128
	(std)	0.013	0.002	0.001	0.008	0.002	0.002	0.006	0.001	0.001
	LOCLBDG	0.985	0.152	0.223	0.986	0.323	0.415	1.034	0.354	0.386
	(std)	0.171	0.018	0.017	0.450	0.037	0.046	0.368	0.034	0.042
	PARABDG	0.994	0.158	0.356	1.047	0.333	0.363	0.975	0.340	0.437
	(std)	0.110	0.013	0.017	0.541	0.085	0.056	0.298	0.045	0.030
KR	EDGEIND	0.061	0.014	0.025	0.132	0.069	0.120	0.032	0.033	0.052
	(std)	0.002	0.000	0.001	0.002	0.001	0.002	0.001	0.000	0.001
	LOCLBDG	0.943	0.118	0.187	0.990	0.175	0.312	1.444	0.181	0.277
	(std)	0.759	0.055	0.028	2.112	0.098	0.077	3.610	0.132	0.079
	PARABDG	1.049	0.161	0.378	1.001	0.279	0.461	1.069	0.346	0.581
	(std)	0.319	0.032	0.017	0.757	0.098	0.044	1.165	0.152	0.035
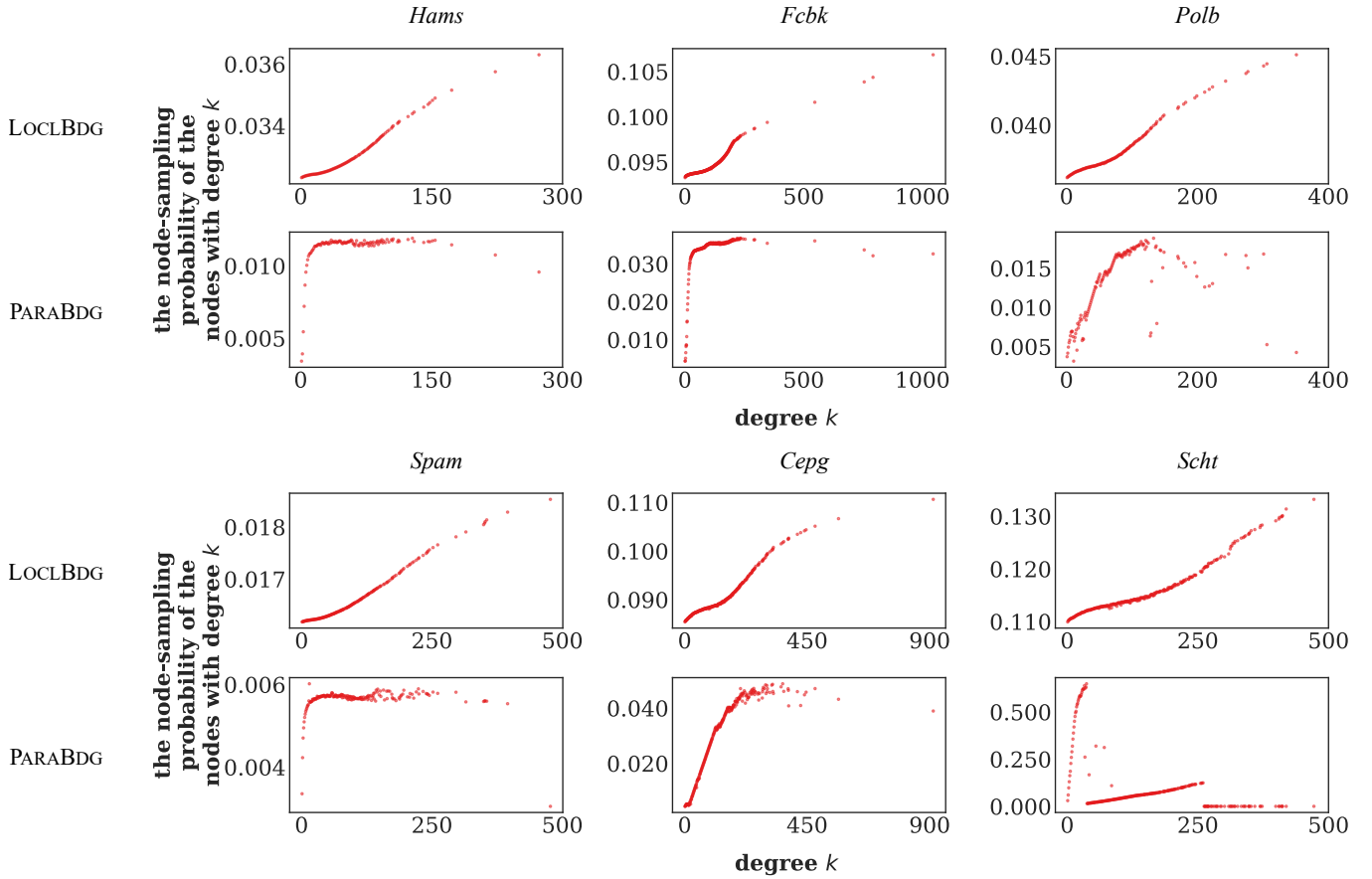
Fig. 5: The relations between node degrees and node-sampling probabilities.

Hardware and software. All the experiments of fitting are run on a machine with two Intel Xeon® Silver 4210R (10 cores, 20 threads) processors, a 512GB RAM, and RTX A6000 (48GB) GPUs. A single GPU is used for each fitting process. The code for fitting is written in Python, using Pytorch [39]. All the experiments of graph generation are run on a machine with one Intel i9-10900K (10 cores, 20 threads) processor, a 64GB RAM. The code for generation is written in C++, compiled with G++ with O2 optimization and OpenMP [40] parallelization.

B. P1: clustering

As mentioned in Section VI-B, the results in Table II are averaged on 100 random trials. In Table VIII, we show the full results with standard deviations. With binding, the variance is higher since the covariances between edges are higher with dependency. We also compute the mean squared errors w.r.t. each metric. The results are in Table IX. Notably, for graph generators, variability is desirable in many cases [13], [84].

Exchangeable network models. We tried the method by [85] for graph generation for exchangeable network models. We used the official MATLAB code by the authors,[9] to conduct inference and graph generation on the real-world graph datasets used in our experiments. In most cases, the generated graphs have much lower clustering than the ground truth. See Table XII for the detailed results.

Exponential random graph models. We tried to fit ERGMs to the datasets we use w.r.t. two features: The number of edges and the number of triangles. For each dataset, when given 5 hours for fitting, the fit ERGM model generates near-empty graphs in most cases (most generated graphs have fewer than 100 edges), likely because the used datasets are too large for ERGMs to converge to a meaningful distribution. See, e.g., the discussions by [86], [87], and [88]. We used an online open-source implementation of ERGMs.[10] Notably, fitting ERGMs to large graphs is an active research topic itself, see, e.g., the work by [89].

---

[9]https://github.com/airoldilab/SAS

[10]https://github.com/jcatw/ergm

Fig. 6: The degree (top) and distance (bottom) distributions of graphs generated by different realization methods. All the plots are in a log-log scale. Each shaded area represents one standard deviation.

TABLE IX: The mean squared errors w.r.t. clustering metrics of graphs generated by different realization methods. The number of triangles (△) is normalized.

dataset		*Hams*			*Fcbk*			*Polb*		
metric		△	GCC	ALCC	△	GCC	ALCC	△	GCC	ALCC
model	GROUNDT	0.000	0.000	0.000	0.000	0.000	0.000	0.000	0.000	0.000
ER	EDGEIND	0.974	0.049	0.283	0.983	0.258	0.354	0.934	0.042	0.089
	LOCLBDG	0.078	0.009	0.093	0.199	0.011	0.148	0.104	0.013	0.007
	PARABDG	0.007	0.024	0.010	0.024	0.004	0.044	0.019	0.035	0.115
CL	EDGEIND	0.492	0.026	0.233	0.767	0.207	0.295	0.044	0.002	0.022
	LOCLBDG	0.125	0.005	0.082	1.068	0.079	0.093	0.017	0.000	0.001
	PARABDG	0.021	0.002	0.005	0.068	0.035	0.001	0.005	0.000	0.022
SB	EDGEIND	0.544	0.022	0.252	0.718	0.140	0.276	0.273	0.007	0.025
	LOCLBDG	0.177	0.002	0.091	0.539	0.015	0.081	0.149	0.001	0.002
	PARABDG	0.014	0.000	0.001	0.255	0.004	0.004	3.303	0.008	0.008
KR	EDGEIND	0.664	0.036	0.230	0.898	0.234	0.317	0.809	0.034	0.060
	LOCLBDG	0.346	0.008	0.097	1.194	0.092	0.115	4.989	0.018	0.010
	PARABDG	0.044	0.005	0.022	0.157	0.033	0.000	0.364	0.006	0.011

dataset		*Spam*			*Cepg*			*Scht*		
metric		△	GCC	ALCC	△	GCC	ALCC	△	GCC	ALCC
model	GROUNDT	0.000	0.000	0.000	0.000	0.000	0.000	0.000	0.000	0.000
ER	EDGEIND	0.990	0.020	0.080	0.927	0.083	0.171	0.947	0.121	0.103
	LOCLBDG	0.025	0.037	0.003	0.310	0.013	0.039	0.473	0.011	0.014
	PARABDG	0.002	0.066	0.143	0.035	0.037	0.093	0.039	0.035	0.198
CL	EDGEIND	0.254	0.005	0.051	0.100	0.008	0.050	0.126	0.017	0.014
	LOCLBDG	0.046	0.001	0.001	0.058	0.001	0.001	0.136	0.004	0.016
	PARABDG	0.006	0.000	0.023	0.012	0.000	0.017	1.682	0.013	0.069
SB	EDGEIND	0.223	0.003	0.062	0.114	0.004	0.061	0.127	0.011	0.049
	LOCLBDG	0.030	0.000	0.004	0.202	0.001	0.003	0.136	0.002	0.003
	PARABDG	0.012	0.000	0.005	0.295	0.007	0.010	0.089	0.003	0.008
KR	EDGEIND	0.882	0.017	0.068	0.754	0.064	0.107	0.936	0.118	0.089
	LOCLBDG	0.579	0.004	0.011	4.462	0.031	0.024	13.233	0.056	0.012
	PARABDG	0.104	0.001	0.009	0.573	0.011	0.002	1.361	0.024	0.054

C. P2: degrees, distances, and other graph statistics

Definition D.2 (Paths and distance). Given a graph $G = (V, E)$, a sequences of nodes $(v_1, v_2, \ldots, v_t)$ consisting of t distinct nodes is a *path* between v_1 and v_t, if $(v_i, v_{i+1}) \in E, \forall i \in [t-1]$, and t is called the length of the path. Given two nodes $u, v \in V$, the *distance* between u and v is the length of the shortest path between u and v.

Definition D.3 (Connected components). Given a graph $G = (V, E)$, and two nodes $u, v \in V$, we say u and v are in the same *connected component*, if and only if there exists at least one path between u and v. This relation of "being in the same connected component" forms equivalent classes among the nodes, and each equivalent class is a connected component. A *largest connected component* is a connected component with the largest size (i.e., the number of nodes in it).[11]

In Figure 6, for each dataset (each column) and each model (each row), we compare the degree distributions and distance distributions in the ground-truth graph and the graphs generated with each realization method, supplementing Figure 1.

In Table X, we provide the detailed numerical results w.r.t. degrees and distances. Specifically, for each dataset, each mode, and each realization method, we report the following statistics:

- the results of the linear regression of node degrees k and the number of nodes with each degree k on a log-log scale: the fit slope (the exponent α in the corresponding power-law fitting) and the r value (the strength of a power law)
- the average path length (APL) and the 90%-effective diameter (d_{eff}) in the largest connected component[12]

With binding, the generated graphs are overall closer to ground truth w.r.t. some other graph metrics: modularity [90], conductance [91], core numbers [92], average vertex betweenness [93], average edge betweenness [94], and natural connectivity [95]. See Tables XIII to XVIII for the detailed results. Modularity is computed after obtaining partitions using the Louvain algorithm [96]. Conductance is computed after obtaining bi-partitions using the Kernighan-Lin bisection algorithm [97].

---

[11]A graph may contain several equal-size largest connected components, but it rarely happens for real-world graphs.

[12]The average path length is the average distance of the pairs in the largest connected component, and the 90%-effective diameter is the minimum distance d such that at least 90% of the pairs in the largest connected component have distances at most d.

TABLE X: The numerical results regarding degrees and distances of graphs generated by different realization methods.

dataset		*Hams*				*Fcbk*				*Polb*			
metric		α	r	APL	d_{eff}	α	r	APL	d_{eff}	α	r	APL	d_{eff}
model	GROUNDT	-1.432	-0.934	3.589	5.000	-1.180	-0.900	3.693	5.000	-1.069	-0.921	2.738	4.000
ER	EDGEIND	-0.058	-0.008	3.004	4.000	-0.046	-0.005	2.606	3.000	0.009	0.007	2.507	3.000
	LOCLBDG	-1.301	-0.850	3.254	4.060	-1.076	-0.869	2.892	3.950	-0.978	-0.828	2.703	3.570
	PARABDG	-0.958	-0.553	2.996	4.000	-2.338	-0.797	2.262	3.000	-1.136	-0.663	2.416	3.000
CL	EDGEIND	-1.414	-0.927	2.938	4.000	-1.185	-0.898	2.608	3.000	-1.055	-0.920	2.585	3.000
	LOCLBDG	-1.262	-0.935	2.772	3.390	-1.058	-0.917	2.493	3.000	-0.974	-0.906	2.414	3.000
	PARABDG	-1.282	-0.924	2.713	3.000	-0.980	-0.877	2.331	3.000	-0.968	-0.900	2.373	3.000
SB	EDGEIND	-1.211	-0.853	3.309	4.000	-0.600	-0.399	3.507	5.000	-0.967	-0.766	2.717	4.000
	LOCLBDG	-1.263	-0.905	3.193	4.420	-1.028	-0.823	4.276	6.480	-0.959	-0.884	2.525	3.020
	PARABDG	-1.209	-0.872	3.000	4.070	-0.409	-0.294	3.429	5.190	-0.954	-0.824	2.595	3.430
KR	EDGEIND	-1.359	-0.909	2.856	3.990	-1.185	-0.806	2.566	3.000	-1.332	-0.912	2.848	3.940
	LOCLBDG	-1.272	-0.937	2.764	3.320	-1.134	-0.924	2.613	3.090	-1.174	-0.924	2.715	3.300
	PARABDG	-1.301	-0.934	2.742	3.010	-1.104	-0.915	2.499	3.000	-1.164	-0.928	2.661	3.050

dataset		*Spam*				*Cepg*				*Scht*			
metric		α	r	APL	d_{eff}	α	r	APL	d_{eff}	α	r	APL	d_{eff}
model	GROUNDT	-1.495	-0.947	3.794	5.000	-0.917	-0.907	2.711	4.000	-0.950	-0.860	2.772	4.000
ER	EDGEIND	-0.054	-0.008	3.384	4.000	-0.067	-0.009	2.119	3.000	-0.078	-0.011	2.135	3.000
	LOCLBDG	-1.551	-0.856	3.601	4.840	-0.843	-0.821	2.482	3.210	-0.848	-0.825	2.532	3.340
	PARABDG	-1.069	-0.541	3.312	4.000	-1.858	-0.765	2.033	2.490	-2.274	-0.800	1.981	2.000
CL	EDGEIND	-1.477	-0.943	3.119	4.000	-0.918	-0.897	2.415	3.000	-0.964	-0.905	2.430	3.000
	LOCLBDG	-1.364	-0.944	2.850	3.440	-0.789	-0.866	2.195	3.000	-0.802	-0.875	2.215	3.000
	PARABDG	-1.389	-0.940	2.811	3.000	-0.715	-0.809	2.096	3.000	-0.779	-0.825	2.201	3.000
SB	EDGEIND	-1.448	-0.893	3.729	5.000	-0.715	-0.644	2.650	4.000	-0.790	-0.749	2.661	4.000
	LOCLBDG	-1.441	-0.938	3.274	4.550	-0.718	-0.803	2.318	3.030	-0.713	-0.814	2.289	3.000
	PARABDG	-1.445	-0.931	3.021	4.000	-0.713	-0.661	2.397	3.000	-0.756	-0.793	2.307	3.000
KR	EDGEIND	-1.602	-0.929	3.466	4.000	-0.976	-0.807	2.303	3.000	-1.338	-0.882	2.747	3.000
	LOCLBDG	-1.457	-0.951	3.177	4.000	-1.010	-0.909	2.343	3.000	-1.100	-0.912	2.649	3.300
	PARABDG	-1.498	-0.953	3.126	4.000	-0.978	-0.904	2.313	3.000	-1.023	-0.891	2.522	3.000

TABLE XI: The time (in seconds) for graph generation with different realization methods.

dataset		*Hams*	*Fcbk*	*Polb*	*Spam*	*Cepg*	*Scht*
ER	EDGEIND	<0.05	<0.05	<0.05	<0.05	<0.05	<0.05
	LOCLBDG	3.2	7.9	2.2	7.7	3.7	4.9
	PARABDG	<0.05	<0.05	<0.05	0.1	<0.05	<0.05
	PARABDG-S	0.2	0.1	<0.05	0.8	<0.05	<0.05
CL	EDGEIND	<0.05	<0.05	<0.05	<0.05	<0.05	<0.05
	LOCLBDG	4.0	48.2	2.4	9.3	6.3	11.5
	PARABDG	0.3	1.1	0.2	0.7	0.3	1.5
	PARABDG-S	3.0	9.4	1.8	6.8	2.6	13.9
SB	EDGEIND	0.1	0.1	0.1	0.1	0.1	0.1
	LOCLBDG	4.0	177.6	4.0	8.9	10.3	10.6
	PARABDG	0.3	6.2	0.9	0.7	1.0	0.7
	PARABDG-S	3.1	33.7	8.6	7.2	9.8	6.6
KR	EDGEIND	0.1	0.1	<0.05	0.1	<0.05	0.1
	LOCLBDG	4.7	49.0	16.6	28.5	81.0	200.1
	PARABDG	0.3	1.7	0.5	1.6	0.9	6.8
	PARABDG-S	3.2	12.6	5.2	14.2	10.5	31.3

In most cases, the metrics in the graphs generated with binding are closer to the ground truth, indicating that binding improves the generation quality in various aspects.

D. Graph generation speed and scalability

In Table XI, for each dataset and each model, we report the running time of graph generation (averaged on 100 random trials) using EDGEIND, LOCLBDG, PARABDG, and serialized PARABDG without parallelization (PARABDG-S). The algorithmic details of EDGEIND for each model are as follows:

- We try to find an optimized and fast algorithm for each model in C++
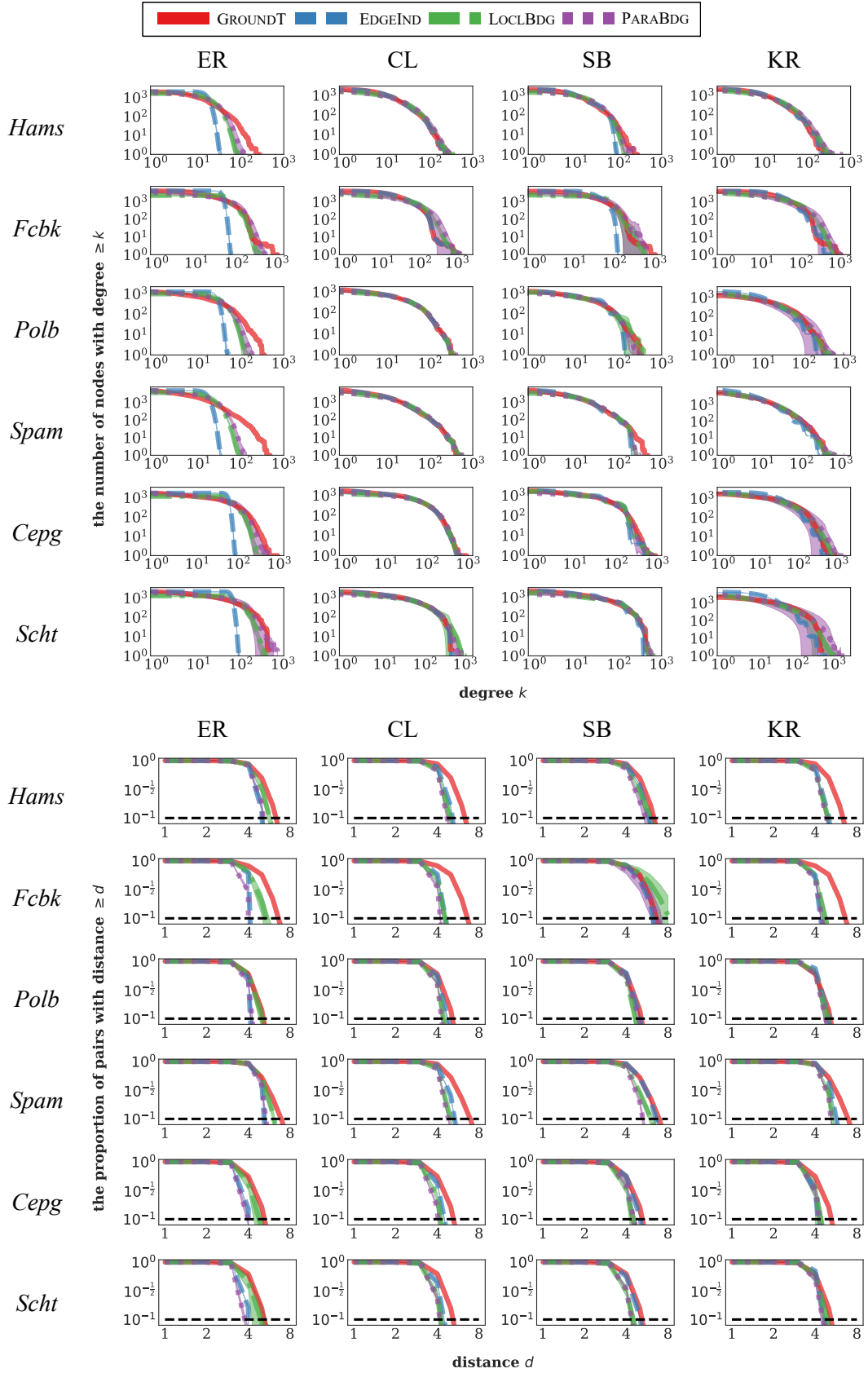- For ER, we use the Boost Graph Library [98]
- For CL, we use NetworKit [99]
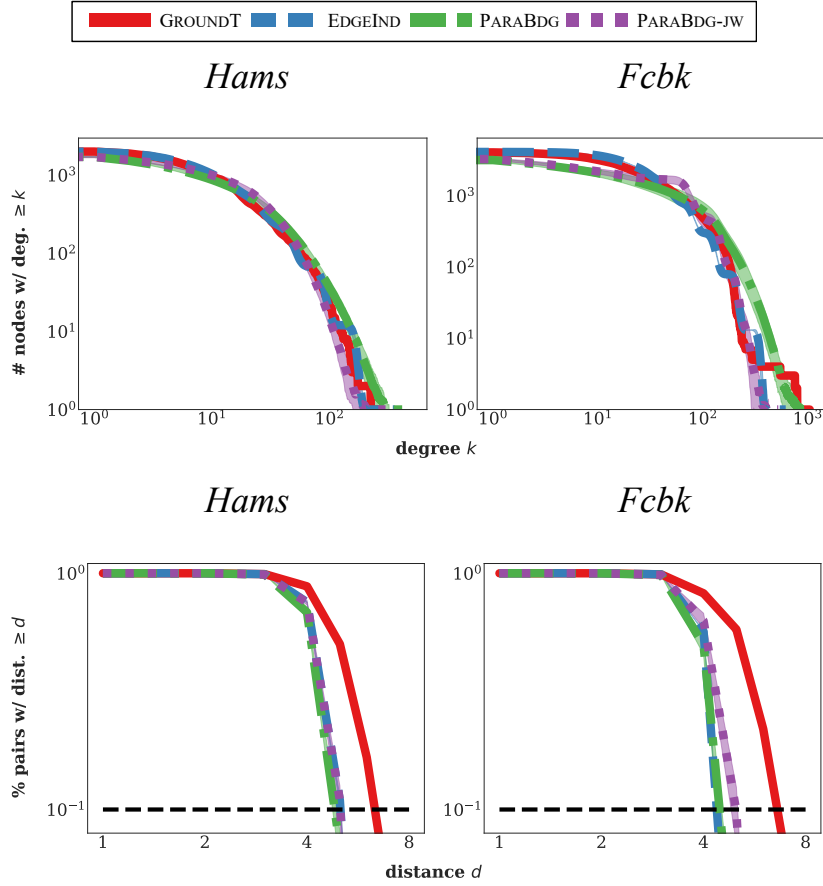
Fig. 7: The degree (top) and distance (bottom) distributions of graphs generated by different realization methods. Each shaded area represents one standard deviation.

TABLE XII: The clustering metrics of graphs generated by exchangeable network models using the method by [85]. The number of triangles ($\triangle$) is normalized.

dataset	$\triangle$	GCC	ALCC
facebook (ground truth)	1.000	0.519	0.606
facebook [85]	0.240	0.129	0.038
hamsterster (ground truth)	1.000	0.229	0.540
hamsterster [85]	0.261	0.067	0.031
web-spam (ground truth)	1.000	0.145	0.286
web-spam [85]	0.470	0.080	0.028
polblogs (ground truth)	1.000	0.226	0.320
polblogs [85]	0.576	0.133	0.132
bio-CE-PG (ground truth)	1.000	0.321	0.447
bio-CE-PG [85]	0.636	0.199	0.201
bio-SC-HT (ground truth)	1.000	0.377	0.350
bio-SC-HT [85]	0.820	0.305	0.153

- For SB, we use online code in a GitHub repo[13]
- For KR, we use `krongen` in SNAP [43]

Consistent with our observation in Section VI-D, EDGEIND is fastest with the simplest algorithmic nature, and between the two binding schemes, PARABDG is noticeably faster than LOCLBDG, and is even faster with parallelization.

We upscale the hamsterster (*Hams*) dataset by duplicating the whole graph multiple times.

- The original dataset contains $|V| = 2000$ nodes.
- For ER, we upscale the total number of nodes.
- For CL, we upscale the number of nodes with each degree.
- For SB, we upscale the number of nodes in each block.

[13]https://github.com/ntamas/blockmodel

TABLE XIII: The modularity in the graphs generated by different realization methods.

	dataset	*Hams*	*Fcbk*	*Polb*	*Spam*	*Cepg*	*Scht*
model	GROUNDT	0.474	0.777	0.427	0.462	0.434	0.253
ER	EDGEIND	0.210	0.120	0.155	0.205	0.104	0.099
	LOCLBDG	0.394	0.443	0.353	0.440	0.321	0.369
	PARABDG	0.365	0.517	0.323	0.394	0.392	0.430
CL	EDGEIND	0.193	0.107	0.127	0.180	0.082	0.078
	LOCLBDG	0.325	0.343	0.184	0.303	0.184	0.205
	PARABDG	0.301	0.332	0.152	0.271	0.118	0.262
SB	EDGEIND	0.317	0.756	0.423	0.370	0.407	0.208
	LOCLBDG	0.386	0.751	0.422	0.396	0.417	0.235
	PARABDG	0.375	0.741	0.482	0.432	0.466	0.263
KR	EDGEIND	0.190	0.114	0.193	0.254	0.107	0.142
	LOCLBDG	0.322	0.357	0.335	0.424	0.248	0.313
	PARABDG	0.314	0.367	0.420	0.411	0.304	0.385

TABLE XIV: The conductance in the graphs generated by different realization methods.

	dataset	*Hams*	*Fcbk*	*Polb*	*Spam*	*Cepg*	*Scht*
model	GROUNDT	0.131	0.012	0.079	0.147	0.075	0.556
ER	EDGEIND	0.330	0.394	0.369	0.327	0.407	0.411
	LOCLBDG	0.235	0.181	0.271	0.201	0.311	0.251
	PARABDG	0.226	0.188	0.253	0.212	0.241	0.226
CL	EDGEIND	0.744	0.830	0.869	0.831	0.901	0.911
	LOCLBDG	0.444	0.265	0.816	0.492	0.813	0.809
	PARABDG	0.540	0.453	0.826	0.687	0.847	0.326
SB	EDGEIND	0.261	0.067	0.081	0.207	0.090	0.615
	LOCLBDG	0.222	0.017	0.080	0.186	0.083	0.597
	PARABDG	0.228	0.021	0.086	0.245	0.067	0.472
KR	EDGEIND	0.814	0.776	0.863	0.828	0.883	0.853
	LOCLBDG	0.411	0.406	0.420	0.265	0.474	0.216
	PARABDG	0.432	0.282	0.211	0.288	0.359	0.208

TABLE XV: The max core number in the graphs generated by different realization methods.

	dataset	*Hams*	*Fcbk*	*Polb*	*Spam*	*Cepg*	*Scht*
model	GROUNDT	24.0	115.0	36.0	35.0	80.0	100.0
ER	EDGEIND	11.0	32.7	19.5	10.9	42.9	46.9
	LOCLBDG	29.5	120.9	42.6	33.9	94.3	117.3
	PARABDG	18.7	70.4	28.1	20.9	61.7	79.8
CL	EDGEIND	16.9	43.7	33.5	25.6	66.7	79.4
	LOCLBDG	30.6	104.3	35.9	35.3	76.6	96.2
	PARABDG	24.4	105.7	35.3	27.1	73.1	96.9
SB	EDGEIND	21.4	71.8	33.9	37.6	99.8	96.4
	LOCLBDG	31.4	88.7	34.8	40.4	85.1	98.4
	PARABDG	26.3	121.3	37.4	38.4	107.8	109.0
KR	EDGEIND	15.5	32.0	15.9	13.0	36.2	25.0
	LOCLBDG	31.6	98.4	33.7	37.9	68.8	84.9
	PARABDG	26.3	107.6	38.5	37.7	86.1	109.4

TABLE XVI: The average vertex betweenness (normalized w.r.t. the ground-truth value) in the graphs generated by different realization methods.

	dataset	*Hams*	*Fcbk*	*Polb*	*Spam*	*Cepg*	*Scht*
model	GROUNDT	1.000	1.000	1.000	1.000	1.000	1.000
ER	EDGEIND	0.794	0.610	0.863	0.876	0.666	0.647
	LOCLBDG	0.975	0.888	1.065	1.078	0.938	1.103
	PARABDG	0.954	0.945	1.038	1.089	0.944	0.954
CL	EDGEIND	0.790	0.605	0.940	0.835	0.893	0.817
	LOCLBDG	0.903	0.808	0.998	0.965	0.983	0.919
	PARABDG	0.873	0.755	0.985	0.946	0.929	0.792
SB	EDGEIND	0.898	0.961	0.999	1.024	0.976	0.929
	LOCLBDG	1.084	1.234	1.133	1.202	1.064	1.169
	PARABDG	1.126	1.446	1.000	1.081	0.917	0.945
KR	EDGEIND	0.730	0.582	0.654	0.626	0.628	0.503
	LOCLBDG	0.809	0.751	0.817	0.754	0.715	0.668
	PARABDG	0.818	0.757	0.815	0.762	0.804	0.715

TABLE XVII: The average edge betweenness (normalized w.r.t. the ground-truth value) in the graphs generated by different realization methods.

	dataset	Hams	Fcbk	Polb	Spam	Cepg	Scht
model	GROUNDT	1.000	1.000	1.000	1.000	1.000	1.000
ER	EDGEIND	0.855	0.718	0.913	0.910	0.792	0.776
	LOCLBDG	0.996	1.047	1.152	1.155	0.984	3.350
	PARABDG	1.010	1.435	1.170	1.163	1.345	1.402
CL	EDGEIND	0.863	0.719	0.995	0.911	0.962	0.902
	LOCLBDG	1.062	1.159	1.122	1.090	1.186	1.050
	PARABDG	0.983	0.970	1.090	1.073	1.138	0.877
SB	EDGEIND	0.927	0.972	1.009	1.023	0.985	0.958
	LOCLBDG	1.055	2.142	1.358	1.297	1.274	1.480
	PARABDG	1.233	1.406	1.029	1.170	0.935	1.129
KR	EDGEIND	0.770	0.704	0.689	0.666	0.742	0.566
	LOCLBDG	0.886	1.141	0.952	0.807	1.089	1.088
	PARABDG	0.897	1.151	0.913	0.850	1.191	1.095

TABLE XVIII: The natural connectivity (normalized w.r.t. the ground-truth value) in the graphs generated by different realization methods.

	dataset	Hams	Fcbk	Polb	Spam	Cepg	Scht
model	GROUNDT	1.000	1.000	1.000	1.000	1.000	1.000
ER	EDGEIND	0.863	0.719	0.995	0.911	0.962	0.902
	LOCLBDG	1.062	1.159	1.122	1.090	1.186	1.050
	PARABDG	0.983	0.970	1.090	1.073	1.138	0.877
CL	EDGEIND	0.878	0.633	1.050	0.884	0.960	0.895
	LOCLBDG	1.090	1.074	1.093	0.971	1.042	1.017
	PARABDG	0.993	0.900	1.095	0.930	1.032	1.003
SB	EDGEIND	0.771	0.523	0.787	0.912	0.872	0.890
	LOCLBDG	1.119	0.716	0.892	0.951	0.933	0.936
	PARABDG	0.869	0.864	1.070	0.926	1.000	0.924
KR	EDGEIND	0.789	0.475	0.518	0.427	0.561	0.316
	LOCLBDG	1.160	0.923	0.971	1.000	1.288	0.966
	PARABDG	0.947	0.807	1.024	0.684	0.889	0.837

TABLE XIX: The results of the scalability experiments when upscaling the input graph (time: seconds).

model	$|V|$	2k	4k	8k	16k	32k	64k	128k
ER	LOCLBDG	3.194	6.505	16.365	45.648	143.394	494.536	1859.232
	PARABDG	0.034	0.058	0.113	0.232	0.601	1.705	5.381
CL	LOCLBDG	3.962	9.595	35.364	123.902	472.281	2162.315	8402.245
	PARABDG	0.302	0.495	1.027	2.114	4.404	11.184	31.129
SB	LOCLBDG	3.989	9.493	29.557	99.167	362.930	1648.392	8398.062
	PARABDG	0.266	0.489	0.994	2.132	5.335	14.861	45.983
KR	LOCLBDG	8.611	31.241	124.453	506.921	2097.190	8680.988	33918.420
	PARABDG	0.428	1.209	4.277	20.339	113.452	705.571	4351.573

- For KR, we upscale the number of nodes by increasing the Kronecker power.
- With 32GB RAM, all the proposed methods can run with $|V| = 128000$ (64× of the original graph).

See Table XIX for the detailed results.

To handle even large graphs, we further provide an alternative implementation with parallel binding (PARABDG), where we

- Save the memory usage by considering the classes of node pairs with the same probability.
  - For ER, it would be all the pairs.
  - For CL, each class contains node pairs with the same node degrees.
  - For SB, each class contains node pairs from the same blocks.
- Directly save the cliques among nodes in the same group and bi-cliques between nodes in two different groups, instead of individual edges.
- Directly save the generated edges to the hard disk, instead of storing them in RAM.

By doing so, we are able to scale to even large graphs. See Table XX for the detailed results.

E. Joint optimization

As shown in Section VI-E, in some "difficult" cases where PARABDG well preserves the number of triangles but not the number of wedges, with joint optimization, PARABDG-JW does better, well preserving both the number of triangles and the

TABLE XX: The results of the scalability experiments when upscaling the input graph using parallel binding (PARABDG) with additional optimization for large graphs.

(a) Runtime (seconds).

model	$|V|$	1m	2m	4m	8m	16m	32m	64m
ER	PARABDG	5.942	12.449	28.174	60.975	121.889	262.736	490.985
CL	PARABDG	102.150	220.177	423.836	815.883	1685.561	3135.217	6179.357
SB	PARABDG	106.026	213.722	428.980	869.002	1798.333	3829.563	8638.938
KR	PARABDG	105.062	219.351	439.110	875.381	1751.339	3504.719	7014.911

(b) Memory (MB).

model	$|V|$	1m	2m	4m	8m	16m	32m	64m
ER	PARABDG	20.94	38.23	68.78	135.71	259.30	547.09	1080.80
CL	PARABDG	137.80	254.16	508.07	953.98	1899.38	3713.34	7371.52
SB	PARABDG	241.62	473.59	943.81	1797.39	3557.76	6867.88	12801.86
KR	PARABDG	1754.9	3113.07	5248.23	10657.96	14151.30	22161.09	38100.75

TABLE XXI: Additional empirical evaluation on other models.

dataset	*Hams*				*Fcbk*				*Polb*			
metric	△	GCC	ALCC	overlap	△	GCC	ALCC	overlap	△	GCC	ALCC	overlap
GROUNDT	1.000	0.229	0.540	N/A	1.000	0.519	0.606	N/A	1.000	0.226	0.320	N/A
EDGEIND-CL	0.299	0.067	0.058	0.059	0.124	0.064	0.063	0.063	0.792	0.183	0.173	0.182
LOCLBDG-CL	0.992	0.165	0.255	0.058	1.026	0.255	0.305	0.063	1.002	0.214	0.341	0.181
PARABDG-CL	1.000	0.185	0.471	0.059	1.006	0.336	0.626	0.062	1.010	0.221	0.468	0.181
PA	0.198	0.049	0.049	0.047	0.120	0.061	0.061	0.062	0.324	0.100	0.101	0.097
RGG (d = 1)	1.252	0.751	0.751	0.008	0.607	0.751	0.752	0.011	1.127	0.751	0.753	0.022
RGG (d = 2)	1.011	0.595	0.604	0.003	0.492	0.596	0.607	0.033	0.933	0.601	0.615	0.029
RGG (d = 3)	0.856	0.491	0.513	0.003	0.421	0.494	0.518	0.033	0.807	0.503	0.534	0.029
BTER	0.991	0.290	0.558	0.538	0.880	0.525	0.605	0.680	1.028	0.342	0.375	0.501
TCL	0.280	0.075	0.126	0.223	0.223	0.117	0.094	0.192	0.490	0.138	0.160	0.411
LFR (μ = 0.0)	1.140	0.262	0.546	0.435	N/A	N/A	N/A	N/A	1.114	0.252	0.414	0.336
LFR (μ = 0.5)	0.296	0.068	0.081	0.175	0.161	0.084	0.120	0.170	0.571	0.145	0.170	0.170
LFR (μ = 1.0)	0.197	0.045	0.047	0.070	0.105	0.055	0.059	0.067	0.019	0.005	0.040	0.281

dataset	*Spam*				*Cepg*				*Scht*			
metric	△	GCC	ALCC	overlap	△	GCC	ALCC	overlap	△	GCC	ALCC	overlap
GROUNDT	1.000	0.145	0.286	N/A	1.000	0.321	0.447	N/A	1.000	0.377	0.350	N/A
EDGEIND-CL	0.496	0.072	0.060	0.067	0.683	0.230	0.223	0.232	0.644	0.245	0.234	0.243
LOCLBDG-CL	1.028	0.124	0.260	0.067	0.996	0.293	0.430	0.231	1.036	0.318	0.469	0.241
PARABDG-CL	1.007	0.131	0.436	0.067	0.999	0.310	0.578	0.231	1.135	0.294	0.610	0.237
PA	0.112	0.027	0.026	0.025	0.288	0.130	0.130	0.129	0.226	0.121	0.123	0.116
RGG (d = 1)	1.144	0.750	0.750	0.003	0.834	0.752	0.754	0.033	0.678	0.752	0.754	0.029
RGG (d = 2)	0.899	0.592	0.597	0.003	0.704	0.604	0.622	0.033	0.567	0.603	0.620	0.029
RGG (d = 3)	0.772	0.485	0.501	0.003	0.611	0.509	0.544	0.033	0.492	0.507	0.541	0.029
BTER	1.003	0.194	0.325	0.402	0.991	0.484	0.504	0.631	0.658	0.397	0.383	0.544
TCL	0.201	0.044	0.087	0.223	0.356	0.166	0.165	0.362	0.218	0.130	0.146	0.312
LFR (μ = 0.0)	1.283	0.187	0.406	0.370	N/A	N/A	N/A	N/A	1.081	0.506	0.850	0.977
LFR (μ = 0.5)	0.426	0.062	0.072	0.120	0.649	0.209	0.294	0.337	0.596	0.224	0.291	0.332
LFR (μ = 1.0)	0.332	0.048	0.042	0.081	0.516	0.166	0.217	0.303	0.476	0.179	0.212	0.292

number of wedges. In Figure 7, for both *Hams* and *Fcbk*, we compare the degree and distance distributions in the ground-truth graph and in the graphs generated by EDGEIND, PARABDG, and PARABDG-JW. With joint optimization, both degree and distance distributions do not change much (compare PARABDG and PARABDG-JW in Figure 7).

F. On advanced EIGMs, other edge-dependent RGMs, and deep graph generative models

As discussed in Section III-A, there exist methods that shift edge probabilities by various mechanisms, while they are still essentially EIGMs. Hence, they inevitably trade-off between variability and the ability to generate high-clustering graphs. Such methods include Binning Chung Lu (BCL) proposed by [19] that uses accept-reject and Block Two-level Erdos-Renyi (BTER) proposed by [20] that uses a mixture of different EIGMs (specifically, Erdos-Renyi and Chung-Lu). Also, as discussed in Section III-B, there are also existing methods that use additional mechanisms to improve upon existing EIGMs. For example,

TABLE XXII: The ρ values (i.e., the probability of taking the triangle-forming step) used by TCL for each dataset.

dataset	*Hams*	*Fcbk*	*Polb*	*Spam*	*Cepg*	*Scht*
TCL ρ	0.877	0.986	0.035	0.652	0.263	0.411

[7] proposed Transitive Chung-Lu (TCL) that uses an additional mechanism to directly insert triangles on top of the original edge-independent Chung-Lu.

Differences. In this work, we aim to improve upon EIGMs by further exploring models without assuming edge independency. The key point is to preserve individual edge probabilities and thus have high tractability, but the existing methods usually use mixed models and thus change the underlying edge probabilities. The consequence is that they either have less tractability or less variability (i.e., high overlap; see Theorems 3.2 and 4.7).

- TCL uses an additional mechanism to directly form triangles and is thus less tractable;
- BTER forms many small dense communities and has very high overlap.

As shown in Property IV.3, EPGMs have the same overlap as the corresponding EIGM, i.e., the variability is perfectly maintained even though we introduce edge dependency.

Below, we compare the performance of (1) the original edge-independent Chung-Lu, (2) Chung-Lu with local binding, (3) Chung-Lu with parallel binding, (4) TCL, and (5) BTER.

Evaluation. In addition to the clustering-related metrics (the number of triangles, global clustering coefficient, and the average local clustering coefficient) we used in our main experiments, we further compare the "overlap" of the generated graphs. Roughly, the overlap of a random graph model is the expected proportion of overlapping edges between two randomly generated graphs (i.e., the edges that exist in both randomly generated graphs). Higher overlap values imply lower variability; when overlap approaches 1, the generated graphs are almost identical.

Implementation.

- For TCL, we use online Python code;[14]
- For BTER, we use the official MATLAB implementation.[15]

Results. In Table XXI, we show the detailed results. Overall, we have the following observations.

- For some datasets (e.g., *facebook*), TCL almost-always (i.e., $\rho \approx 1$) uses the mechanism that directly forms triangles. Even so, TCL often fails to well preserve the clustering-related metrics in real-world graphs.
  - TCL mixes two types of steps: (1) original Chung-Lu with probability $(1-\rho)$ and (2) a triangle-forming step with probability ρ.
  - See Table XXII for the ρ values used by TCL for each dataset.
- As expected, although BTER generates graphs with high clustering as intended, it has very high overlap, which implies that it well reproduces high-clustering graphs by largely duplicating the input graphs.
- Our methods with binding schemes have the same overlap as the corresponding EIGM, while well preserving clustering-related metrics in real-world graphs.

Other edge-dependent RMGs. For the experiments on other edge-dependent RMGs in Section VI-F, we provide more details here.

- For random geometric graphs (RGG), we tried dimensions $d \in \{1, 2, 3\}$, while setting the number of nodes as that in the input graph, and setting the diameter to fit the number of edges in the input graph. Note that the clustering in the generated graph is only determined by the dimension, and smaller dimensions give higher clustering.
- For preferential attachment (PA), we tried the extended Barabási-Albert model.[16] We set the number of nodes as that in the input graph, and set the parameter m to fit the number of edges in the input graph. We tried $p, q \in \{0, 0.1, 0.2, 0.3\}$. We report the variant that gives the highest clustering.
- For the Lancichinetti-Fortunato-Radicchi (LFR) model, we set the degrees as the ground-truth degrees, set the community sizes as the sizes of the communities detected using the Louvain algorithm, and tried different mixing parameters $\mu \in \{0, 0.5, 1.0\}$.

Discussions on deep graph generative models. Recently, deep graph generative models have become more and more popular. Typically, deep graph generative models aim to fit a population of small graphs, while this work focuses on fitting random graph models to individual input graphs. We empirically tested three deep graph generative models: CELL [45], GraphVAE [46], and GrpahRNN [47].

We summarize our empirical observations as follows:

- CELL often fails to generate high clustering, and also generates high overlap (i.e., low variability). CELL is essentially an EIGM. See also the discussions by [15].

---

[14]https://github.com/pdsteele/socialNetworksProject/blob/master/proj-TransChungLu.py

[15]https://www.mathsci.ai/feastpack

[16]See, e.g., https://networkx.org/documentation/stable/reference/generated/networkx.generators.random_graphs.extended_barabasi_albert_graph.html.

TABLE XXIII: The clustering metrics of generated graphs without fitting specific graphs using ER as the underlying edge-probability model.

average $g(v)$	$\triangle$	GCC	ALCC
0 (EIGM)	179.21	0.010	0.010
0.001	1957.88	0.100	0.119
0.002	3721.49	0.177	0.249
0.003	5499.17	0.240	0.379
0.004	7323.14	0.296	0.489
0.005	9489.65	0.344	0.568
0.006	10796.54	0.386	0.635
0.007	12742.98	0.422	0.681
0.008	14342.90	0.464	0.723
0.009	16122.18	0.491	0.749
0.01	18116.62	0.514	0.772

(a) ER + PARABDG

average $g(v)$	$\triangle$	GCC	ALCC
0 (EIGM)	179.21	0.010	0.010
0.001	338.67	0.019	0.018
0.002	1006.9	0.054	0.047
0.003	1864.64	0.092	0.088
0.004	2567.84	0.121	0.125
0.005	3178.68	0.143	0.151
0.006	3797.42	0.165	0.171
0.007	4301.58	0.183	0.187
0.008	5080.94	0.202	0.200
0.009	5542.13	0.218	0.210
0.01	6441.86	0.236	0.222

(b) ER + LOCLBDG

TABLE XXIV: The clustering metrics of generated graphs without fitting specific graphs using CL as the underlying edge-probability model.

α	average $g(v)$	$\triangle$	GCC	ALCC
	0 (EIGM)	13668.59	0.167	0.337
	0.01	12506.14	0.153	0.493
	0.02	13160.15	0.156	0.536
	0.03	13844.84	0.161	0.559
	0.04	15182.06	0.172	0.568
-0.3	0.05	15610.28	0.168	0.584
	0.06	17647.33	0.179	0.588
	0.07	16757.68	0.172	0.588
	0.08	16119.25	0.173	0.593
	0.09	15417.53	0.160	0.594
	0.1	18102.03	0.176	0.605
	0 (EIGM)	13668.59	0.167	0.337
	0.01	13051.15	0.159	0.539
	0.02	14274.04	0.171	0.585
	0.03	15724.32	0.181	0.602
	0.04	16188.49	0.182	0.614
0	0.05	19404.04	0.200	0.622
	0.06	20993.48	0.209	0.634
	0.07	19845.02	0.198	0.639
	0.08	23823.32	0.215	0.634
	0.09	30700.56	0.232	0.644
	0.1	26477.88	0.215	0.646
	0 (EIGM)	13668.59	0.167	0.337
	0.01	14245.14	0.173	0.598
	0.02	17062.43	0.195	0.643
	0.03	19329.61	0.215	0.660
	0.04	22821.36	0.232	0.673
0.3	0.05	23128.39	0.238	0.684
	0.06	28266.25	0.250	0.697
	0.07	30571.88	0.265	0.703
	0.08	27047.89	0.250	0.717
	0.09	38293.91	0.286	0.728
	0.1	34335.56	0.278	0.731

(a) CL + PARABDG

α	average $g(v)$	$\triangle$	GCC	ALCC
	0 (EIGM)	13668.59	0.167	0.337
	0.01	11962.88	0.148	0.426
	0.02	12417.21	0.149	0.462
	0.03	12688.25	0.153	0.475
	0.04	12847.39	0.151	0.486
-0.3	0.05	13543.07	0.159	0.495
	0.06	14457.40	0.163	0.504
	0.07	13856.21	0.155	0.511
	0.08	14942.73	0.156	0.530
	0.09	15551.34	0.163	0.524
	0.1	14264.12	0.154	0.532
	0 (EIGM)	13668.59	0.167	0.337
	0.01	12155.44	0.152	0.433
	0.02	12651.05	0.154	0.463
	0.03	13348.38	0.160	0.480
	0.04	13249.86	0.157	0.495
0	0.05	14450.43	0.167	0.503
	0.06	15668.08	0.171	0.518
	0.07	14949.55	0.169	0.519
	0.08	14733.55	0.164	0.525
	0.09	19401.58	0.182	0.528
	0.1	18072.88	0.182	0.529
	0 (EIGM)	13668.59	0.167	0.337
	0.01	12544.92	0.154	0.433
	0.02	13383.98	0.160	0.461
	0.03	13901.56	0.166	0.476
	0.04	15005.39	0.175	0.493
0.3	0.05	16448.43	0.181	0.506
	0.06	16623.27	0.182	0.503
	0.07	18159.03	0.186	0.523
	0.08	16835.26	0.185	0.522
	0.09	18177.49	0.188	0.538
	0.1	18459.21	0.195	0.546

(b) CL + LOCLBDG

- GraphVAE learns to duplicate the training graph (i.e., 100% overlap). This is likely because GraphVAE was designed to learn from a population of graphs instead of a single graph, as discussed above.
- GraphRNN often generates graphs with far more edges but still low clustering. This is likely because GraphRNN was designed mainly for relatively small graphs and cannot fit well to individual large graphs.

As discussed by [15], several deep graph generative models also output edge probabilities (e.g., CELL), and this work provides a new perspective to potentially enhance them with edge dependency.

G. On graph generation without fitting specific graphs

Instead of fitting specific graphs as done in our main experiments, one can also use the proposed models to generate graphs "from scratch" without specific graphs as references by freely choosing the parameters.

First, one needs to choose the underlying edge probabilities. Typically, one can use an underlying edge-probability model and choose it according to the required properties. For example, if one wants to generate graphs with power-law degree distributions, Chung-Lu with a prescribed power-law degree sequence can be used. Or, if one wants to generate a graph with community structures, the stochastic block model can be used.

TABLE XXV: The clustering metrics of generated graphs without fitting specific graphs using SB as the underlying edge-probability model.

(a) SB + PARABDG

α	average $g(v)$	$\triangle$	GCC	ALCC
-0.5	0 (EIGM)	297.15	0.167	0.337
	0.01	1070.80	0.153	0.493
	0.02	1857.45	0.156	0.536
	0.03	2587.32	0.161	0.559
	0.04	3393.55	0.172	0.568
	0.05	4140.39	0.168	0.584
	0.06	4980.47	0.179	0.588
	0.07	5662.74	0.172	0.588
	0.08	6440.77	0.173	0.593
	0.09	7169.38	0.160	0.594
	0.1	7949.71	0.176	0.605
0	0 (EIGM)	297.15	0.167	0.337
	0.01	1460.17	0.159	0.539
	0.02	2656.48	0.171	0.585
	0.03	3821.19	0.181	0.602
	0.04	4995.17	0.182	0.614
	0.05	6135.86	0.200	0.622
	0.06	7271.69	0.209	0.634
	0.07	8458.58	0.198	0.639
	0.08	9924.68	0.215	0.634
	0.09	10945.15	0.232	0.644
	0.1	12061.47	0.215	0.646
0.5	0 (EIGM)	297.15	0.167	0.337
	0.01	1527.10	0.173	0.598
	0.02	2746.08	0.195	0.643
	0.03	3989.85	0.215	0.660
	0.04	5209.86	0.232	0.673
	0.05	6516.78	0.238	0.684
	0.06	7707.59	0.250	0.697
	0.07	8833.38	0.265	0.703
	0.08	10119.58	0.250	0.717
	0.09	11197.86	0.286	0.728
	0.1	12589.62	0.278	0.731

(b) SB + LOCLBDG

α	average $g(v)$	$\triangle$	GCC	ALCC
-0.5	0 (EIGM)	297.15	0.015	0.014
	0.01	3139.06	0.133	0.147
	0.02	6016.54	0.215	0.208
	0.03	8872.29	0.272	0.239
	0.04	11101.77	0.313	0.256
	0.05	13093.51	0.331	0.261
	0.06	19008.57	0.368	0.274
	0.07	18992.58	0.378	0.270
	0.08	23138.66	0.412	0.276
	0.09	24280.39	0.412	0.271
	0.1	30652.89	0.432	0.280
0	0 (EIGM)	297.15	0.015	0.014
	0.01	4257.22	0.172	0.170
	0.02	7764.28	0.265	0.221
	0.03	11887.79	0.327	0.247
	0.04	16886.04	0.379	0.253
	0.05	20868.18	0.405	0.257
	0.06	23889.00	0.436	0.256
	0.07	29247.06	0.451	0.264
	0.08	30123.19	0.450	0.253
	0.09	36971.23	0.451	0.254
	0.1	45597.38	0.468	0.264
0.5	0 (EIGM)	297.15	0.015	0.014
	0.01	4348.57	0.170	0.156
	0.02	8368.21	0.269	0.215
	0.03	12679.81	0.331	0.235
	0.04	17480.57	0.380	0.246
	0.05	19396.23	0.412	0.242
	0.06	24362.75	0.418	0.247
	0.07	30949.97	0.453	0.250
	0.08	33129.43	0.437	0.252
	0.09	36050.41	0.463	0.253
	0.1	41233.18	0.458	0.260

Below, we shall discuss the graph statistics of random graphs generated by EPGMs using binding with varying parameters. Let us first provide the parameter ranges.

For the Erdős-Rényi (ER) model:

- The number n of nodes is fixed as 1024.
- The edge probability $p(u,v)$ is 0.01, the same for all the node pairs. The value 0.01 is chosen in the typical range of real-world graphs [100].
- The node-sampling probability $g(v)$ is the same for all the nodes (as discussed in Section V-D), with varying values.
- The number R of rounds is 100000, as in our main experiments.

For the Chung-Lu (CL) model:

- The number n of nodes is fixed as 1024.
- The degree sequence d_v's are generated as a power-law sequence with power-law exponent 2, so that the average edge probability $p(u,v)$ is around 0.01. The exponent 2 is chosen in the typical range of real-world graphs [8].
- The node-sampling probability $g(v)$ is the same for nodes with the same degree (as discussed in Section V-D), with varying mean values and varying correlation with degrees. Specifically, for each node v, we set the node-sampling probability $g(v)$ proportional to $d(v)^\alpha$ with different α values (-0.3, 0, and 0.3), where $d(v)$ is the degree of node v. The α values are chosen so that no node has a node-sampling probability exceeding 1. The node-sampling probabilities are positively (resp., negatively) correlated with node degrees with a positive (resp., negative) α value. When $\alpha = 0$, the node-sampling probability is the same for all the nodes.
- The number R of rounds is 100000, as in our main experiments.

For the stochastic block (SB) model:

- The number n of nodes is fixed as 1024.
- The number of communities (i.e., blocks) is fixed as 10.
- The community sizes are generated as a power-law with power-law exponent 1.5. The exponent 1.5 is chosen in the typical range of real-world graphs [101].
- The intra-community edge probability and inter-community edge probability are the same for different communities, and are chosen so that the average edge probability $p(u,v)$ is around 0.01.

TABLE XXVI: The clustering metrics of generated graphs without fitting specific graphs using KR as the underlying edge-probability model.

α	average $g(v)$	$\triangle$	GCC	ALCC	α	average $g(v)$	$\triangle$	GCC	ALCC
	0 (EIGM)	1044.88	0.031	0.033		0 (EIGM)	1044.88	0.031	0.033
	0.01	6586.23	0.157	0.327		0.01	3086.48	0.081	0.147
	0.02	11809.86	0.240	0.422		0.02	5166.20	0.122	0.188
	0.03	17238.21	0.305	0.471		0.03	7636.03	0.158	0.211
	0.04	22369.54	0.334	0.508		0.04	9707.45	0.180	0.227
-1	0.05	27207.33	0.361	0.530	-1	0.05	10435.17	0.189	0.232
	0.06	37717.33	0.409	0.556		0.06	13325.55	0.207	0.243
	0.07	38131.85	0.418	0.559		0.07	16207.68	0.225	0.250
	0.08	46682.81	0.432	0.580		0.08	18169.74	0.236	0.261
	0.09	52381.99	0.435	0.595		0.09	21601.60	0.234	0.267
	0.1	56996.55	0.439	0.604		0.1	23594.77	0.241	0.270
	0 (EIGM)	1044.88	0.031	0.033		0 (EIGM)	1044.88	0.031	0.033
	0.01	8860.73	0.198	0.402		0.01	3726.94	0.094	0.154
	0.02	16677.24	0.307	0.499		0.02	6239.78	0.141	0.187
	0.03	23927.22	0.373	0.549		0.03	8729.61	0.176	0.209
	0.04	33434.06	0.430	0.582		0.04	11659.48	0.209	0.218
0	0.05	33908.84	0.436	0.600	0	0.05	15550.88	0.238	0.230
	0.06	51113.67	0.488	0.624		0.06	17557.07	0.241	0.232
	0.07	56890.50	0.503	0.631		0.07	22365.64	0.271	0.243
	0.08	57262.88	0.492	0.637		0.08	20931.69	0.266	0.237
	0.09	73944.66	0.517	0.656		0.09	20406.49	0.240	0.237
	0.1	71084.79	0.486	0.642		0.1	26693.30	0.254	0.249
	0 (EIGM)	1044.88	0.031	0.033		0 (EIGM)	1044.88	0.031	0.033
	0.01	11202.40	0.242	0.472		0.01	4118.72	0.103	0.152
	0.02	21129.53	0.360	0.572		0.02	7056.13	0.155	0.181
	0.03	30490.92	0.443	0.619		0.03	10525.82	0.196	0.201
	0.04	42543.89	0.501	0.648		0.04	12531.47	0.217	0.198
1	0.05	48769.38	0.535	0.664	1	0.05	16213.98	0.245	0.207
	0.06	57292.62	0.562	0.665		0.06	22050.84	0.276	0.221
	0.07	62270.76	0.558	0.682		0.07	19337.29	0.256	0.212
	0.08	68569.86	0.522	0.689		0.08	25260.46	0.276	0.220
	0.09	99628.36	0.565	0.708		0.09	24525.96	0.263	0.213
	0.1	109134.19	0.547	0.702		0.1	33226.16	0.276	0.236

(a) KR + PARABDG   (b) KR + LOCLBDG

- The node-sampling probability $g(v)$ is the same for nodes with the same community (as discussed in Section V-D), with varying mean values and varying correlation with community sizes. Specifically, for each node v, we set the node-sampling probability $g(v)$ proportional to $s(v)^\alpha$ with different α values (-0.5, 0, and 0.5), where $s(v)$ is the size of the community v is in. The α values are chosen so that no node has a node-sampling probability exceeding 1. The node-sampling probabilities are positively (resp., negatively) correlated with community sizes with a positive (resp., negative) α value. When $\alpha = 0$, the node-sampling probability is the same for all the nodes.
- The number R of rounds is 100000, as in our main experiments.

  For the stochastic Kronecker (KR) model:

- The number n of nodes is fixed as 1024. Specifically, the seed matrix is two-by-two, and we take the order-10 Kronecker power of the seed matrix.
- The seed matrix is [0.95, 0.63; 0.63, 0.32]. The values in the seed matrix are chosen so that the average edge probability $p(u, v)$ is around 0.01, and the value distribution is similar to those in the original paper of Kronecker [12].
- The node-sampling probability $g(v)$ is the same for nodes with the same number of ones in their binary node labels (as discussed in Section V-D), with varying mean values and varying correlation with the number of ones. Specifically, for each node v, we set the node-sampling probability $g(v)$ proportional to $(i(v) + 1)^\alpha$ with different α values (-1, 0, and 1), where $i(v)$ is the number of ones in the binary node label of v. The α values are chosen so that no node has a node-sampling probability exceeding 1. The node-sampling probabilities are positively (resp., negative) correlated with the number of ones with a positive (resp., negative) α value. When $\alpha = 0$, the node-sampling probability is the same for all the nodes.

  In Tables XXIII to XXVI, we show the clustering metrics of graphs generated without fitting specific graphs as described above, with different underlying edge-probability models.

  Below, let us discuss the insights we have based on the results. Overall, in line with our theoretical analysis, in most cases, when we increase node-sampling probabilities, the generated graphs have higher clustering. By varying node-sampling probabilities, one can generate graphs with different levels of clustering. Also, with the same node-sampling probabilities, PARABDG generates graphs with higher clustering than LOCLBDG.

  There are also interesting observations on the correlation between node-sampling probabilities and some parameters in the underlying edge-probability models, indicated by the value of α. For CL, with the same average node-sampling probability,

when we make node-sampling probabilities positively correlated to the node degrees, the generated graphs have higher clustering. For SB, with the same average node-sampling probability, when we make node-sampling probabilities negatively correlated to the node degrees, the generated graphs have relatively lower clustering, while positive correlation and no correlation give similar results. For KR, with the same average node-sampling probability, when we make node-sampling probabilities positively correlated to the number of ones, the generated graphs have higher clustering.